Journal of Medicinal Chemistry

pubs.acs.org/jmc

Article

Potent Inhibition of SARS-CoV-2 nsp14 *N*7-Methyltransferase by Sulfonamide-Based Bisubstrate Analogues

Rostom Ahmed-Belkacem, Marcel Hausdorff, Adrien Delpal, Priscila Sutto-Ortiz, Agathe M. G. Colmant, Franck Touret, Natacha S. Ogando, Eric J. Snijder, Bruno Canard, Bruno Coutard, Jean-Jacques Vasseur, Etienne Decroly,* and Françoise Debart*

Cite This: *J. Med. Chem.* 2022, 65, 6231−6249

Read Online

ACCESS | Metrics & More | Article Recommendations | Supporting Information

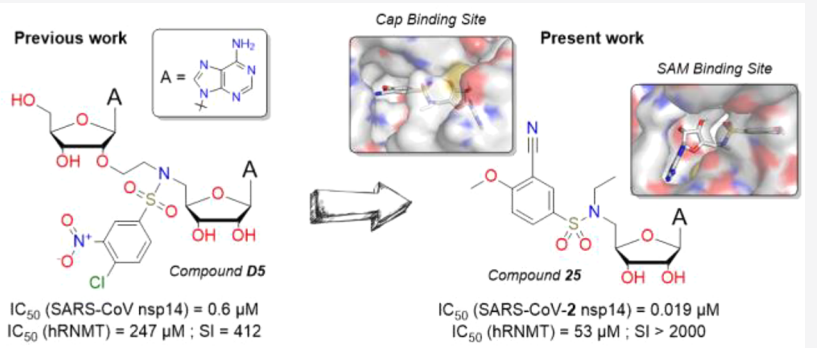

ABSTRACT: Enzymes involved in RNA capping of SARS-CoV-2 are essential for the stability of viral RNA, translation of mRNAs, and virus evasion from innate immunity, making them attractive targets for antiviral agents. In this work, we focused on the design and synthesis of nucleoside-derived inhibitors against the SARS-CoV-2 nsp14 (*N*7-guanine)-methyltransferase (*N*7-MTase) that catalyzes the transfer of the methyl group from the *S*-adenosyl-L-methionine (SAM) cofactor to the *N*7-guanosine cap. Seven compounds out of 39 SAM analogues showed remarkable double-digit nanomolar inhibitory activity against the *N*7-MTase nsp14. Molecular docking supported the structure−activity relationships of these inhibitors and a bisubstrate-based mechanism of action. The three most potent inhibitors significantly stabilized nsp14 ($\Delta T_m \approx 11$ °C), and the best inhibitor demonstrated high selectivity for nsp14 over human RNA *N*7-MTase.

INTRODUCTION

Severe acute respiratory syndrome coronavirus 2 (SARS-CoV-2) is the third highly pathogenic coronavirus, emerging in the human population in 2019, after SARS-CoV and Middle East respiratory syndrome coronavirus (MERS-CoV) emerged in 2003[1] and 2012,[2] respectively. Currently, treatments for diseases caused by CoVs are still limited. Therefore, this health emergency highlights the crucial need to identify effective treatments for SARS-CoV-2 and its variants. Until now, the promising drug repurposing strategy has failed to find an effective treatment for COVID-19. The alternative strategy is to develop new direct-acting antiviral drugs with a rational design.[3,4] Although more time-consuming, this second approach of exploring the structure−activity relationships (SARs) of compounds in an attempt to understand their mode of action is more compelling for medicinal chemists.

CoVs have a genome composed of a large, single-stranded, positive-sense RNA with a cap structure at its 5′ end that ensures mRNA stability by protecting it from cellular 5′-exo-ribonucleases. This structure consists of an *N*7-methylguanosine linked by a 5′-5′-triphosphate bridge to the 5′-terminal nucleotide (adenosine in CoVs) (cap 0: ^{7m}GpppA), which can be further methylated at its 2′-*O* position (cap 1: ^{7m}GpppA$_m$).[5,6] Specifically, *N*7-methylation of the viral RNA cap plays a key role in the translation of viral RNA into proteins. Furthermore, inhibition of the SARS-CoV-2 nsp14 *N*7-methyltransferase (MTase) blocks the enzymatic cascade of viral RNA methylations, as the 2′-*O*-MTase (nsp16) only recognizes *N*7-methylated cap substrates.[7,8] Nsp14 is also considered as an antiviral target because the replication of *N*7-MTase catalytic mutants is strongly impaired.[9] Therefore, this crucial yet uncommon and under-explored enzyme seemed an enticing target to us for the development of antiviral therapies.[9−11]

Received: January 21, 2022
Published: April 19, 2022

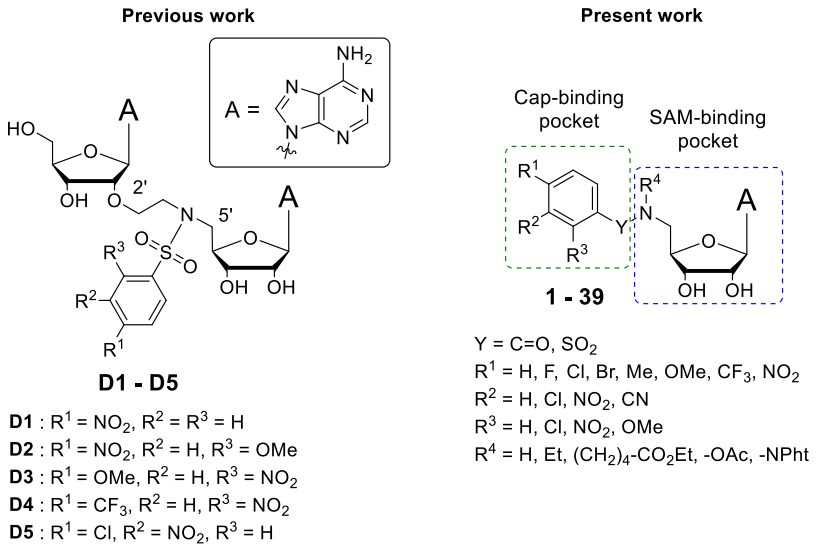

Figure 1. Design of SARS-CoV-2 nsp14 inhibitors **1**−**39** derived from initial dinucleoside inhibitors **D1**−**D5** of SARS-CoV nsp14.[21]

Curiously, until recently, few inhibitors of the viral MTase nsp14 have been developed, and the lack of selective inhibitors is an exciting challenge not only for new antiviral therapies but also for functional studies of this enzyme.[12] It is noteworthy that nsp14 has an original fold,[13] which is not the canonical Rossmann fold, and that the *N*7-MTase domains of CoVs are highly conserved. This particular structural organization and sequence conservation could facilitate the development of specific inhibitors. Recently, several studies have reported high-throughput screening of existing libraries of small molecules against nsp14 activity. However, very few compounds have been identified as potential inhibitors of SARS-CoV-2.[14−18] In addition to the drug-repurposing approach, the method of *de novo* drug discovery with structure-guided design of nsp14 substrates yielded potent inhibitors with IC_{50} values in the nanomolar to submicromolar range.[19,20] However, both articles did not report studies on the inhibitory activity of these nsp14 inhibitors in SARS-CoV-2-infected cells. Before the emergence of SARS-CoV-2, our group had pioneered the synthesis of selective inhibitors targeting the SARS-CoV nsp14 *N*7-MTase using dinucleosides as mimetics of the *S*-adenosyl-L-methionine (SAM) that is the methyl donor in the *N*7-methylation of the cap (Figure 1).[21] Initially, these compounds were designed to interact with 2′-*O*-MTases in a selective manner by mimicking the structure of the transition state of viral cap-mRNA during the 2′-*O*-methylation of $^{7m}GpppN_1$-RNA. Unexpectedly, while all of the synthesized compounds were barely active against 2′-*O*-MTases, some of them (**D1**−**D5**, Figure 1, Table 1) exhibited inhibition of the SARS-CoV nsp14 *N*7-MTase in the submicromolar range. These dinucleosides consisted of two adenosines, linked in 2′-5′ by a substituted benzenesulfonamide ethyl linker. Molecular docking studies suggested that the phenyl ring binds to the cap-binding pocket of SARS-CoV nsp14 and establishes $\pi-\pi$ stacking interactions with the Phe426 amino acid that naturally stacks the guanosine of the viral mRNA cap structure (Supporting Information, Figures S1 and S2).[22] Thus, this work demonstrated that dinucleosides could act as competitive bisubstrate inhibitors by occupying both the SAM-binding pocket and the cap-binding pocket (Supporting Information, Figure S2). Unfortunately, none of the developed compounds exhibited antiviral activity in SARS-CoV-infected VeroE6 cells (unpublished results). This lack of efficacy could be explained by poor cellular internalization of these large, high-molecular-weight dinucleosides, which could impair targeting of the nsp14 enzyme in the cytoplasm.[23]

Table 1. Comparison of IC_{50} Values of Sinefungin, Dinucleosides D1−D5, and Compounds 2, 3, 5, 6, and 7 on SARS-CoV nsp14 and SARS-CoV-2 nsp14

	IC_{50}[a] (μM)	
compound	SARS-CoV nsp14	SARS-CoV-2 nsp14
sinefungin	0.36[b]	0.278 ± 0.008
D1[c]	2.6 ± 0.3	n.d.
D2[c]	70.4 ± 4.9	n.d.
D3[c]	3.9 ± 0.4	n.d.
D4[c]	5.7 ± 0.5	n.d.
D5[c]	0.6 ± 0.1	n.d.
2	7.6 ± 1.2	14.1 ± 1.0
3	25 ± 6.1	5.1 ± 2.0
5	2.6 ± 0.3	1.4 ± 0.2
6	3.3 ± 0.2	3.5 ± 0.2
7	1.4 ± 0.2	2.1 ± 0.2

[a]Concentration inhibiting *N*7-MTase activity by 50%; mean value from three independent experiments. [b]Values from the literature.[10] [c]Values from the literature.[21] n.d.: not determined.

Here, with the aim to obtain smaller and presumably more efficient molecules to enter cells, we designed and developed SAM nucleoside analogues **1**−**39** of a reduced size and molecular weight relative to our initial dinucleoside nsp14 inhibitors (Figure 1). These nucleosides, designed as bisubstrates, consist of an adenosine interacting with the SAM-binding pocket and various benzenesulfonamide moieties which occupy the cap-binding pocket. Indeed, the arylsulfonamide moiety was crucial for the inhibitory activity of dinucleosides **D1**−**D5** on SARS-CoV nsp14.[21] The synthesized compounds **1**−**39** were screened for their ability to inhibit the *N*7-MTase activity of SARS-CoV-2 *in vitro*.

RESULTS AND DISCUSSION

Design. In the search for effective inhibitors, we started to optimize the structure of novel nucleoside analogues **1**−**9** with the goal in mind to improve interactions with the SARS-CoV-2 *N*7-MTase nsp14. A thorough structural analysis highlighted

https://doi.org/10.1021/acs.jmedchem.2c00120
J. Med. Chem. 2022, 65, 6231−6249

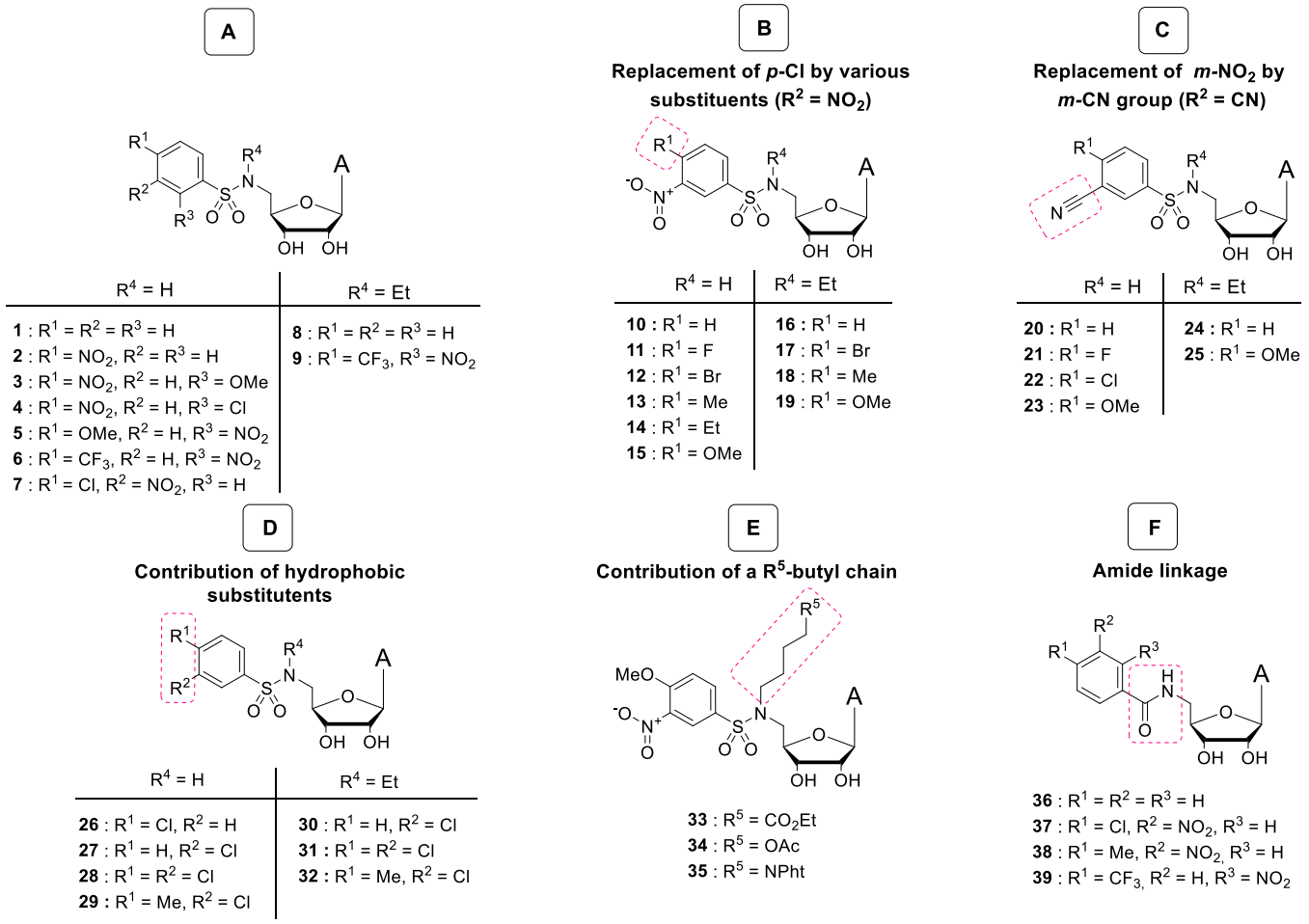

Figure 2. Rational design of nucleoside analogues **1**−**39** as inhibitors of SARS-CoV-2 nsp14. (A) Initial compounds **1**−**9** mainly derived from **D1**−**D5**. (B) Compounds **10**−**19** derived from *m*-NO_2 compound **7** in which *p*-Cl was replaced by various substituents. (C) Compounds **20**−**25** containing a *m*-CN group replacing a *m*-NO_2 group. (D) Compounds **26**−**32** with hydrophobic substituents (Cl, Me) in the phenyl ring. (E) Compounds **33**−**35** with an *N*-butyl chain terminated with various groups. (F) Compounds **36**−**39** with an amide linkage replacing a sulfonamide linkage.

that three parts of interest in these bisubstrate molecules could be modified to explore SARs: the linker between the 5′-deoxyadenosine and the phenyl ring, the substituents on the phenyl ring, and the functionalization of the 5′-nitrogen atom of the nucleoside (Figure 1). In addition, molecular docking performed prior to synthesis supported the choice of chemical modifications envisioned in the adenosine scaffold of **7**, the nucleoside counterpart of the most active inhibitor, **D5** (Supporting Information, Figure S3). Currently, since the crystal structure of the *N*7-MTase domain of SARS-CoV-2 nsp14 (highly conserved among CoVs) bound to the SAM cofactor is still uncharacterized, the high structural similarity to SARS-CoV nsp14 (95% amino acid sequence homology) enables modeling with the crystallized nsp14-SAM complex (PDB: 5C8T).[24]

First, nucleoside **1** without a substituent in the phenyl ring and nucleosides **2**−**9** with a nitro (NO_2) group at different positions (*ortho* (*o*), *meta* (*m*), or *para* (*p*)) of the aromatic moiety were designed to evaluate whether the monoadenosine structure was not detrimental to the inhibitory activity compared with previous dinucleoside inhibitors **D1**−**D5** (Figure 2A).[21] Furthermore, nucleosides **8** and **9** were functionalized with an ethyl (Et) group on the *N*-sulfonamide moiety. This *N*-substitution has been proposed to improve hydrophobicity and therefore cellular penetration. It could also improve affinity with nsp14, as it could reduce the total nonpolar surface area exposed to water and, therefore, provide beneficial association entropy. Supported by our previous results, the NO_2 group is well *meta*-oriented in the benzenesulfonamide group to provide a double hydrogen bond with Arg310 in nsp14. This amino acid naturally interacts with the triphosphate bridge of the cap structure through two hydrogen bonds.[22] Thus, nucleosides **10**−**19** were designed with the *m*-NO_2 group and bearing various *para* substituents with *N*-H- or *N*-Et-sulfonamide motifs (Figure 2B). Their inhibitory activity was compared with that of compound **7** (*m*-NO_2, *p*-Cl). Due to the narrow cavity surrounding the *para* position in the phenyl ring, only small substituents were inserted (H, F, Br, methyl (Me), Et). In compounds **20**−**25**, the *m*-nitro group was replaced by an *m*-cyano (CN) group to anticipate the mutagenic potential of the NO_2 group *in vivo* (Figure 2C).[25] In addition, upstream docking studies showed a strong similarity between NO_2 and CN overlays facing Arg310 (Figures 3 and 4).

The cap-binding pocket is surrounded by aromatic hydrophobic residues (Phe401, Phe506), forming a cavity near the *meta* and *para* sites of the benzenesulfonamide ring (Figure 4). To take advantage of this, nucleosides **26**−**32** were designed with hydrophobic substituents (Cl, Me) at these positions (Figure 2D). Note that docking studies show a pivot of the benzenesulfonamide ring: *m*-Cl does not face Arg310 but

https://doi.org/10.1021/acs.jmedchem.2c00120
J. Med. Chem. 2022, 65, 6231−6249

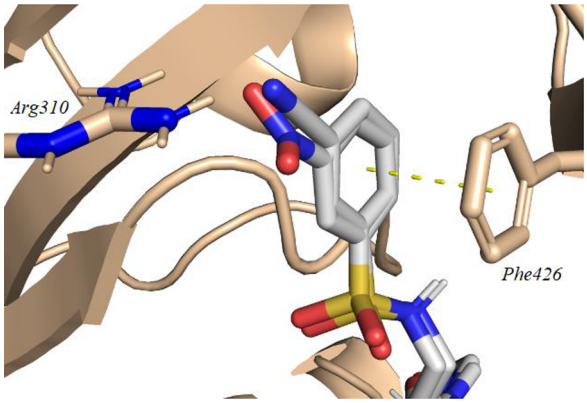

Figure 3. Overlay of *m*-nitro ($d_{O-H\ Arg310}$ = 2.3, 2.1 Å) and *m*-cyano ($d_{N-H\ Arg310}$ = 2.5, 2.0 Å) derivatives **10** and **20**. The $\pi-\pi$ stacking interaction with Phe426 is shown in yellow.

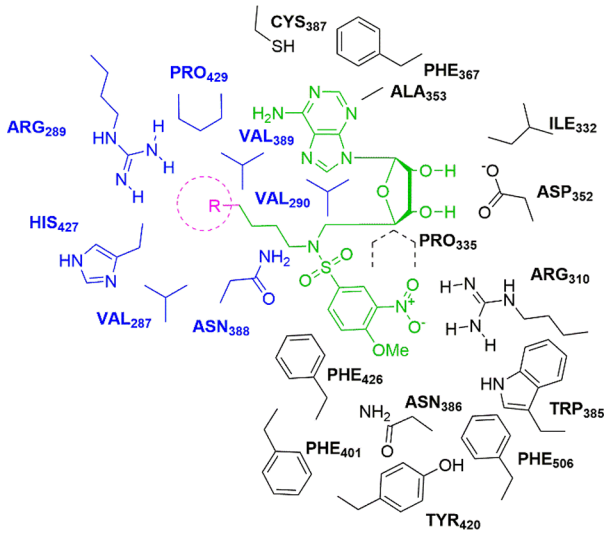

Figure 4. 2D representation of the SARS-CoV nsp14 sites targeted by compounds **33**−**35**. Amino acids surrounding the cap-binding pocket and SAM-binding pocket are shown in black. Amino acids surrounding the targeted pocket are shown in blue. Nucleoside is shown in green. All residues shown here are conserved in the SARS-CoV-2 nsp14.[24]

occupies the hydrophobic cavity, validating our approach to improve affinity (Supporting Information, Figure S4). In addition to the SAM-binding pocket and the cap-binding pocket, a side cavity close to the SAM-binding pocket and surrounded by Arg289, Val290, Asn388, and His427 (Figure 4) was targeted by compounds **33**−**35** (Figure 2E). Their *N*-sulfonamide linker was functionalized with a butyl chain terminated with various groups (CO_2Et, OAc, NPht) that could interact with these residues. In particular, docking studies suggest that a phthalimide (Pht) group could interact via a π*−cation interaction with Arg289 (Figure 4, and Supporting Information, Figure S5). The contribution of this R^5-butyl chain was evaluated by comparing the inhibitory activities of **33**−**35** with that of **15** with a *N*-H-sulfonamide moiety (Figure 2F).

At the same time, Otava et al. reported the synthesis of SARS-CoV-2 inhibitors designed to target the same pocket in nsp14.[20] Because this cavity is also adjacent to the N7 position of the SAM adenine, the authors functionalized the C7 position of the 7-deazaadenosine SAH analogues with aromatic systems. This rational design led to the identification of several compounds with an inhibitory effect against SARS-CoV-2 nsp14 in the low micromolar to nanomolar range, supporting the relevance of our target. Finally, to demonstrate the key role of the sulfonamide linker for significant inhibitory activity, it was replaced by an amide bond in nucleosides **36**−**39**.

Chemical Synthesis. The synthesis of compounds **1**−**32** began with the preparation of the readily accessible 5′-amino-2′,3′-isopropylideneadenosine **40** (Scheme 1).[21] Coupling of **40** with the corresponding commercially available benzenesulfonyl chloride reagents afforded the protected nucleosides **41a**−**u** in 24−81% yield.[21,26] The low yield of 24% associated with the synthesis of the *p*-F-*m*-NO_2-benzenesulfonamide derivative **41i** can be explained by a side reaction of the aromatic nucleophilic substitution at the *p*-F site by **40**. The aromatic nucleophilic substitution to introduce a methoxy (OMe) group at the *para* position was carried out from the *p*-Cl (**41g**) and *p*-F (**41o**) derivatives with sodium methanolate at 50 °C for 48 h, giving the nucleosides **41m** and **41q** in 76% and 98% yield, respectively.[27,28] Fluorinated derivative **41o** was engaged for the S_NAr reaction in place of the *p*-Cl-*m*-CN-benzenesulfonamide derivative **41p** to give the compound **41q** in higher yield (98% instead of 24%). In nucleosides **42a**−**k**, the *N*-sulfonamide linker was functionalized with an ethyl chain using ethyl *p*-toluenesulfonate and potassium iodide in DMF after 18 h at 50 °C in 40−86% yield. Moreover, the *N*-sulfonamide linker was substituted with an R^5-butyl chain in compounds **43a**−**c** with the corresponding alkyl bromide reagent under basic conditions in DMF after 18 h at 50 °C in 55−62% yield (Scheme 2).[29] Finally, the amide bond in nucleosides **44a**−**d** was formed by coupling 5′-NH_2 adenosine **40** with a suitable carboxylic acid (37−92% yield) (Scheme 3). Here, several conditions were screened using various peptide coupling agents (HBTU, EDC, PyBOP) in the presence of various bases (iPr_2NH, DIEA, DMAP) to test the coupling of **40** with benzoic acid.[30,31] It was found that coupling with EDC in the presence of DMAP at 0 °C was the most efficient and had the shortest reaction time (2 h). Finally, the 2′,3′-*O*-isopropylidene-protecting group was removed in all intermediates **41a**−**u**, **42a**−**k**, **43a**−**c**, and **44a**−**d** under the same acidic conditions with a mixture of formic acid and water (1:1) during 24−48 h, giving nucleosides **1**−**39** after purification.[32,33]

SARS-CoV-2 *N*7-MTase nsp14 Inhibition Studies. Compounds **1**−**39** were tested for *N*7-MTase inhibitory activity using a radioactive MTase assay (filter-binding assay) that involves measuring the [^{3}H]-radiolabeled methyl transferred from the SAM methyl donor onto the cap structure of an RNA substrate ($GpppAC_4$).[34] It should be noted that the first synthesized nucleosides, **2**, **3**, and **5**−**7**, were initially tested against SARS-CoV nsp14. Then, after the emergence of SARS-CoV-2, their inhibitory ability was measured against the SARS-CoV-2 nsp14 protein for comparison (Table 1). Similar IC_{50} values in the single-digit micromolar range (except for compound **3**) were obtained with both nsp14 enzymes, in agreement with the high sequence homology between these two viral *N*7-MTases. Moreover, compounds **2**, **3**, and **5**−**7** are derived from the initial dinucleosides **D1**−**D5**,[21] respectively, and their IC_{50} values are comparable in the same micromolar range. Compound **D5**, with a *p*-Cl-*m*-NO_2-phenylsulfonamide moiety, was the best dinucleoside inhibitor of SARS-CoV nsp14 (IC_{50} = 0.6 μM), and its nucleoside derivative **7** showed similar low IC_{50} values of 1.4 μM against SARS-CoV nsp14 and 2.1 μM against SARS-CoV-2 nsp14.

https://doi.org/10.1021/acs.jmedchem.2c00120
J. Med. Chem. 2022, 65, 6231−6249

Scheme 1. Synthetic Route for Compounds 1−32[a]

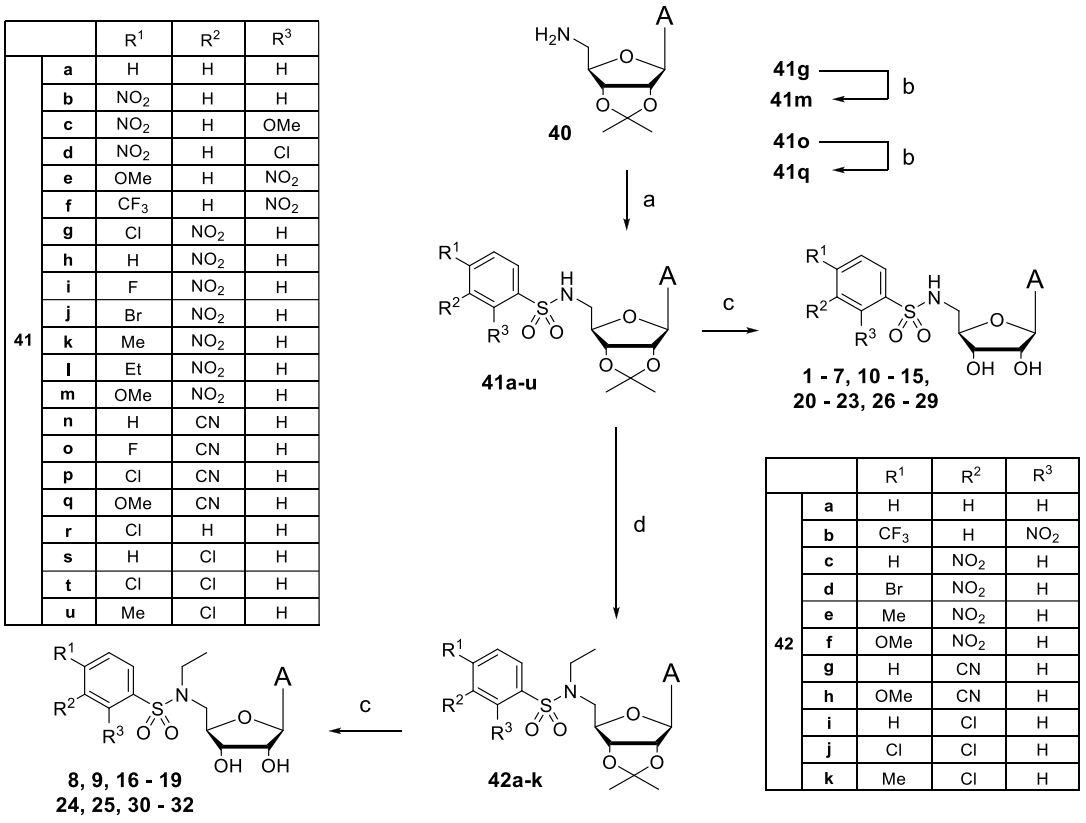

[a]Reagents and conditions: (a) appropriate substituted benzenesulfonyl chloride, Et_3N, DMF, 0 °C, 24−81%; (b) MeONa 0.5 M/MeOH, 50 °C, 48 h, 80−98%; (c) HCO_2H/H_2O 1:1 v/v, 25 °C, 24−48 h, 45−84%; (d) EtOTs, KI, K_2CO_3, DMF, 50 °C, 18 h, 40−81%.

Scheme 2. Synthetic Route for Compounds 33−35[a]

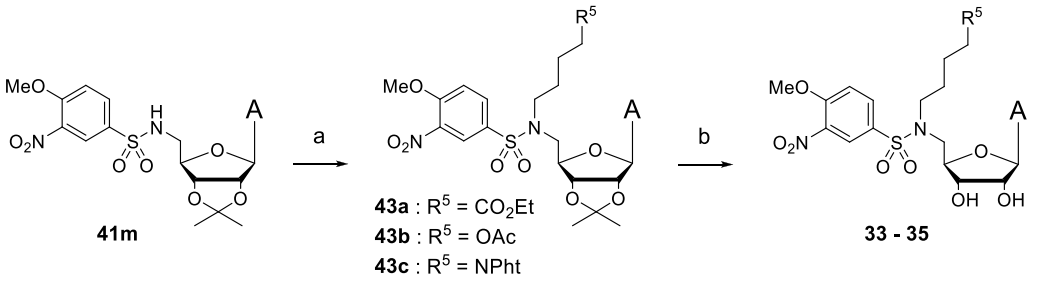

[a]Reagents and conditions: (a) appropriate alkyl bromide, K_2CO_3, DMF, 50 °C, 18 h, 55−62%; (b) HCO_2H/H_2O 1:1 v/v, 25 °C, 58−89%.

Scheme 3. Synthetic Route for Compounds 36−39[a]

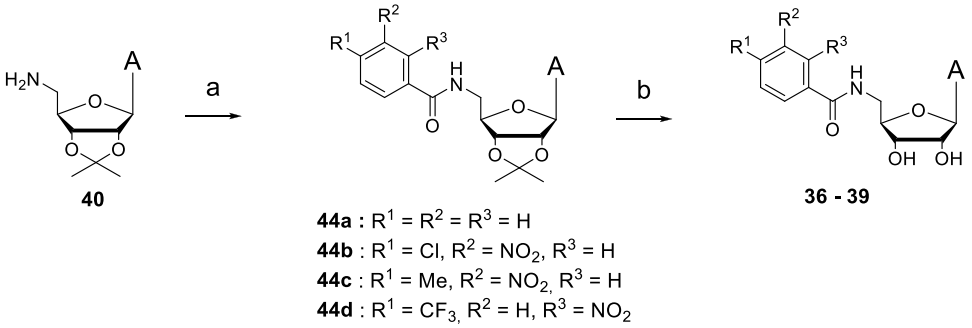

[a]Reagents and conditions: (a) appropriate carboxylic acid, EDC, DMAP, 0 °C, 2 h, 37−92%; (b) HCO_2H/H_2O 1:1 v/v, 25 °C, 62−90%.

https://doi.org/10.1021/acs.jmedchem.2c00120
J. Med. Chem. 2022, 65, 6231−6249

Table 2. Screening for Inhibitory Activity of Sinefungin and Compounds 1−39 at 5 μM on SARS-CoV-2 *N*7-MTase nsp14[a]

compound	inhibition of SARS CoV-2 nsp14 at 5 μM (%)	SARS CoV-2 nsp14 IC_{50} (μM)	compound	inhibition of SARS CoV-2 nsp14 at 5 μM (%)	SARS CoV-2 nsp14 IC_{50} (μM)
sinefungin	100	0.278 ± 0.008	**20**	80	5.3 ± 0.9
1	NI	n.d.	**21**	90	0.899 ± 0.1
2	25	14.12 ± 0.9	**22**	100	1.01 ± 0.2
3	77	n.d.	**23**	100	0.514 ± 0.05
4	21	n.d.	**24**	65	0.960 ± 0.1
5	70	1.44 ± 0.2	**25**	100	0.019 ± 0.02
6	60	3.49 ± 0.1	**26**	25	13.02 ± 0.93
7	75	2.07 ± 0.2	**27**	20	n.d.
8	NI	n.d.	**28**	87	0.482 ± 0.06
9	84	5.0 ± 1.0	**29**	90	0.344 ± 0.04
10	80	3.589 ± 0.9	**30**	65	0.442 ± 0.08
11	87	4.4 ± 0.5	**31**	100	0.100 ± 0.01
12	85	2.9 ± 0.1	**32**	95	0.056 ± 0.01
13	100	0.342 ± 0.04	**33**	100	0.114 ± 0.01
14	98	0.244 ± 0.01	**34**	100	0.080 ± 0.006
15	90	0.146 ± 0.01	**35**	100	0.030 ± 0.001
16	75	0.516 ± 0.08	**36**	NI	n.d.
17	100	0.080 ± 0.01	**37**	NI	n.d.
18	100	0.038 ± 0.002	**38**	NI	n.d.
19	100	0.044 ± 0.003	**39**	NI	n.d.

[a]Values are the mean of three independent experiments. The *N*7-MTase activity was measured using a filter-binding assay. Assays were carried out in reaction mixture [40 mM Tris-HCl (pH 8.0), 1 mM DTT, 1 mM $MgCl_2$, 2 μM SAM, and 0.1 μM ^{3}H-SAM] in the presence of 0.7 μM $GpppAC_4$ synthetic RNA and incubated at 30 °C and SARS-CoV-2 nsp14 (50 nM). Compounds were dissolved in 100% DMSO. NI: no inhibition detected at 5 μM. n.d.: IC_{50} not determined.

The next series of synthesized compounds was then evaluated only against the SARS-CoV-2 nsp14 *N*7-MTase at a fixed concentration of 5 μM. With the exception of eight compounds (**1**, **4**, **8**, **27**, **36**−**39**) that showed no or low inhibitory activity against nsp14, most of the bisubstrate nucleoside analogues displayed at least 65% inhibition. They were then tested in a dose−response assay with increasing compound concentration (Supporting Information, Figure S6), and MTase activity was measured using a filter-binding assay to determine the corresponding IC_{50} (Table 2). Among the 32 potential inhibitors, 11 compounds—**14**, **15**, **17**−**19**, **25**, **31**−**35**—displayed higher inhibitory activity than the broad-spectrum inhibitor, sinefungin (IC_{50} = 278 nM). Remarkably, seven of these compounds—**17**−**19**, **25**, **32**, **34**, **35**—exhibited high activity, with IC_{50} values between 19 and 80 nM. All these potent nsp14 inhibitors bear a similar scaffold: an *N*-alkylsulfonamide linker between adenosine and the phenyl ring that contains a substituent in the *para* position and a substituent in the *meta* position. The N-atom of the linker is substituted with either an ethyl group (R_4) in compounds **17**−**19** and **25**, **32**, an acetyl-ended butyl chain (**34**), or a phthalimide group (**35**) (Figure 2). Finally, it is worth noting that, except for compound **17**, the *para* substituents are electron-donating groups (EDGs: Me or OMe) while the *meta* substituents are rather electron-withdrawing groups (EWGs: such as NO_2, CN, or Cl). Among the seven best inhibitors **17**−**19**, **25**, **32**, **34**, **35**, the most potent one, **25**, is *para*-OMe and *meta*-CN substituted (IC_{50} = 19 nM). Further investigations on the mechanism of action showed that **25** is a SAM-competitive nsp14 inhibitor (Supporting Information, Figure S7).

Structure−Activity Relationships (SARs). As previously mentioned, we aimed to optimize the structure of nucleoside analogues by investigating the SARs upon modification of different parts of the bisubstrate molecules.

From Adenine Dinucleoside Precursors to Monoadenosine SAM Mimics. Inhibition data for compounds **2**, **3**, and **5**−**7** compared with those of **D1**−**D5** clearly indicate that removal of adenosine 2′-O-connected at the arylsulfonamide ethyl linker in **D1**−**D5** is not detrimental to the inhibitory activity of the monoadenosine compounds against the SARS-CoV *N*7-MTase nsp14 (Table 1).

Arylsulfonamide Moieties. Three *N*,*N*-dimethyl-*N*-arylsulfonamide derivatives, corresponding to the arylsulfonamide moieties of compounds **6**, **7**, and **13**, were prepared and evaluated for their potential to inhibit the SARS-CoV-2 *N*7-MTase nsp14 at 5 and 50 μM. None of them induces detectable inhibition, demonstrating the necessity of the 5′-linked nucleoside structure on the phenylsulfonamide core to achieve methylation inhibition.

2′,3′-O-Isopropylidene Adenosine. Two intermediate compounds, **41f** and **41k**, corresponding to the 2′,3′-*O*-protected precursors of **6** and **13**, display no inhibition of nsp14 at 50 μM, showing that the 2′-OH and 3′-OH of ribose may be involved in the inhibitor interactions with SARS-CoV-2 nsp14. In fact, it was previously shown that the 2′-OH and 3′-OH of ribose interact through an H-bond with Asp352 of SARS-CoV nsp14.[22]

Substituents on the Phenyl Ring. The impact of substituents on the phenyl ring was demonstrated with compounds **1** and **8** (without substituents) barely inhibiting nsp14 at 5 μM, compared to most other prepared nucleosides in which the aromatic moiety was decorated with one or two substituents and exhibited 65−100% inhibition of methylation. In addition, the positioning of the EWG seems to be directly correlated with activity, with the efficiency of the compounds increasing from the *ortho* position to the *para* position and then to the *meta* position. In the case of compounds **2** and **26**, the introduction of a nitro group or chlorine atom at the *para* position leads to moderate inhibition (IC_{50} = 14.12 and 13.02 μM, respectively), while in compounds **10** and **20**, with a nitro group or a cyano

https://doi.org/10.1021/acs.jmedchem.2c00120
J. Med. Chem. 2022, 65, 6231−6249

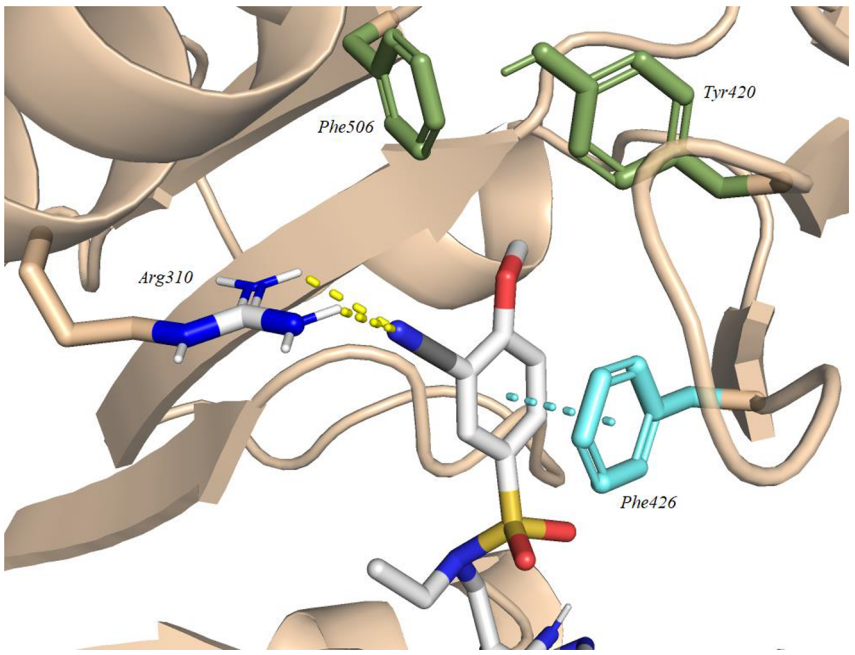

Figure 5. Modeling results of docking compound **25** with the cap-binding pocket of SARS-CoV nsp14 (PDB ID: 5C8T, resolution 3.2 Å). Contribution of the cyanobenzenesulfonamide core of **25**. Tyr420 and Phe506 (both in green), hydrogen bonds (yellow), and the $\pi-\pi$ stacking interaction (cyan) are shown.

group located at the *meta* position, the activity increases to 3.6 and 5.3 μM, respectively. Surprisingly, however, the *m*-Cl-substituted analogue **27** does not show inhibition at 5 μM. A clear improvement was observed when the phenyl ring was doubly substituted in the *para* and *meta* positions. When a *m*-NO_2 group is associated with an EWG such as Cl, F, or Br located at the *para* position in compounds **7**, **11**, and **12**, respectively, IC_{50} values are in the same micromolar range (from 2.07 to 4.4 μM). Moreover, replacement of *m*-NO_2 by *m*-CN in the *p*-F or *p*-Cl analogues **21** or **22** slightly increased the inhibitory effect (IC_{50} = 0.899 and 1.01 μM). Remarkably, the analogue **28**, doubly substituted with chlorine in *para* and *meta* positions, showed better inhibition. Of special interest, an EDG (Me, Et, OMe) in the *para* position significantly enhanced the inhibitory activity of compounds **13**−**15** and **23** (146 nM < IC_{50} < 514 nM). In conclusion, a *meta* EWG substituent (NO_2, CN or Cl) and a *para* EDG substituent (Me or OMe) on the phenyl ring appear to be the best combination to obtain nsp14 inhibitors with an IC_{50} < 0.5 μM (**13**−**15**, **23**, and **29**).

Substituents of the Nitrogen Atom of the Sulfonamide Linker. After identifying several optimal substituted aromatic rings for effective inhibition, we next studied the functionalization of the nitrogen atom in the sulfonamide linker with an ethyl group to give the *meta*-nitro compounds **17**−**19**, a *meta*-CN compound **25**, and the chlorine-containing nucleosides **31** and **32**. Compared to the *N*-H-sulfonamide linker (0.146 μM < IC_{50} < 14 μM), without any exception, the corresponding *N*-ethylsulfonamide linker confers a higher level of *N*7-MTase nsp14 inhibition, in the range of IC_{50} < 100 nM. As an example, the IC_{50} values of the *p*-Me-*m*-NO_2-*N*-Et-sulfonamide derivative **18** and the corresponding NH- derivative **13** were 38 and 342 nM, respectively. The best inhibition was observed for the *m*-CN-*p*-OMe compound **25**, with IC_{50} = 19 nM. Nevertheless, the corresponding *m*-NO_2-*p*-OMe analogue **19** and *m*-Cl-*p*-Me analogue **32** exhibited comparable high potency, with IC_{50} = 44 and 56 nM, respectively. Furthermore, the crucial N-substitution for high nsp14 inhibition was demonstrated with compounds **33**−**35** containing butyl chains with various end groups (CO_2Et, OAc, *N*-phthalimide). Complete inhibition of SARS-CoV-2 nsp14 was observed at 5 μM of **33**−**35**. Notably, nucleoside **35**, carrying the phthalimide moiety, appeared to be the best inhibitor in the series (IC_{50} = 30 nM). This result can be compared to recent work by Otava et al., who identified several compounds with a similar aromatic ring attached to the N7 position of adenine that inhibited SARS-CoV-2 nsp14 in the same low nanomolar range.[20]

Linker Modification. To support the crucial role of the sulfonamide linker in bisubstrate molecules, a series of analogues of compounds **1**, **7**, **13**, and **6** were designed with an amide linkage to give compounds **36**−**39**, respectively. One of the most striking results was the lack of inhibition of the *N*7-MTase nsp14 by the amide-linked compounds **36**−**39**, thus endorsing the sulfonamide linkage in the scaffold.

Molecular Docking Studies of SARS-CoV nsp14 in Complex with 25. In this work, molecular modeling experiments were performed both before and after the nucleoside synthesis. Before, these experiments allowed us to design the aromatic moiety combining various EWG and EDG substituents at positions suitable to strongly interact with the viral protein. To corroborate our results in the enzymatic assays, we performed computational docking studies with the most potent inhibitor **25**, using Autodock Vina.[35] The docking was based on the structure of the SARS-CoV nsp14-nsp10 complex solved in the presence of SAM (PDB ID: 5C8T).[22] Compound **25** was modeled in the SAM- and cap-binding pockets of the SARS-CoV nsp14 structure, which shares 95% identity in the sequence with SARS-CoV-2 nsp14. At first sight, nucleoside **25** perfectly overlays with the adenosine of the SAM-bound structure (Supporting Information, Figure S8). As with previous dinucleoside bisubstrates,[21] the benzenesulfonamide ring interacts with Phe426 through $\pi-\pi$ stacking interactions (d = 3.6 Å) (Figure 5). Formation of a double hydrogen-bond

https://doi.org/10.1021/acs.jmedchem.2c00120
J. Med. Chem. 2022, 65, 6231−6249

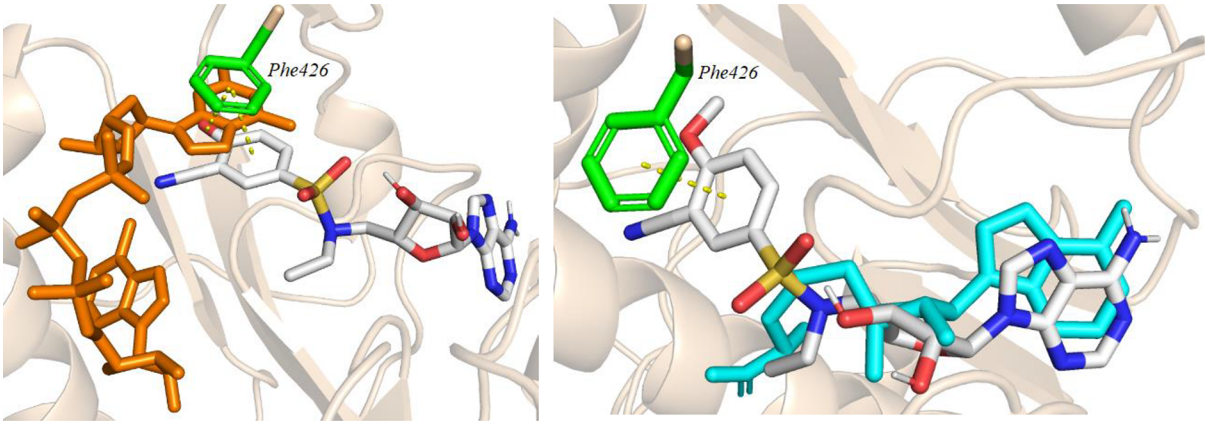

Figure 6. Modeling results in the cap-binding (left) and SAM/SAH-binding pocket (right) of SARS-CoV nsp14 (PDB ID: 5C8S, resolution 3.3 Å) with **25**. GpppA and SAH are shown in orange and cyan, respectively. Phe426 is shown in green. $\pi-\pi$ stacking interactions (yellow) are shown.

interaction was observed between the cyano group and Arg310 (d = 2.5, 2.6 Å), which normally interacts with the second phosphate group of the triphosphate bond in the cap structure, also equivalent to what had been observed with dinucleosides bearing a nitro group in the *meta* position. Specifically for compound **25**, a π−alkyl interaction occurs between the CH_3 of the OMe group and two aromatic residues, Tyr420 and Phe506, that naturally hold the purine portion of guanosine in the cap structure.[22]

To support the hypothesis of a bisubstrate mechanism, we also performed docking studies with **25** and the structure of the SARS-CoV nsp14-nsp10 complex in the presence of SAH and GpppA. Here, we show that the 3-cyano-4-methoxybenzene-sulfonamide ring of compound **25** clearly occupies the cap-guanosine binding pocket surrounded by Phe401, Tyr420, Phe426, Thr428, and Phe506 residues, while the overlay with SAH is correct (Figure 6).

Thermal Shift Assays for SARS-CoV-2 nsp14. To further confirm the direct interaction between compounds **25**, **32**, and **35** and the *N*7-MTase nsp14, we performed thermal shift assays (TSAs) (Supporting Information, Figure S9). We observed a significant shift in melting temperature (T_m) of nsp14 with high concentrations of the compounds (>2 μM). Data in Table S1 (Supporting Information) show that the ΔT_m of approximately +11 °C at 0.5 mM **25**, **32**, and **35** indicates remarkable stabilization of nsp14 with these three inhibitors. Dose−response curves showing the T_m's of **25**, **32**, and **35** as a function of each compound's concentration indicate that these three inhibitors increased the stability of the protein more efficiently than the pan-inhibitor sinefungin or the natural co-substrate SAM (Supporting Information, Figure S9). This suggests that these bisubstrates have potent interactions with the nsp14 protein, leading to a substantial inhibition (19 nM < IC_{50} < 56 nM). Moreover, it is noteworthy that all three nucleoside analogues increased the stability of nsp14 more effectively at 0.5 mM than the dinucleoside **D5** that was used at 1 mM in the previous study (T_m shift was 10.8 °C).[21] Comparing the structures of the newly designed compounds with **D5**, this demonstrates that the second adenosine in **D5** is not required in the structure of the sulfonamide-containing bisubstrates to interact with SARS-CoV-2 nsp14 effectively.

Dose−Response Testing of Compound 25 against SARS-CoV-2 nsp14 and Other MTases. To support the observed inhibition of compound **25** against SARS-CoV-2 nsp14, we also tested the compound in a dose−response assay. After pre-incubation of nsp14 with increasing concentrations of **25**, MTase activity was measured by a filter-binding assay (FBA). The IC_{50} of compound **25**, deduced from the Hill slope equation (Y = 100/[1 + ((X/IC_{50})^Hillslope)]) curve-fitting, was 11.81 ± 1.80 nM, confirming its inhibitory activity in the low nanomolar range (Figure 7). In addition, we evaluated the

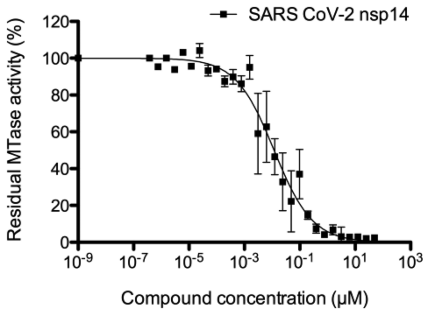

Figure 7. IC_{50} curve monitored by FBA. Increasing concentrations of compound **25** were incubated with 50 nM SARS-CoV-2 nsp14 in the reaction mixture [40 mM Tris-HCl (pH 8.0), 1 mM DTT, 1 mM $MgCl_2$, 2 μM SAM, and 0.1 μM ^{3}H-SAM (Perkin Elmer)] in the presence of 0.7 μM $GpppAC_4$ synthetic RNA. Reactions were incubated at 30 °C during 30 min, and the enzymatic activity was determined by FBA. Values were normalized and fitted with Prism (GraphPad) using the following equation: Y = 100/[1 + ((X/IC_{50})^Hillslope)] (n = 3; mean value ± SD).

inhibition of compound **25** in the presence of other viral *N*7- and 2′-*O*-MTases: *N*7-MTase from vaccinia virus (D1/D12 complex) and 2′-*O*-MTases from Dengue virus (NS5 MTase), vaccinia virus (VP39), and SARS-CoV-2 (nsp10/nsp16 complex). The dose−response assay showed no inhibition of these enzymes by compound **25** up to 50 μM (Supporting Information, Figure S10). Moreover, human RNA *N*7-MTase (hRNMT), which exhibit N7 activity, was also tested in a dose−response assay. The results showed some inhibition of *N*7-MTase activity at a high concentration (50 μM), IC_{50} = 52.8 ± 8.31 μM. Compound **25** specifically inhibits SARS-CoV-2 *N*7-MTase nsp14 with a high selectivity of ∼2000-fold, in comparison with dinucleoside **D5**, which showed a selectivity of 413-fold.[21] This evidences that compound **25** has high specificity to target SARS-CoV-2 *N*7-MTase nsp14.

https://doi.org/10.1021/acs.jmedchem.2c00120
J. Med. Chem. 2022, 65, 6231−6249

CONCLUSIONS

Using a rational structure-guided design consistent with a bisubstrate strategy targeting the SARS-CoV-2 *N*7-MTase nsp14, we designed and synthesized 39 SAM-derived compounds with a similar scaffold containing a 5′-aminoadenosine linked to a disubstituted phenyl ring through either a sulfonamide linker or an amide linker. In a biochemical assay, seven out of the 39 compounds tested were found to strongly inhibit *N*7-MTase nsp14, with IC_{50} values ranging from 19 to 80 nM. The three most potent inhibitors, **25**, **32**, and **35**, are high-affinity ligands for nsp14, as judged by TSA. Compound **25** is selective for the *N*7-MTase nsp14 over other viral *N*7- or 2′-*O*-MTases and, interestingly, over human *N*7-MTase (SI > 2000). SAR studies consistent with our modeling results reveal an effective bisubstrate structure: adenosine (occupying SAM-binding site) linked to a *p*-EDG-*m*-EWG-substituted phenyl group (occupying the cap RNA substrate binding site) through an *N*-ethylsulfonamide motif. These promising results pave the way to develop new *N*-arylsulfonamide-containing bisubstrate SAM analogues. Indeed, based on docking studies, our particular scaffold interacts with two key conserved residues—Arg310 and Phe426 in SARS-CoV nsp14—of the catalytic pocket that have been identified as critical for *N*7-MTase nsp14 activity and consequently for SARS-CoV-2 replication.[9] Our results strengthen the emerging status of this enzyme as a valid target for antiviral rational-designed inhibitors. Further optimizations are underway to increase the cellular permeability of this series of potent nsp14 inhibitors with physicochemical properties tailored for cellular activity, which will enable the characterization of their mode of action.

EXPERIMENTAL SECTION

Chemistry General Procedures. All dry solvents and reagents were purchased from commercial suppliers and were used without further purification. DIEA was distilled over calcium hydride. Thin-layer chromatography (TLC) analyses were carried out on silica plate 60 F_{254}. Purifications by column chromatography were performed using Biotage Isolera 1 system with FlashPure cartridges (Buchi). NMR experiments were recorded on Bruker 400, 500, or 600 MHz spectrometers at 20 °C. HRMS analyses were obtained with electrospray ionization (ESI) in positive mode on a Q-TOF Micromass spectrometer. Analytical HPLC was performed on a UHPLC Thermoscientific Ultimate 3000 system equipped with a LPG-3400RS pump, a DAD 3000 detector, and a WPS-3000TBRS autosampler, Column Oven TCC-3000SD. Compounds were analyzed by RP-HPLC on a Column Nucleodur C_{18} ec 100-3, 4.6 × 75 mm (Macherey Nagel) at 30 °C. The following HPLC solvent systems were used: 1% CH_3CN in 12.5 mM TEAAc (buffer A), 80% CH_3CN in 12.5 mM TEEAc (buffer B). Flow rate was 1 mL/min. UV detection was performed at 260 nm. Solid compounds **1**−**39** were stored at −20 °C for several months without any degradation. Compounds **1**−**32** were analyzed by HPLC and are >95% pure.

General Procedure A for the Synthesis of Compounds 41a, 41d, 41h−**l, 41n**−**p, and 41r**−**u.** To a solution at 0 °C under argon of 5′-deoxy-5′-amino-2′,3′-isopropylideneadenosine **40** (1.00 equiv) in anhydrous DMF (*C* = 0.05 M) were added Et_3N (2.00 equiv) and the corresponding benzenesulfonyl chloride reactant (1.25 equiv) in three portions. After stirring at 0 °C (−10 °C for **41i**) for 1.5−3 h, the reaction mixture was diluted with AcOEt and brine. The aqueous layer was extracted with AcOEt and the combined organic extracts were washed with brine, dried over Na_2SO_4, and concentrated under vacuum. The residue was purified by flash column chromatography (dry sample, silica gel, linear gradient 0−4% MeOH in CH_2Cl_2) to give desired compounds as colorless solids.

*N-{[(4R,6R)-6-(6-amino-9H-purin-9-yl)-2,2-dimethyl-tetrahydro-2H-furo[3,4-d][1,3]dioxol-4-yl]methyl}benzenesulfonamide (**41a**).* Following method A with **40** (300 mg, 0.98 mmol, 1.00 equiv) and benzenesulfonyl chloride, **41a** (280 mg, 76%) was obtained as a white solid. R_f = 0.51 (1:9 MeOH/CH_2Cl_2). ^{1}H NMR (600 MHz, DMSO-d_6): δ 8.29 (s, 1H), 8.21 (t, *J* = 5.9 Hz, 1H), 8.14 (s, 1H), 7.75−7.70 (m, 2H), 7.63−7.57 (m, 1H), 7.54 (dd, *J* = 8.3, 6.9 Hz, 2H), 7.39 (br s, 2H), 6.11 (d, *J* = 3.0 Hz, 1H), 5.34 (dd, *J* = 6.3, 3.0 Hz, 1H), 4.89 (dd, *J* = 6.3, 2.9 Hz, 1H), 4.18 (td, *J* = 5.7, 2.9 Hz, 1H), 3.15−2.97 (m, 2H), 1.52 (s, 3H), 1.28 (s, 3H). ^{13}C NMR (150 MHz, DMSO-d_6): δ 156.3, 152.5, 148.4, 140.2, 140.2, 132.4, 129.2, 126.3, 119.3, 113.4, 89.6, 84.2, 82.8, 81.6, 44.5, 27.0, 25.1. HRMS (ESI+): *m*/*z* calculated for $C_{19}H_{23}N_6O_5S$ $[M+H]^+$: 447.1445, found 447.1446.

*N-{[(4R,6R)-6-(6-amino-9H-purin-9-yl)-2,2-dimethyl-tetrahydro-2H-furo[3,4-d][1,3]dioxol-4-yl]methyl}-4-nitrobenzene-1-sulfonamide (**41b**).* See ref 21.

*N-{[(4R,6R)-6-(6-amino-9H-purin-9-yl)-2,2-dimethyl-tetrahydro-2H-furo[3,4-d][1,3]dioxol-4-yl]methyl}-2-methoxy-4-nitrobenzene-1-sulfonamide (**41c**).* See ref 21.

*N-{[(4R,6R)-6-(6-amino-9H-purin-9-yl)-2,2-dimethyl-tetrahydro-2H-furo[3,4-d][1,3]dioxol-4-yl]methyl}-2-chloro-4-nitrobenzene-1-sulfonamide (**41d**).* Following method A with **40** (300 mg, 0.98 mmol, 1.00 equiv) and 2-chloro-4-nitrobenzenesulfonyl chloride, **41d** (270 mg, 52%) was obtained as a white solid. R_f = 0.51 (1:9 MeOH/CH_2Cl_2). ^{1}H NMR (600 MHz, DMSO-d_6): δ 8.74 (br s, 1H), 8.32 (d, *J* = 2.2 Hz, 1H), 8.19 (s, 1H), 8.12 (s, 1H), 8.04 (dd, *J* = 8.7, 2.3 Hz, 1H), 7.92 (d, *J* = 8.7 Hz, 1H), 7.35 (br s, 2H), 6.03 (d, *J* = 2.8 Hz, 1H), 5.31 (dd, *J* = 6.3, 2.8 Hz, 1H) 4.91 (dd, *J* = 6.4, 3.1 Hz, 1H), 4.17 (ddd, *J* = 6.7, 5.2, 3.1 Hz, 1H), 3.36−3.26 (m, 2H), 1.^{49} (s, 3H), 1.27 (s, 3H). ^{13}C NMR (150 MHz, DMSO-d_6): δ 156.2, 152.6, 149.3, 148.2, 143.2, 140.1, 131.9, 131.1, 126.2, 122.1, 119.2, 113.4, 89.3, 84.6, 83.0, 81.5, 44.7, 26.9, 25.0. HRMS (ESI+): *m*/*z* calculated for $C_{19}H_{21}ClN_7O_7S$ $[M+H]^+$: 526.0906, found 526.0901.

*N-{[(4R,6R)-6-(6-amino-9H-purin-9-yl)-2,2-dimethyl-tetrahydro-2H-furo[3,4-d][1,3]dioxol-4-yl]methyl}-4-methoxy-2-nitrobenzene-1-sulfonamide (**41e**).* See ref 21.

*N-{[(4R,6R)-6-(6-amino-9H-purin-9-yl)-2,2-dimethyl-tetrahydro-2H-furo[3,4-d][1,3]dioxol-4-yl]methyl}-2-nitro-4-(trifluoromethyl)-benzene-1-sulfonamide (**41f**).* See ref 21.

*N-{[(4R,6R)-6-(6-amino-9H-purin-9-yl)-2,2-dimethyl-tetrahydro-2H-furo[3,4-d][1,3]dioxol-4-yl]methyl}-4-chloro-3-nitrobenzene-1-sulfonamide (**41g**).* See ref 21.

*N-{[(4R,6R)-6-(6-amino-9H-purin-9-yl)-2,2-dimethyl-tetrahydro-2H-furo[3,4-d][1,3]dioxol-4-yl]methyl}-3-nitrobenzene-1-sulfonamide (**41h**).* Following method A with **40** (300 mg, 0.98 mmol, 1.00 equiv) and 3-nitrobenzenesulfonyl chloride, **41h** (330 mg, 69%) was obtained as a white solid. R_f = 0.47 (1:9 MeOH/CH_2Cl_2). ^{1}H NMR (500 MHz, DMSO-d_6): δ 8.50 (br s, 1H), 8.44 (t, *J* = 2.0 Hz, 1H), 8.42−8.35 (m, 1H), 8.25 (s, 1H), 8.13−8.06 (m, 2H), 7.78 (t, *J* = 8.0 Hz, 1H), 7.36 (br s, 2H), 6.10 (d, *J* = 2.7 Hz, 1H), 5.33 (dd, *J* = 6.3, 2.8 Hz, 1H), 4.91 (dd, *J* = 6.3, 3.1 Hz, 1H), 4.16 (td, *J* = 6.0, 3.1 Hz, 1H), 3.25−3.06 (m, 2H), 1.50 (s, 3H), 1.28 (s, 3H). ^{13}C NMR (125 MHz, DMSO-d_6): δ 156.2, 152.5, 148.4, 147.8, 142.0, 140.1, 132.4, 131.1, 126.9, 121.3, 119.3, 113.5, 89.3, 84.3, 82.9, 81.6, 44.5, 26.9, 25.1. HRMS (ESI+): *m*/*z* calculated for $C_{19}H_{22}N_7O_7S$ $[M+H]^+$: 492.1301, found 492.1308.

*N-{[(4R,6R)-6-(6-amino-9H-purin-9-yl)-2,2-dimethyl-tetrahydro-2H-furo[3,4-d][1,3]dioxol-4-yl]methyl}-4-fluoro-3-nitrobenzene-1-sulfonamide (**41i**).* Following method A with **40** (300 mg, 0.98 mmol, 1.00 equiv) and 4-fluoro-3-nitrobenzenesulfonyl chloride, **41i** (119 mg, 24%) was obtained as a pale yellow solid. R_f = 0.45 (8:92 MeOH/CH_2Cl_2). ^{1}H NMR (500 MHz, DMSO-d_6): δ 8.52 (t, *J* = 5.7 Hz, 1H), 8.40 (dd, *J* = 7.0, 2.4 Hz, 1H), 8.26 (s, 1H), 8.11 (s, 1H), 8.06 (ddd, *J* = 8.7, 3.9, 2.4 Hz, 1H), 7.69 (dd, *J* = 10.9, 8.8 Hz, 1H), 7.40 (br s, 2H), 6.11 (d, *J* = 2.8 Hz, 1H), 5.34 (dd, *J* = 6.3, 2.8 Hz, 1H), 4.91 (dd, *J* = 6.3, 3.1 Hz, 1H), 4.16 (td, *J* = 6.0, 3.1 Hz, 1H), 3.27−3.07 (m, 2H), 1.51 (s, 3H), 1.28 (s, 3H). ^{13}C NMR (125 MHz, DMSO-d_6): δ 157.7, 155.6, 156.2, 152.6, 148.4, 140.1, 137.3, 137.3, 136.8, 136.7, 134.2, 134.1, 125.0, 120.0, 119.9, 119.3, 113.5, 89.3, 84.3, 83.0, 81.6, 44.5, 27.0, 25.1. ^{19}F NMR (378 MHz, DMSO-d_6): δ −112.3. HRMS (ESI+): *m*/*z* calculated for $C_{19}H_{21}FN_7O_7S$ $[M+H]^+$: 510.1207, found 510.1212.

*N-{[(4R,6R)-6-(6-amino-9H-purin-9-yl)-2,2-dimethyl-tetrahydro-2H-furo[3,4-d][1,3]dioxol-4-yl]methyl}-4-bromo-3-nitrobenzene-1-sulfonamide (**41j**).* Following method A with **40** (300 mg, 0.98 mmol,

https://doi.org/10.1021/acs.jmedchem.2c00120
J. Med. Chem. 2022, 65, 6231−6249

1.00 equiv) and 4-bromo-3-nitrobenzenesulfonyl chloride, **41j** (294 mg, 53%) was obtained as a white solid. R_f = 0.50 (8:92 MeOH/CH_2Cl_2). ^{1}H NMR (500 MHz, DMSO-d_6): δ 8.59 (t, J = 5.8 Hz, 1H), 8.34 (d, J = 2.2 Hz, 1H), 8.28 (s, 1H), 8.13 (s, 1H), 8.06 (d, J = 8.4, 1H), 7.85 (dd, J = 8.4, 2.2 Hz, 1H), 7.42 (br s, 2H), 6.11 (d, J = 2.9 Hz, 1H), 5.33 (dd, J = 6.4, 2.9 Hz, 1H), 4.87 (dd, J = 6.3, 3.1 Hz, 1H), 4.15 (td, J = 5.9, 3.0 Hz, 1H), 3.29−3.11 (m, 2H), 1.50 (s, 3H), 1.27 (s, 3H). ^{13}C NMR (125 MHz, DMSO-d_6): δ 156.2, 152.6, 149.5, 148.4, 141.2, 140.1, 136.1, 130.9, 123.7, 119.5, 118.0, 113.5, 89.3, 84.2, 82.9, 81.5, 44.5, 27.0, 25.1. HRMS (ESI+): m/z calculated for $C_{19}H_{21}BrN_7O_7S$ $[M+H]^+$: 570.0401, found 570.0405.

*N-{[(4R,6R)-6-(6-amino-9H-purin-9-yl)-2,2-dimethyl-tetrahydro-2H-furo[3,4-d][1,3]dioxol-4-yl]methyl}-4-methyl-3-nitrobenzene-1-sulfonamide (**41k**).* Following method A with **40** (280 mg, 0.92 mmol, 1.00 equiv) and 4-methyl-3-nitrobenzenesulfonyl chloride, **41k** (235 mg, 51%) was obtained as a beige solid. R_f = 0.50 (8:92 MeOH/CH_2Cl_2). ^{1}H NMR (600 MHz, DMSO-d_6): δ 8.40 (br s, 1H), 8.26 (d, J = 1.9 Hz, 1H), 8.25 (s, 1H), 8.11 (s, 1H), 7.87 (dd, J = 8.2, 2.0 Hz, 1H), 7.60 (dd, J = 8.2, 0.8 Hz, 1H), 7.36 (br s, 2H), 6.09 (d, J = 2.9 Hz, 1H), 5.32 (dd, J = 6.2, 2.9 Hz, 1H), 4.89 (dd, J = 6.3, 3.1 Hz, 1H), 4.16 (ddd, J = 6.4, 5.4, 3.0 Hz, 1H), 3.24−3.09 (m, 2H), 2.55 (s, 3H), 1.51 (s, 3H), 1.27 (s, 3H). ^{13}C NMR (150 MHz, DMSO-d_6): δ 156.2, 152.5, 148.5, 148.4, 140.1, 139.4, 137.6, 133.9, 130.4, 122.6, 119.3, 113.5, 89.3, 84.2, 82.9, 81.5, 44.5, 26.9, 25.1, 19.7. HRMS (ESI+): m/z calculated for $C_{20}H_{24}N_7O_7S$ $[M+H]^+$: 506.1452, found 506.1451.

*N-{[(4R,6R)-6-(6-amino-9H-purin-9-yl)-2,2-dimethyl-tetrahydro-2H-furo[3,4-d][1,3]dioxol-4-yl]methyl}-4-ethyl-3-nitrobenzene-1-sulfonamide (**41l**).* Following method A with **40** (213 mg, 0.70 mmol, 1.00 equiv) and 4-ethyl-3-nitrobenzenesulfonyl chloride, **41l** (183 mg, 51%) was obtained as a white solid. R_f = 0.53 (8:92 MeOH/CH_2Cl_2). ^{1}H NMR (500 MHz, DMSO-d_6): δ 8.46 (br s, 1H), 8.27 (s, 1H), 8.22 (d, J = 1.9 Hz, 1H), 8.11 (s, 1H), 7.91 (dd, J = 8.1, 2.0 Hz, 1H), 7.65 (d, J = 8.2, 1H), 7.41 (br s, 2H), 6.10 (d, J = 2.9 Hz, 1H), 5.32 (dd, J = 6.3, 2.9 Hz, 1H), 4.89 (dd, J = 6.3, 3.0 Hz, 1H), 4.16 (td, J = 5.8, 3.0 Hz, 1H), 3.25−3.09 (m, 2H), 2.85 (q, J = 7.5 Hz, 2H), 1.50 (s, 3H), 1.27 (s, 3H), 1.20 (t, J = 7.5 Hz, 3H). ^{13}C NMR (125 MHz, DMSO-d_6): δ 156.2, 152.6, 148.6, 148.3, 142.5, 140.2, 139.4, 132.6, 130.5, 122.6, 119.3, 113.5, 89.4, 84.3, 82.9, 81.6, 44.5, 27.0, 25.3, 25.1, 14.5. HRMS (ESI+): m/z calculated for $C_{21}H_{26}N_7O_7S$ $[M+H]^+$: 520.1609, found 520.1611.

*N-{[(4R,6R)-6-(6-amino-9H-purin-9-yl)-2,2-dimethyl-tetrahydro-2H-furo[3,4-d][1,3]dioxol-4-yl]methyl}-4-methoxy-3-nitrobenzene-1-sulfonamide (**41m**).* To a suspension of **41g** (800 mg, 1.52 mmol, 1.00 equiv) in MeOH (6.6 mL) was added sodium methoxide (15 mL, 0.5 M solution in MeOH). The reaction mixture was stirred at 50 °C for 48 h. After cooling to room temperature, the reaction mixture was diluted with AcOEt and washed with saturated NH_4Cl aqueous solution. The aqueous layer was extracted with AcOEt and the combined organic extracts were washed with brine, dried over Na_2SO_4 and concentrated under vacuum. The residue was purified by flash column chromatography (dry sample, silica gel, linear gradient 0−6% MeOH in CH_2Cl_2) to give **41m** as a white solid (640 mg, 80%). R_f = 0.41 (8:92 MeOH/CH_2Cl_2). ^{1}H NMR (600 MHz, DMSO-d_6): δ 8.29 (t, J = 6.2 Hz, 1H), 8.27 (s, 1H), 8.21 (d, J = 2.3 Hz, 1H), 8.13 (s, 1H), 7.92 (dd, J = 9.0, 2.3 Hz, 1H), 7.45 (d, J = 9.0, 1H), 7.37 (br s, 2H), 6.11 (d, J = 2.9 Hz, 1H), 5.34 (dd, J = 6.3, 2.9 Hz, 1H), 4.90 (dd, J = 6.3, 3.0 Hz, 1H), 4.17 (td, J = 5.9, 3.0 Hz, 1H), 3.99 (s, 3H), 3.21−3.06 (m, 2H), 1.51 (s, 3H), 1.28 (s, 3H). ^{13}C NMR (150 MHz, DMSO-d_6): δ 156.2, 154.7, 152.5, 148.4, 140.1, 138.5, 132.4, 132.0, 123.8, 119.3, 115.1, 113.5, 89.4, 84.2, 82.9, 81.5, 57.3, 44.4, 26.9, 25.1. HRMS (ESI+): m/z calculated for $C_{20}H_{24}N_7O_8S$ $[M+H]^+$: 522.1402, found 522.1399.

*N-{[(4R,6R)-6-(6-amino-9H-purin-9-yl)-2,2-dimethyl-tetrahydro-2H-furo[3,4-d][1,3]dioxol-4-yl]methyl}-3-cyanobenzene-1-sulfonamide (**41n**).* Following method A with **40** (300 mg, 0.98 mmol, 1.00 equiv) and 3-cyanobenzenesulfonyl chloride, **41n** (360 mg, 78%) was obtained as a white solid. R_f = 0.72 (1:9 MeOH/CH_2Cl_2). ^{1}H NMR (500 MHz, DMSO-d_6): δ 8.40 (br s, 1H), 8.27 (s, 1H), 8.17−8.09 (m, 2H), 8.05 (dt, J = 7.8, 1.4 Hz, 1H), 7.99 (dt, J = 8.3, 1.3 Hz, 1H), 7.71 (t, J = 7.9 Hz, 1H), 7.38 (br s, 2H), 6.11 (d, J = 2.9 Hz, 1H), 5.34 (dd, J = 6.3, 2.9 Hz, 1H), 4.89 (dd, J = 6.3, 3.0 Hz, 1H), 4.16 (td, J = 5.9, 3.0 Hz, 1H), 3.25−3.05 (m, 2H), 1.51 (s, 3H), 1.28 (s, 3H). ^{13}C NMR (125 MHz, DMSO-d_6): δ 156.2, 152.6, 148.4, 141.7, 140.1, 135.9, 130.8, 130.6, 130.0, 119.3, 117.5, 113.5, 112.4, 89.4, 84.3, 82.9, 81.6, 44.5, 27.0, 25.1. HRMS (ESI+): m/z calculated for $C_{20}H_{22}N_7O_5S$ $[M+H]^+$: 472.1403, found 472.1409.

*N-{[(4R,6R)-6-(6-amino-9H-purin-9-yl)-2,2-dimethyl-tetrahydro-2H-furo[3,4-d][1,3]dioxol-4-yl]methyl}-3-cyano-4-fluorobenzene-1-sulfonamide (**41o**).* Following method A with **40** (300 mg, 0.98 mmol, 1.00 equiv) and 3-cyano-4-fluorobenzenesulfonyl chloride, **41o** (360 mg, 75%) was obtained as a white solid. R_f = 0.49 (1:9 MeOH/CH_2Cl_2). ^{1}H NMR (600 MHz, DMSO-d_6): δ 8.40 (br s, 1H), 8.27 (s, 1H) 8.25 (dd, J = 5.9, 2.4 Hz, 1H), 8.13 (s, 1H), 8.04 (ddd, J = 8.9, 4.9, 2.4 Hz, 1H), 7.62 (t, J = 8.9 Hz, 1H), 7.38 (br s, 2H), 6.11 (d, J = 2.9 Hz, 1H), 5.34 (dd, J = 6.3, 2.8 Hz, 1H), 4.89 (dd, J = 6.3, 3.1 Hz, 1H), 4.16 (td, J = 6.0, 3.1 Hz, 1H), 3.24−3.10 (m, 2H), 1.52 (s, 3H), 1.29 (s, 3H). ^{13}C NMR (150 MHz, DMSO-d_6): δ 165.0, 163.3, 156.2, 152.6, 148.4, 140.1, 137.9, 134.2, 134.1, 132.6, 119.3, 117.8, 117.7, 113.5, 112.8, 101.4, 101.3, 89.3, 84.3, 82.9, 81.5, 44.5, 27.0, 25.1. HRMS (ESI+): m/z calculated for $C_{20}H_{21}FN_7O_5S$ $[M+H]^+$: 490.1303, found 490.1302.

*N-{[(4R,6R)-6-(6-amino-9H-purin-9-yl)-2,2-dimethyl-tetrahydro-2H-furo[3,4-d][1,3]dioxol-4-yl]methyl}-4-chloro-3-cyanobenzene-1-sulfonamide (**41p**).* Following method A with **40** (300 mg, 0.98 mmol, 1.00 equiv) and 4-chloro-3-cyanobenzenesulfonyl chloride, **41p** (400 mg, 81%) was obtained as a white solid. R_f = 0.60 (1:9 MeOH/CH_2Cl_2). ^{1}H NMR (600 MHz, DMSO-d_6): δ 8.46 (br s, 1H), 8.27 (s, 1H), 8.25 (d, J = 2.1 Hz, 1H), 8.13 (s, 1H), 7.96 (dd, J = 8.6, 2.3 Hz, 1H), 7.85 (d, J = 8.6 Hz, 1H), 7.38 (br s, 2H), 6.11 (d, J = 2.9 Hz, 1H), 5.33 (dd, J = 6.3, 2.9 Hz, 1H), 4.87 (dd, J = 6.3, 3.0 Hz, 1H), 4.15 (td, J = 6.0, 3.1 Hz, 1H), 3.25−3.13 (m, 2H), 1.51 (s, 3H), 1.28 (s, 3H). ^{13}C NMR (150 MHz, DMSO-d_6): δ 156.2, 152.6, 148.4, 140.3, 140.1, 139.4, 132.4, 132.3, 131.0, 119.3, 114.9, 113.5, 113.1, 89.3, 84.3, 82.9, 81.5, 44.4, 27.0, 25.1. HRMS (ESI+): m/z calculated for $C_{20}H_{21}ClN_7O_5S$ $[M+H]^+$: 506.1008, found 506.1011.

*N-{[(4R,6R)-6-(6-amino-9H-purin-9-yl)-2,2-dimethyl-tetrahydro-2H-furo[3,4-d][1,3]dioxol-4-yl]methyl}-3-cyano-4-methoxybenzene-1-sulfonamide (**41q**).* To a suspension of **41o** (150 mg, 0.31 mmol, 1.00 equiv) in MeOH (1.5 mL) was added sodium methoxide (3 mL, 0.5 M solution in MeOH). The reaction mixture was stirred at 50 °C for 48 h. After cooling to room temperature, the reaction mixture was diluted with AcOEt and washed with saturated NH_4Cl aqueous solution. The aqueous layer was extracted with AcOEt and the combined organic extracts were washed with brine, dried over Na_2SO_4 and concentrated under vacuum. The residue was purified by flash column chromatography (dry sample, silica gel, linear gradient 0−6% MeOH in CH_2Cl_2) to give **41q** as a white solid (150 mg, 98%). R_f = 0.48 (9:1 AcOEt/MeOH). ^{1}H NMR (600 MHz, DMSO-d_6): δ 8.27 (s, 1H), 8.21 (dd, J = 6.6, 5.4 Hz, 1H), 8.13 (s, 1H), 8.04 (d, J = 2.4 Hz, 1H), 7.92 (dd, J = 9.0, 2.4 Hz, 1H), 7.38 (br s, 2H), 7.33 (d, J = 9.0 Hz, 1H), 6.11 (d, J = 2.9 Hz, 1H), 5.33 (dd, J = 6.4, 2.9 Hz, 1H), 4.89 (dd, J = 6.4, 3.0 Hz, 1H), 4.16 (td, J = 5.9, 3.1 Hz, 1H), 3.98 (s, 3H), 3.18−3.04 (m, 2H), 1.52 (s, 3H), 1.28 (s, 3H). ^{13}C NMR (150 MHz, DMSO-d_6): δ 163.3, 156.2, 152.6, 148.4, 140.1, 133.3, 132.8, 132.3, 119.3, 115.1, 113.5, 112.9, 100.9, 89.4, 84.3, 82.9, 81.6, 57.1, 44.4, 27.0, 25.1. HRMS (ESI+): m/z calculated for $C_{21}H_{24}N_7O_6S$ $[M+H]^+$: 502.1503, found 502.1503.

*N-{[(4R,6R)-6-(6-amino-9H-purin-9-yl)-2,2-dimethyl-tetrahydro-2H-furo[3,4-d][1,3]dioxol-4-yl]methyl}-4-chlorobenzene-1-sulfonamide (**41r**).* Following method A with **40** (200 mg, 0.65 mmol, 1.00 equiv) and 4-chlorobenzenesulfonyl chloride, **41r** (157 mg, 50%) was obtained as a white solid. R_f = 0.49 (1:9 MeOH/CH_2Cl_2). ^{1}H NMR (600 MHz, DMSO-d_6): δ 8.31 (t, J = 5.3 Hz, 1H), 8.28 (s, 1H), 8.14 (s, 1H), 7.75−7.69 (m, 2H), 7.63−7.55 (m, 2H), 7.38 (br s, 2H), 6.10 (d, J = 3.0 Hz, 1H), 5.33 (dd, J = 6.2, 3.0 Hz, 1H), 4.86 (dd, J = 6.3, 2.9 Hz, 1H), 4.16 (td, J = 5.8, 3.0 Hz, 1H), 3.17−3.01 (m, 2H), 1.51 (s, 3H), 1.28 (s, 3H). ^{13}C NMR (150 MHz, DMSO-d_6): δ 156.2, 152.6, 148.4, 140.1, 139.2, 137.3, 129.3, 128.3, 119.3, 113.5, 89.5, 84.2, 82.8, 81.6, 44.5, 27.0, 25.1. HRMS (ESI+): m/z calculated for $C_{19}H_{22}ClN_6O_5S$ $[M+H]^+$: 481.1055, found 481.1062.

N-{[(4R,6R)-6-(6-amino-9H-purin-9-yl)-2,2-dimethyl-tetrahydro-2H-furo[3,4-d][1,3]dioxol-4-yl]methyl}-3-chlorobenzene-1-sulfon-

https://doi.org/10.1021/acs.jmedchem.2c00120
J. Med. Chem. 2022, 65, 6231−6249

*amide (**41s**).* Following method A with **40** (300 mg, 0.98 mmol, 1.00 equiv) and 3-chlorobenzenesulfonyl chloride, **41s** (154 mg, 33%) was obtained as a white solid. R_f = 0.50 (1:9 MeOH/CH_2Cl_2). ^{1}H NMR (600 MHz, DMSO-d_6): δ 8.32 (s, 1H), 8.28 (s, 1H), 8.14 (s, 1H), 7.73 (t, J = 1.9 Hz, 1H), 7.70−7.65 (m, 2H), 7.56 (t, J = 7.9 Hz, 1H), 7.38 (br s, 2H), 6.12 (d, J = 2.9 Hz, 1H), 5.34 (dd, J = 6.3, 2.9 Hz, 1H), 4.90 (dd, J = 6.4, 3.0 Hz, 1H), 4.16 (td, J = 5.8, 3.0 Hz, 1H), 3.20−3.04 (m, 2H), 1.52 (s, 3H), 1.29 (s, 3H). ^{13}C NMR (150 MHz, DMSO-d_6): δ 156.2, 152.5, 148.4, 142.2, 140.1, 133.8, 132.4, 131.2, 126.0, 125.1, 119.3, 113.5, 89.4, 84.3, 82.9, 81.6, 44.5, 26.9, 25.1. HRMS (ESI+): m/z calculated for $C_{19}H_{22}ClN_6O_5S$ $[M+H]^+$: 481.1055, found 481.1047.

*N-{[(4R,6R)-6-(6-amino-9H-purin-9-yl)-2,2-dimethyl-tetrahydro-2H-furo[3,4-d][1,3]dioxol-4-yl]methyl}-3,4-dichlorobenzene-1-sulfonamide (**41t**).* Following method A with **40** (300 mg, 0.98 mmol, 1.00 equiv) and 3,4-dichlorobenzenesulfonyl chloride, **41t** (230 mg, 46%) was obtained as a beige solid. R_f = 0.58 (8:92 MeOH/CH_2Cl_2). ^{1}H NMR (600 MHz, DMSO-d_6): δ 8.38 (br s, 1H), 8.28 (s, 1H), 8.13 (s, 1H), 7.90 (d, J = 2.1 Hz, 1H), 7.78 (d, J = 8.3, 1H), 7.66 (dd, J = 8.5, 2.1 Hz, 1H), 7.37 (br s, 2H), 6.11 (d, J = 2.9 Hz, 1H), 5.34 (dd, J = 6.4, 2.9 Hz, 1H), 4.88 (dd, J = 6.3, 3.1 Hz, 1H), 4.15 (td, J = 5.9, 3.0 Hz, 1H), 3.24−3.06 (m, 2H), 1.51 (s, 3H), 1.28 (s, 3H). ^{13}C NMR (150 MHz, DMSO-d_6): δ 156.2, 152.5, 148.4, 140.7, 140.1, 135.5, 132.0, 131.5, 128.2, 126.5, 119.3, 113.5, 89.3, 84.2, 82.8, 81.5, 44.4, 27.0, 25.1. HRMS (ESI+): m/z calculated for $C_{19}H_{21}Cl_2N_6O_5S$ $[M+H]^+$: 515.0666, found 515.0669.

*N-{[(4R,6R)-6-(6-amino-9H-purin-9-yl)-2,2-dimethyl-tetrahydro-2H-furo[3,4-d][1,3]dioxol-4-yl]methyl-3-chloro-4-methylbenzene-1-sulfonamide (**41u**).* Following method A with **40** (300 mg, 0.98 mmol, 1.00 equiv) and 3-chloro-4-methylbenzenesulfonyl chloride, **41u** (362 mg, 69%) was obtained as a white solid. R_f = 0.46 (1:9 MeOH/CH_2Cl_2). ^{1}H NMR (600 MHz, DMSO-d_6): δ 8.28 (s, 1H), 8.24 (dd, J = 6.6, 5.4 Hz, 1H), 8.13 (s, 1H), 7.70 (d, J = 1.9 Hz, 1H), 7.55 (dd, J = 8.0, 1.9 Hz, 1H), 7.47 (d, J = 8.0 Hz, 1H), 7.38 (br s, 2H), 6.11 (d, J = 2.9 Hz, 1H), 5.33 (dd, J = 6.3, 3.0 Hz, 1H), 4.89 (dd, J = 6.3, 3.0 Hz, 1H), 4.17 (td, J = 5.8, 2.9 Hz, 1H), 3.18−3.02 (m, 2H), 2.36 (s, 3H), 1.51 (s, 3H), 1.28 (s, 3H). ^{13}C NMR (150 MHz, DMSO-d_6): δ 156.2, 152.5, 148.4, 140.6, 140.2, 139.5, 133.8, 131.9, 126.5, 125.1, 119.3, 113.5, 89.5, 84.2, 82.8, 81.6, 44.5, 27.0, 25.1, 19.6. HRMS (ESI+): m/z calculated for $C_{20}H_{24}ClN_6O_5S$ $[M+H]^+$: 495.1212, found 495.1213.

General Method B for the Synthesis of Compounds 42a−k. A suspension of synthesis intermediates **41** (1.00 equiv), ethyl *p*-toluenesulfonate (1.50 equiv), KI (0.10 equiv) and K_2CO_3 (3.00 equiv) in anhydrous DMF (C = 0.1 M) was stirred under argon at 50 °C for 16 h. After cooling to room temperature, the reaction mixture was diluted with AcOEt and brine. The aqueous layer was extracted with AcOEt and the combined organic extracts were washed with brine, dried over Na_2SO_4 and concentrated under vacuum. The residue was purified by flash column chromatography (dry sample, silica gel, linear gradient 0−4% MeOH in CH_2Cl_2) to give the desired compound as a colorless solid.

*N-{[(4R,6R)-6-(6-amino-9H-purin-9-yl)-2,2-dimethyl-tetrahydro-2H-furo[3,4-d][1,3]dioxol-4-yl]methyl}-N-ethylbenzenesulfonamide (**42a**).* Following method B with **41a** (140 mg, 0.31 mmol, 1.00 equiv), **42a** (108 mg, 72%) was obtained as a white solid. R_f = 0.50 (8:92 MeOH/CH_2Cl_2). ^{1}H NMR (600 MHz, DMSO-d_6): δ 8.32 (s, 1H), 8.17 (s, 1H), 7.73−7.51 (m, 5H), 7.34 (br s, 2H), 6.20 (d, J = 2.1 Hz, 1H), 5.50 (dd, J = 6.3, 2.3 Hz, 1H), 5.09 (dd, J = 6.3, 3.0 Hz, 1H), 4.29 (ddd, J = 7.7, 5.7, 3.1 Hz, 1H), 3.56 (dd, J = 14.7, 5.7 Hz, 1H), 3.21 (dd, J = 14.7, 7.8 Hz, 1H), 3.06 (q, J = 7.1 Hz, 2H), 1.53 (s, 3H), 1.33 (s, 3H), 0.78 (t, J = 7.1 Hz, 3H). ^{13}C NMR (150 MHz, DMSO-d_6): δ 156.2, 152.7, 148.6, 140.3, 139.3, 132.8, 129.3, 126.7, 119.2, 113.3, 89.3, 85.3, 83.0, 82.1, 48.9, 43.4, 26.9, 25.1, 13.2. HRMS (ESI+): m/z calculated for $C_{21}H_{27}N_6O_5S$ $[M+H]^+$: 475.1758, found 475.1764.

*N-{[(4R,6R)-6-(6-amino-9H-purin-9-yl)-2,2-dimethyl-tetrahydro-2H-furo[3,4-d][1,3]dioxol-4-yl]methyl}-N-ethyl-2-nitro-4-(trifluoromethyl)benzene-1-sulfonamide (**42b**).* Following method B with **41f** (150 mg, 0.29 mmol, 1.00 equiv), **42b** (130 mg, 76%) was obtained as a beige solid. R_f = 0.43 (8:92 MeOH/CH_2Cl_2). ^{1}H NMR (600 MHz, DMSO-d_6): δ 8.55−8.51 (m, 1H), 8.30 (s, 1H), 8.16 (s, 1H), 8.08 (d, J = 8.2 Hz, 1H), 8.03 (dd, J = 8.6, 1.8 Hz, 1H), 7.33 (br s, 2H), 6.20 (d, J = 2.1 Hz, 1H), 5.42 (dd, J = 6.3, 2.2 Hz, 1H), 5.05 (dd, J = 6.4, 3.4 Hz, 1H), 4.29 (ddd, J = 8.3, 4.6, 3.3 Hz, 1H), 3.75 (dd, J = 15.0, 4.7 Hz, 1H), 3.60 (dd, J = 15.1, 8.5 Hz, 1H), 3.30−3.17 (m, 2H), 1.51 (s, 3H), 1.31 (s, 3H), 0.86 (t, J = 7.0 Hz, 3H). ^{13}C NMR (150 MHz, DMSO-d_6): δ 156.2, 152.7, 148.5, 147.6, 140.2, 135.6, 134.0, 133.8, 133.6, 133.4, 131.1, 129.1, 124.9, 123.1, 121.3, 119.5, 121.9, 119.2, 113.5, 89.1, 84.9, 83.2, 82.0, 48.7, 43.3, 26.9, 25.1, 13.1. HRMS (ESI+): m/z calculated for $C_{22}H_{24}F_3N_7O_7S$ $[M+H]^+$: 588.1483, found 588.1485.

*N-{[(4R,6R)-6-(6-amino-9H-purin-9-yl)-2,2-dimethyl-tetrahydro-2H-furo[3,4-d][1,3]dioxol-4-yl]methyl}-N-ethyl-3-nitrobenzene-1-sulfonamide (**42c**).* Following method B with **41h** (150 mg, 0.305 mmol, 1.00 equiv), **42c** (400 mg, 81%) was obtained as a white solid. R_f = 0.60 (1:9 MeOH/CH_2Cl_2). ^{1}H NMR (600 MHz, DMSO-d_6): δ 8.42 (ddd, J = 8.0, 2.2, 1.0 Hz, 1H), 8.38 (t, J = 2.0 Hz, 1H), 8.29 (s, 1H), 8.16 (s, 1H), 8.12−8.10 (m, 1H), 7.79 (t, J = 8.0 Hz, 1H), 7.33 (br s, 2H), 6.19 (d, J = 2.2 Hz, 1H), 5.45 (dd, J = 6.3, 2.2 Hz, 1H), 5.07 (dd, J = 6.2, 3.2 Hz, 1H), 4.31 (ddd, J = 8.3, 5.1, 3.2 Hz, 1H), 3.65 (dd, J = 14.8, 5.1 Hz, 1H), 3.39 (dd, J = 14.7, 8.3 Hz, 1H), 3.15 (q, J = 7.1 Hz, 2H), 1.52 (s, 3H), 1.32 (s, 3H), 0.85 (t, J = 7.1 Hz, 3H). ^{13}C NMR (150 MHz, DMSO-d_6): δ 156.6, 153.1, 149.0, 148.3, 141.5, 140.8, 133.2, 131.8, 127.8, 121.9, 119.7, 113.9, 89.7, 85.4, 83.7, 82.5, 49.3, 43.9, 27.4, 25.6, 13.8. HRMS (ESI+): m/z calculated for $C_{21}H_{26}N_7O_7S$ $[M+H]^+$: 520.1614, found 520.1626.

*N-{[(4R,6R)-6-(6-amino-9H-purin-9-yl)-2,2-dimethyl-tetrahydro-2H-furo[3,4-d][1,3]dioxol-4-yl]methyl}-N-ethyl-4-bromo-3-nitrobenzene-1-sulfonamide (**42d**).* Following method B with **41j** (190 mg, 0.33 mmol, 1.00 equiv), **42d** (122 mg, 61%) was obtained as a white solid. R_f = 0.50 (8:92 MeOH/CH_2Cl_2). ^{1}H NMR (600 MHz, $CDCl_3$): δ 8.33 (s, 1H), 8.15 (d, J = 2.0 Hz, 1H), 7.82 (s, 1H), 7.71 (d, J = 8.5, 1H), 7.65 (dd, J = 8.4, 2.2 Hz, 1H), 6.02 (d, J = 1.8 Hz, 1H), 5.82 (br s, 2H), 5.44 (dd, J = 6.3, 1.8 Hz, 1H), 5.12 (dd, J = 6.4, 3.4 Hz, 1H), 4.40 (ddd, J = 8.4, 5.1, 3.5 Hz, 1H), 3.67 (dd, J = 14.9, 5.0 Hz, 1H), 3.56 (dd, J = 14.9, 8.4 Hz, 1H), 3.30−3.14 (m, 2H), 1.59 (s, 3H), 1.37 (s, 3H). ^{13}C NMR (150 MHz, $CDCl_3$): δ 155.8, 153.3, 149.8, 149.1, 141.4, 140.4, 135.9, 131.0, 124.3, 120.6, 119.1, 114.8, 91.1, 86.0, 84.2, 82.8, 48.8, 43.7, 27.2, 25.4, 13.7. HRMS (ESI+): m/z calculated for $C_{21}H_{25}BrN_7O_7S$ $[M+H]^+$: 598.0714, found 598.0723.

*N-{[(4R,6R)-6-(6-amino-9H-purin-9-yl)-2,2-dimethyl-tetrahydro-2H-furo[3,4-d][1,3]dioxol-4-yl]methyl}-N-ethyl-4-methyl-3-nitrobenzene-1-sulfonamide (**42e**).* Following method B with **41k** (135 mg, 0.27 mmol, 1.00 equiv), **42e** (66 mg, 46%) was obtained as a beige solid. R_f = 0.50 (8:92 MeOH/CH_2Cl_2). ^{1}H NMR (600 MHz, $CDCl_3$): δ 8.34 (s, 1H), 8.30 (d, J = 2.0 Hz, 1H), 7.82 (s, 1H), 7.76 (dd, J = 8.0, 1.9 Hz, 1H), 7.34 (d, J = 8.1 Hz, 1H), 6.02 (d, J = 1.9 Hz, 1H), 5.71 (br s, 2H), 5.46 (dd, J = 6.4, 2.0 Hz, 1H), 5.14 (dd, J = 6.4, 3.4 Hz, 1H), 4.42 (ddd, J = 8.4, 5.3, 3.4 Hz, 1H), 3.69 (dd, J = 14.7, 5.3 Hz, 1H), 3.45 (dd, J = 14.7, 8.0 Hz, 1H), 3.31−3.14 (m, 2H), 2.62 (s, 3H), 1.59 (s, 3H), 1.38 (s, 3H), 1.02 (t, J = 7.1 Hz, 3H). ^{13}C NMR (150 MHz, $CDCl_3$): δ 155.7, 153.3, 149.1, 140.5, 139.7, 138.2, 133.6, 131.0, 123.7, 120.6, 114.7, 91.1, 86.1, 84.1, 82.8, 48.9, 43.8, 27.2, 25.4, 20.6, 13.7. HRMS (ESI+): m/z calculated for $C_{22}H_{28}N_7O_7S$ $[M+H]^+$: 534.1765, found 534.1768.

*N-{[(4R,6R)-6-(6-amino-9H-purin-9-yl)-2,2-dimethyl-tetrahydro-2H-furo[3,4-d][1,3]dioxol-4-yl]methyl}-N-ethyl-4-methoxy-3-nitrobenzene-1-sulfonamide (**42f**).* Following method B with **41m** (127 mg, 0.24 mmol, 1.00 equiv), **42f** (102 mg, 79%) was obtained as a beige solid. R_f = 0.52 (8:92 MeOH/CH_2Cl_2). ^{1}H NMR (600 MHz, $CDCl_3$): δ 8.32 (s, 1H), 8.22 (d, J = 2.3 Hz, 1H), 8.16 (s, 1H), 7.92 (dd, J = 8.9, 2.4 Hz, 1H), 7.51−7.25 (m, 3H), 6.20 (d, J = 2.2 Hz, 1H), 5.71 (br s, 2H), 5.46 (dd, J = 6.3, 2.2 Hz, 1H), 5.06 (dd, J = 6.3, 3.1 Hz, 1H), 4.31 (ddd, J = 8.3, 5.3, 3.0 Hz, 1H), 3.99 (s, 3H), 3.59 (dd, J = 14.8, 5.4 Hz, 1H), 3.31 (dd, J = 14.7, 7.4 Hz, 1H), 3.07 (q, J = 7.0 Hz, 2H), 1.52 (s, 3H), 1.32 (s, 3H), 0.80 (t, J = 7.0 Hz, 3H).^{13}C NMR (150 MHz, DMSO-d_6): δ 163.5, 156.2, 152.7, 148.6, 140.3, 133.7, 132.7, 131.9, 119.2, 113.3, 112.9, 101.2, 89.2, 85.2, 83.1, 82.0, 57.1, 48.8, 43.4, 26.9, 25.1, 13.3. HRMS (ESI+): m/z calculated for $C_{22}H_{28}N_7O_8S$ $[M+H]^+$: 550.1720, found 550.1726.

*N-{[(4R,6R)-6-(6-amino-9H-purin-9-yl)-2,2-dimethyl-tetrahydro-2H-furo[3,4-d][1,3]dioxol-4-yl]methyl}-N-ethyl-3-cyanobenzene-1-sulfonamide (**42g**).* Following method B with **41n** (230 mg, 0.49

https://doi.org/10.1021/acs.jmedchem.2c00120
J. Med. Chem. 2022, 65, 6231−6249

mmol, 1.00 equiv), **42g** (100 mg, 41%) was obtained as a beige solid. R_f = 0.50 (8:92 MeOH/CH_2Cl_2). ^{1}H NMR (600 MHz, DMSO-d_6): δ 8.31 (s, 1H), 8.21 (t, J = 1.8 Hz, 1H), 8.17 (s, 1H), 8.09 (dt, J = 7.9, 1.4 Hz, 1H), 7.99 (ddd, J = 7.9, 1.8, 1.0 Hz, 1H), 7.70 (t, J = 8.0 Hz, 1H), 7.34 (br s, 2H), 6.20 (d, J = 2.3 Hz, 1H), 5.46 (dd, J = 6.3, 2.2 Hz, 1H), 5.06 (dd, J = 6.3, 3.1 Hz, 1H), 4.30 (ddd, J = 8.3, 5.1, 3.1 Hz, 1H), 3.63 (dd, J = 14.8, 5.2 Hz, 1H), 3.40−3.32 (m, 1H), 3.11 (q, J = 7.1 Hz, 2H), 1.53 (s, 3H), 1.33 (s, 3H), 0.80 (t, J = 7.1 Hz, 3H). ^{13}C NMR (150 MHz, DMSO-d_6): δ 156.2, 152.7, 148.5, 140.7, 140.3, 136.3, 131.2, 130.6, 130.4, 119.2, 117.5, 113.4, 112.7, 89.2, 85.1, 83.1, 82.0, 48.8, 43.5, 26.9, 25.1, 13.2. HRMS (ESI+): m/z calculated for $C_{22}H_{26}N_7O_5S$ $[M+H]^+$: 500.1716, found 500.1720.

*N-{[(4R,6R)-6-(6-amino-9H-purin-9-yl)-2,2-dimethyl-tetrahydro-2H-furo[3,4-d][1,3]dioxol-4-yl]methyl}-N-ethyl-3-cyano-4-methoxybenzene-1-sulfonamide (**42h**).* Following method B with **41q** (95 mg, 0.19 mmol, 1.00 equiv), **42h** (40 mg, 40%) was obtained as a beige solid. R_f = 0.50 (8:92 MeOH/CH_2Cl_2). ^{1}H NMR (600 MHz, DMSO-d_6): δ 8.32 (s, 1H), 8.17 (s, 1H), 8.11 (d, J = 2.4 Hz, 1H), 7.93 (dd, J = 9.0, 2.4 Hz, 1H), 7.35 (br s, 2H), 7.30 (d, J = 9.0 Hz, 1H), 6.20 (d, J = 2.3 Hz, 1H), 5.47 (dd, J = 6.2, 2.3 Hz, 1H), 5.05 (dd, J = 6.3, 3.1 Hz, 1H), 4.29 (ddd, J = 8.3, 5.3, 3.1 Hz, 1H), 3.99 (s, 3H), 3.58 (dd, J = 14.8, 5.4 Hz, 1H), 3.36−3.25 (m, 1H), 3.07 (qd, J = 7.2, 3.4 Hz, 2H), 1.53 (s, 3H), 1.33 (s, 3H), 0.81 (t, J = 7.1 Hz, 3H). ^{13}C NMR (150 MHz, DMSO-d_6): δ 163.5, 156.2, 152.7, 148.6, 140.3, 133.7, 132.7, 131.9, 119.2, 115.0, 113.3, 112.9, 101.2, 89.2, 85.2, 83.1, 82.0, 57.1, 48.8, 43.4, 26.9, 25.1, 13.3. HRMS (ESI+): m/z calculated for $C_{23}H_{28}N_7O_6S$ $[M+H]^+$: 530.1816, found 530.1814.

*N-{[(4R,6R)-6-(6-amino-9H-purin-9-yl)-2,2-dimethyl-tetrahydro-2H-furo[3,4-d][1,3]dioxol-4-yl]methyl}-N-ethyl-3-chlorobenzene-1-sulfonamide (**42i**).* Following method B with **41s** (95 mg, 0.20 mmol, 1.00 equiv), **42i** (45 mg, 45%) was obtained as a white solid. R_f = 0.54 (8:92 MeOH/CH_2Cl_2). ^{1}H NMR (600 MHz, DMSO-d_6): δ 8.32 (s, 1H), 8.18 (s, 1H), 7.75−7.53 (m, 5H), 7.34 (br s, 2H), 6.21 (d, J = 2.2 Hz, 1H), 5.48 (dd, J = 6.3, 2.2 Hz, 1H), 5.08 (dd, J = 6.3, 3.1 Hz, 1H), 4.30 (ddd, J = 7.7, 5.7, 3.1 Hz, 1H), 3.61 (dd, J = 14.7, 5.5 Hz, 1H), 3.35−3.27 (m, 1H), 3.09 (q, J = 7.2 Hz, 2H), 1.53 (s, 3H), 1.33 (s, 3H), 0.81 (t, J = 7.1 Hz, 3H). ^{13}C NMR (150 MHz, DMSO-d_6): δ 156.2, 152.7, 148.5, 141.3, 140.3, 134.0 132.8, 129.3, 126.7, 119.2, 113.3, 89.3, 85.3, 83.0, 82.1, 48.9, 43.4, 26.9, 25.1, 13.2. HRMS (ESI+): m/z calculated for $C_{21}H_{27}N_6O_5S$ $[M+H]^+$: 475.1758, found 475.1764.

*N-{[(4R,6R)-6-(6-amino-9H-purin-9-yl)-2,2-dimethyl-tetrahydro-2H-furo[3,4-d][1,3]dioxol-4-yl]methyl}-N-ethyl-3,4-dichlorobenzene-1-sulfonamide (**42j**).* Following method B with **41t** (140 mg, 0.27 mmol, 1.00 equiv), **42j** (120 mg, 81%) was obtained as a beige solid. R_f = 0.58 (8:92 MeOH/CH_2Cl_2). ^{1}H NMR (600 MHz, DMSO-d_6): δ 8.32 (s, 1H), 8.17 (s, 1H), 7.92 (d, J = 2.2 Hz, 1H), 7.76 (d, J = 8.5, 1H), 7.65 (dd, J = 8.4, 2.2 Hz, 1H), 7.34 (br s, 2H), 6.20 (d, J = 2.2 Hz, 1H), 5.46 (dd, J = 6.4, 2.3 Hz, 1H), 5.06 (dd, J = 6.4, 3.1 Hz, 1H), 4.29 (ddd, J = 8.4, 5.4, 3.2 Hz, 1H), 3.61 (dd, J = 14.9, 5.3 Hz, 1H), 3.35 (dd, J = 14.9, 8.2 Hz, 1H), 3.11 (q, J = 7.2 Hz, 2H), 1.52 (s, 3H), 1.32 (s, 3H), 0.84 (t, J = 7.1 Hz, 3H). ^{13}C NMR (150 MHz, DMSO-d_6): δ 156.2, 152.7, 148.5, 140.3, 139.8, 135.9, 132.3, 131.6, 128.5, 126.9, 119.2, 113.3, 89.2, 85.0, 83.1, 82.0, 48.8, 43.4, 26.9, 25.1, 13.3. HRMS (ESI+): m/z calculated for $C_{21}H_{24}Cl_2N_6O_5S$ $[M+H]^+$: 543.0979, found 543.0978.

*N-{[(4R,6R)-6-(6-amino-9H-purin-9-yl)-2,2-dimethyl-tetrahydro-2H-furo[3,4-d][1,3]dioxol-4-yl]methyl}-N-ethyl-3-chloro-4-methylbenzene-1-sulfonamide (**42k**).* Following method B with **41u** (200 mg, 0.41 mmol, 1.00 equiv), **42k** (140 mg, 66%) was obtained as a white solid. R_f = 0.57 (8:92 MeOH/CH_2Cl_2). ^{1}H NMR (600 MHz, DMSO-d_6): δ 8.31 (s, 1H), 8.17 (s, 1H), 7.70 (d, J = 2.2 Hz, 1H), 7.55 (dd, J = 8.0, 1.9 Hz, 1H), 7.49 (dd, J = 8.0, 0.8 Hz, 1H), 7.34 (br s, 2H), 6.20 (d, J = 2.3 Hz, 1H), 5.47 (dd, J = 6.2, 2.3 Hz, 1H), 5.07 (dd, J = 6.3, 3.1 Hz, 1H), 4.29 (ddd, J = 8.4, 5.5, 3.2 Hz, 1H), 3.59 (dd, J = 14.7, 5.5 Hz, 1H), 3.27 (dd, J = 14.7, 8.0 Hz, 1H), 3.08 (q, J = 7.0 Hz, 2H), 2.37 (s, 3H), 1.53 (s, 3H), 1.32 (s, 3H), 0.82 (t, J = 7.1 Hz, 3H). ^{13}C NMR (150 MHz, DMSO-d_6): δ 156.2, 152.6, 148.5, 141.0, 140.3, 138.6, 134.0, 132.0, 126.8, 125.4, 119.2, 113.3, 89.2, 85.0, 83.1, 82.0, 48.8, 43.4, 26.9, 25.1, 19.6, 13.3. HRMS (ESI+): m/z calculated for $C_{22}H_{27}ClN_6O_5S$ $[M+H]^+$: 523.1530, found 523.1530.

General Method C for the Synthesis of Compounds 43a-c. A suspension of **41m** (1.00 equiv), the corresponding alkyl bromide reagent (1.50 equiv), and K_2CO_3 (3.00 equiv) in anhydrous DMF was stirred under argon at 50 °C for 16 h. After cooling to room temperature, the reaction mixture was diluted with AcOEt and brine. The aqueous layer was extracted with AcOEt and the combined organic extracts were washed with brine, dried over Na_2SO_4 and concentrated under vacuum. The residue was purified by flash column chromatography (dry sample, silica gel, linear gradient 0−3% MeOH in CH_2Cl_2) to give the desired compound as a colorless solid.

*ethyl 5-(N-{[(4R,6R)-6-(6-amino-9H-purin-9-yl)-2,2-dimethyl-tetrahydro-2H-furo[3,4-d][1,3]dioxol-4-yl]methyl}4-methoxy-3-nitrobenzenesulfonamido)pentanoate (**43a**).* Following method C with **41m** (200 mg, 0.38 mmol, 1.00 equiv) and ethyl 5-bromovalerate, **43a** (149 mg, 60%) was obtained as a white foam. R_f = 0.50 (5:95 MeOH/CH_2Cl_2). ^{1}H NMR (600 MHz, $CDCl_3$): δ 8.33 (s, 1H), 8.19 (d, J = 2.4 Hz, 1H), 7.84 (s, 1H), 7.80 (dd, J = 8.8, 2.3 Hz, 1H), 7.01 (d, J = 8.8, 1H), 6.02 (d, J = 1.8 Hz, 1H), 5.80 (br s, 2H), 5.45 (dd, J = 6.3, 1.9 Hz, 1H), 5.11 (dd, J = 6.3, 3.4 Hz, 1H), 4.40 (ddd, J = 8.4, 4.9, 3.4 Hz, 1H), 4.10 (q, J = 7.1 Hz, 2H), 4.00 (s, 3H), 3.65 (dd, J = 14.9, 5.0 Hz, 1H), 3.43 (dd, J = 14.9, 8.5 Hz, 1H), 3.17−2.97 (m, 2H), 2.22−2.13 (m, 2H), 1.58 (s, 3H), 1.48−1.40 (m, 4H), 1.37 (s, 3H), 1.23 (t, J = 7.2 Hz, 3H). ^{13}C NMR (150 MHz, $CDCl_3$): δ 173.2, 155.8, 155.6, 153.3, 149.1, 140.5, 139.2, 133.0, 132.1, 125.2, 120.5, 114.7, 113.6, 91.1, 86.1, 84.1, 82.8, 60.5, 57.1, 49.7, 48.7, 33.7, 27.7, 27.2, 25.4, 21.9, 14.4. HRMS (ESI+): m/z calculated for $C_{27}H_{36}N_7O_{10}S$ $[M+H]^+$: 650.2239, found 650.2244.

*4-(N-{[(4R,6R)-6-(6-amino-9H-purin-9-yl)-2,2-dimethyl-tetrahydro-2H-furo[3,4-d][1,3]dioxol-4-yl]methyl}4-methoxy-3-nitrobenzenesulfonamido)butyl acetate (**43b**).* Following method C with **41m** (200 mg, 0.38 mmol, 1.00 equiv) and 4-bromobutyl acetate, **43b** (151 mg, 62%) was obtained as a beige foam. R_f = 0.50 (5:95 MeOH/CH_2Cl_2). ^{1}H NMR (600 MHz, $CDCl_3$): δ 8.33 (s, 1H), 8.18 (d, J = 2.3 Hz, 1H), 7.84 (s, 1H), 7.80 (dd, J = 8.8, 2.3 Hz, 1H), 7.01 (d, J = 8.9, 1H), 6.02 (d, J = 1.8 Hz, 1H), 5.87 (br s, 2H), 5.45 (dd, J = 6.3, 1.9 Hz, 1H), 5.12 (dd, J = 6.3, 3.4 Hz, 1H), 4.41 (ddd, J = 8.4, 4.9, 3.1 Hz, 1H), 4.00 (s, 3H), 3.96−3.86 (m, 2H), 3.66 (dd, J = 14.8, 4.9 Hz, 1H), 3.43 (dd, J = 14.8, 8.5 Hz, 1H), 3.18−2.97 (m, 2H), 2.02 (s, 3H), 1.58 (s, 3H), 1.52−1.40 (m, 4H), 1.37 (s, 3H). ^{13}C NMR (150 MHz, $CDCl_3$): δ 171.2, 155.8, 155.6, 153.3, 149.1, 140.5, 139.2, 132.9, 132.0, 125.2, 120.5, 114.7, 113.6, 91.1, 86.1, 84.1, 82.9, 63.8, 57.1, 49.8, 48.7, 27.2, 25.7, 25.4, 24.9, 21.1. HRMS (ESI+): m/z calculated for $C_{26}H_{34}N_7O_{10}S$ $[M+H]^+$: 636.2082, found 636.2092.

*N-{[(4R,6R)-6-(6-amino-9H-purin-9-yl)-2,2-dimethyl-tetrahydro-2H-furo[3,4-d][1,3]dioxol-4-yl]methyl}-N-[4-(1,3-dioxo-2,3-dihydro-1H-isoindol-2-yl)butyl]-4-methoxy-3-nitrobenzene-1-sulfonamide (**43c**).* Following method C with **41m** (200 mg, 0.38 mmol, 1.00 equiv) and 4-bromobutylphthalimide, **43c** (152 mg, 55%) was obtained as a beige foam. R_f = 0.60 (5:95 MeOH/CH_2Cl_2). ^{1}H NMR (600 MHz, DMSO-d_6): δ 8.29 (s, 1H), 8.19 (d, J = 2.4 Hz, 1H), 8.15 (s, 1H), 7.89 (dd, J = 9.0, 2.4 Hz, 1H), 7.86−7.81 (m, 4H), 7.7 (d, J = 9.0, 1H), 7.37 (br s, 2H), 6.16 (d, J = 2.3 Hz, 1H), 5.42 (dd, J = 6.2, 2.3 Hz, 1H), 5.03 (dd, J = 6.3, 3.1 Hz, 1H), 4.30 (ddd, J = 8.4, 5.4, 3.1 Hz, 1H), 3.97 (s, 3H), 3.59 (dd, J = 14.8, 5.5 Hz, 1H), 3.42 (td, J = 6.8, 2.5 Hz, 2H), 3.28 (dd, J = 14.7, 8.0 Hz, 1H), 3.07−2.94 (m, 2H), 3.18−2.97 (m, 2H), 1.49 (s, 3H), 1.40−1.23 (m, 7H). ^{13}C NMR (150 MHz, DMSO-d_6): δ 167.8, 156.1, 154.7, 152.6, 148.5, 140.3, 138.7, 134.3, 131.5, 130.7, 124.0, 123.0, 119.2, 115.0, 113.3, 89.2, 85.0, 83.1, 82.0, 57.3, 49.7, 48.4, 36.8, 26.8, 25.2, 25.1, 25.0. HRMS (ESI+): m/z calculated for $C_{32}H_{35}N_8O_{10}S$ $[M+H]^+$: 723.2191, found 723.2189.

General Method D for the Synthesis of Compounds 44a−d. To a solution at 0 °C under argon of 5′-amino-5′-deoxy-2′,3′-isopropylideneadenosine **40** (1.00 equiv) were successively added corresponding benzoic acid (1.80 equiv), EDC (2.00 equiv) and DMAP (0.30 equiv) in anhydrous DMF (C = 0.35 M). After stirring at 0 °C for 2 h, the reaction mixture was diluted with AcOEt and saturated NH_4Cl solution. The aqueous layer was extracted three times with AcOEt and the combined organic extracts were washed with brine, dried over Na_2SO_4 and concentrated under vacuum. The residue was purified by flash column chromatography (dry sample, silica gel, linear

https://doi.org/10.1021/acs.jmedchem.2c00120
J. Med. Chem. 2022, 65, 6231−6249

gradient 0−5% MeOH in CH_2Cl_2) to give the desired compound as a foam.

*N-{[(4R,6R)-6-(6-amino-9H-purin-9-yl)-2,2-dimethyl-tetrahydro-2H-furo[3,4-d][1,3]dioxol-4-yl]methyl}benzamide (**44a**).* Following method D with **40** (300 mg, 0.98 mmol, 1.00 equiv) and benzoic acid, **44a** (369 mg, 92%) was obtained as a beige foam. R_f = 0.42 (1:9 MeOH/CH_2Cl_2). ^{1}H NMR (600 MHz, DMSO-d_6): δ 8.64 (t, J = 5.7 Hz, 1H), 8.33 (s, 1H), 8.08 (s, 1H), 7.86−7.81 (m, 2H), 7.56−7.50 (m, 1H), 7.49−7.42 (m, 2H), 7.33 (br s, 2H), 6.16 (d, J = 2.7 Hz, 1H), 5.49 (dd, J = 6.4, 2.8 Hz, 1H), 5.06 (dd, J = 6.3, 3.4 Hz, 1H), 4.31 (td, J = 6.2, 3.4 Hz, 1H), 3.60−3.46 (m, 2H), 1.53 (s, 3H), 1.32 (s, 3H). ^{13}C NMR (150 MHz, DMSO-d_6): δ 166.7, 156.2, 152.7, 148.8, 140.1, 134.2, 131.3, 128.3, 127.3, 119.3, 113.5, 89.0, 84.3, 83.0, 81.9, 41.4, 27.0, 25.3. HRMS (ESI+): m/z calculated for $C_{20}H_{23}N_6O_4$ $[M+H]^+$: 411.1775, found 411.1777.

*N-{[(4R,6R)-6-(6-amino-9H-purin-9-yl)-2,2-dimethyl-tetrahydro-2H-furo[3,4-d][1,3]dioxol-4-yl]methyl}-4-chloro-3-nitrobenzamide (**44b**).* Following method D with **40** (300 mg, 0.98 mmol, 1.00 equiv) and 4-chloro-3-nitrobenzoic acid, **44b** (400 mg, 83%) was obtained as a beige foam. R_f = 0.52 (1:9 MeOH/CH_2Cl_2). ^{1}H NMR (600 MHz, DMSO-d_6): δ 8.99 (t, J = 5.8 Hz, 1H), 8.48 (d, J = 2.2 Hz, 1H), 8.33 (s, 1H), 8.11 (dd, J = 8.5, 2.1 Hz, 1H), 8.07 (s, 1H), 7.89 (d, J = 8.5 Hz, 1H), 7.32 (br s, 2H), 6.17 (d, J = 2.6 Hz, 1H), 5.49 (dd, J = 6.4, 2.6 Hz, 1H), 5.07 (dd, J = 6.3, 3.6 Hz, 1H), 4.30 (td, J = 6.1, 3.5 Hz, 1H), 3.64−3.50 (m, 2H), 1.53 (s, 3H), 1.32 (s, 3H). ^{13}C NMR (150 MHz, DMSO-d_6): δ 163.7, 156.2, 152.7, 148.8, 147.3, 140.2, 134.1, 132.4, 131.9, 127.9, 124.5, 119.3, 113.5, 88.9, 84.2, 83.1, 81.8, 41.7, 27.0, 25.3. HRMS (ESI+): m/z calculated for $C_{20}H_{21}ClN_7O_6$ $[M+H]^+$: 490.1236, found 490.1240.

*N-{[(4R,6R)-6-(6-amino-9H-purin-9-yl)-2,2-dimethyl-tetrahydro-2H-furo[3,4-d][1,3]dioxol-4-yl]methyl}-3-nitro-4-methylbenzamide (**44c**).* Following method D with **40** (300 mg, 0.98 mmol, 1.00 equiv) and 4-methyl-3-nitrobenzoic acid, **44c** (390 mg, 84%) was obtained as a beige foam. R_f = 0.56 (1:9 MeOH/CH_2Cl_2). ^{1}H NMR (600 MHz, DMSO-d_6): δ 8.91 (t, J = 5.8 Hz, 1H), 8.43 (d, J = 1.8 Hz, 1H), 8.33 (s, 1H), 8.09 (s, 1H), 8.06 (dd, J = 8.0, 1.9 Hz, 1H), 7.60 (d, J = 8.1 Hz, 1H), 7.32 (br s, 2H), 6.17 (d, J = 2.5 Hz, 1H), 5.49 (dd, J = 6.4, 2.6 Hz, 1H), 5.07 (dd, J = 6.3, 3.5 Hz, 1H), 4.31 (td, J = 6.2, 3.5 Hz, 1H), 3.64−3.49 (m, 2H), 2.56 (s, 3H), 1.53 (s, 3H), 1.32 (s, 3H). ^{13}C NMR (150 MHz, DMSO-d_6): δ 164.4, 156.2, 152.7, 148.8, 148.7, 140.1, 136.0, 133.1, 133.0, 131.7, 123.2, 119.3, 113.5, 88.9, 84.3, 83.1, 81.9, 41.6, 27.0, 25.3, 19.5. HRMS (ESI+): m/z calculated for $C_{21}H_{24}N_7O_6$ $[M+H]^+$: 470.1783, found 470.1779.

*N-{[(4R,6R)-6-(6-amino-9H-purin-9-yl)-2,2-dimethyl-tetrahydro-2H-furo[3,4-d][1,3]dioxol-4-yl]methyl}-2-nitro-4-(trifluoromethyl)-benzamide (**44d**).* Following method D with **40** (300 mg, 0.98 mmol, 1.00 equiv) and 4-trifluoro-2-nitrobenzoic acid, **44d** was obtained as a beige foam (190 mg, 37%). R_f = 0.56 (1:9 MeOH/CH_2Cl_2). ^{1}H NMR (600 MHz, DMSO-d_6): δ 9.18 (t, J = 5.8 Hz, 1H), 8.43 (d, J = 1.7 Hz, 1H), 8.33 (s, 1H), 8.23 (dd, J = 8.0, 1.7 Hz, 1H), 7.88 (d, J = 8.0 Hz, 1H), 7.82 (s, 1H), 7.36 (br s, 2H), 6.15 (d, J = 3.3 Hz, 1H), 5.42 (dd, J = 6.2, 3.3 Hz, 1H), 5.02 (dd, J = 6.3, 3.0 Hz, 1H), 4.35 (td, J = 5.4, 3.0 Hz, 1H), 3.66−3.55 (m, 2H), 1.57 (s, 3H), 1.35 (s, 3H). ^{13}C NMR (150 MHz, DMSO-d_6): δ 164.7, 156.2, 152.4, 148.6, 147.1, 140.2, 135.7, 131.2, 131.0, 130.7, 130.5, 130.6, 130.5, 125.4, 123.6, 121.8, 120.0, 121.6, 119.4, 113.6, 89.5, 83.6, 82.7, 81.7, 41.3, 27.0, 25.2. HRMS (ESI+): m/z calculated for $C_{21}H_{21}F_3N_7O_6$ $[M+H]^+$: 524.1500, found 524.1488.

General Method E for the Synthesis of Final Compounds 1−39. Synthesis intermediates were treated with a formic acid/water (1/1 v:v, C = 0.05 M) solution. After stirring at 25 °C for 24−48 h until completion of the reaction, solvents were removed under vacuum and the crude was co-evaporated three times with absolute EtOH. The residues were purified by flash column chromatography (dry sample, silica gel, linear gradient 0−10% MeOH in CH_2Cl_2). Fractions containing pure product were concentrated and trituration in Et_2O afforded desired compounds as solids.

*N-{[(2R,5R)-5-(6-amino-9H-purin-9-yl)-3,4-dihydroxyoxolan-2-yl]methyl}benzenesulfonamide (**1**).* Following method E with **41a** (100 mg, 0.22 mmol), **1** was obtained as a white solid (69 mg, 76%) with 99% purity determined by HPLC analysis at 260 nm. R_f = 0.55 (1:9 MeOH/CH_2Cl_2). ^{1}H NMR (600 MHz, DMSO-d_6): δ 8.51 (t, J = 6.0 Hz, 1H), 8.30 (s, 1H), 8.14 (s, 1H), 7.82−7.77 (m, 2H), 7.66−7.60 (m, 1H), 7.60−7.55 (m, 2H), 7.38 (br s, 2H), 5.82 (d, J = 6.6 Hz, 1H), 5.47 (d, J = 6.2 Hz, 1H), 5.28 (d, J = 4.5 Hz, 1H), 4.69 (td, J = 6.4, 5.2 Hz, 1H), 4.07 (td, J = 4.9, 2.7 Hz, 1H), 4.00 (td, J = 4.7, 2.8 Hz, 1H), 3.12−3.04 (m, 2H). ^{13}C NMR (150 MHz, DMSO-d_6): δ 156.3, 152.2, 148.8, 140.5, 140.3, 132.4, 129.3, 126.4, 119.6, 88.2, 83.5, 72.3, 71.2, 44.9. HRMS (ESI+): m/z calculated for $C_{16}H_{19}N_6O_5S$ $[M+H]^+$: 407.1132, found 407.1121.

*N-{[(2R,5R)-5-(6-amino-9H-purin-9-yl)-3,4-dihydroxyoxolan-2-yl]methyl}-4-nitrobenzenesulfonamide (**2**).* Following method E with **41b** (100 mg, 0.20 mmol), **2** was obtained as a beige solid (73 mg, 80%). R_f = 0.51 (1:9 MeOH/CH_2Cl_2). ^{1}H NMR (600 MHz, DMSO-d_6): δ 8.84 (t, J = 6.6 Hz, 1H), 8.41−8.33 (m, 2H), 8.28 (s, 1H), 8.13 (s, 1H), 8.07−7.97 (m, 2H), 7.37 (br s, 2H), 5.80 (d, J = 6.4 Hz, 1H), 5.49 (d, J = 6.1 Hz, 1H), 5.30 (d, J = 4.7 Hz, 1H), 4.65 (td, J = 6.4, J = 5.0 Hz, 1H), 4.05 (td, J = 4.9, J = 3.0 Hz, 1H), 3.98 (td, J = 4.8, J = 3.0 Hz, 1H), 3.24−3.12 (m, 2H). ^{13}C NMR (600 MHz, DMSO-d_6): δ 156.3, 152.3, 149.5, 148.8, 146.0, 140.4, 128.0, 124.5, 119.5, 88.1, 83.4, 72.4, 71.1, 44.9. HRMS (ESI+): m/z calculated for $C_{16}H_{18}N_7O_7S$ $[M+H]^+$: 452.0983, found 452.0995.

*N-{[(2R,5R)-5-(6-amino-9H-purin-9-yl)-3,4-dihydroxyoxolan-2-yl]methyl}-2-methoxy-4-nitrobenzenesulfonamide (**3**).* Following method E with **41c** (95 mg, 0.18 mmol), **3** was obtained as a beige solid (56 mg, 64%). R_f = 0.44 (1:9 MeOH/CH_2Cl_2). ^{1}H NMR (600 MHz, DMSO-d_6): δ 8.76 (t, J = 5.8 Hz, 1H), 8.27 (s, 1H), 8.12 (s, 1H), 7.96 (d, J = 8.5 Hz, 1H), 7.87 (d, J = 2.1 Hz, 1H), 7.83 (dd, J = 8.6, 2.2 Hz, 1H), 7.38 (br s, 2H), 5.78 (d, J = 6.7 Hz, 1H), 5.46 (d, J = 6.3 Hz, 1H), 5.26 (d, J = 4.4 Hz, 1H), 4.72 (td, J = 6.6, 5.2 Hz, 1H), 4.07 (td, J = 4.8, 2.6 Hz, 1H), 3.99 (td, J = 4.5, 2.5 Hz, 1H), 3.85 (s, 3H), 3.21−3.09 (m, 2H). ^{13}C NMR (150 MHz, DMSO-d_6): δ 156.8, 156.3, 152.2, 150.9, 148.7, 140.7, 133.5, 130.7, 119.6, 115.0, 107.8, 88.4, 83.6, 72.2, 71.2, 56.8, 45.0. HRMS (ESI+): m/z calculated for $C_{17}H_{20}N_7O_8S$ $[M+H]^+$: 482.1089, found 482.1094.

*N-{[(2R,5R)-5-(6-amino-9H-purin-9-yl)-3,4-dihydroxyoxolan-2-yl]methyl}-2-chloro-4-nitrobenzenesulfonamide (**4**).* Following method E using **41d** (75 mg, 0.143 mmol), **4** was obtained as a white solid (43 mg, 62%) with 99% purity determined by HPLC analysis at 260 nm. R_f = 0.26 (1:9 MeOH/CH_2Cl_2). ^{1}H NMR (600 MHz, DMSO-d_6): δ 9.09 (br s, 1H), 8.36 (d, J = 1.7 Hz, 1H), 8.25 (s, 1H), 8.13−8.05 (m, 3H), 7.36 (br s, 2H), 5.75 (d, J = 6.5 Hz, 1H), 5.47 (d, J = 6.2 Hz, 1H), 5.27 (d, J = 4.6 Hz, 1H) 4.70 (q, J = 6.0 Hz, 1H), 4.07 (td, J = 4.9, 3.2 Hz, 1H), 3.98 (ddd, J = 5.6, 4.2, 3.0 Hz, 1H), 3.31−3.23 (m, 2H). ^{13}C NMR (150 MHz, DMSO-d_6): δ 156.2, 152.3, 149.5, 148.7, 143.3, 140.4, 131.8, 131.5, 126.3, 122.3, 119.5, 88.2, 83.5, 72.3, 71.1, 45.1. HRMS (ESI+): m/z calculated for $C_{16}H_{17}ClN_7O_7S$ $[M+H]^+$: 486.0593, found 486.0580.

*N-{[(2R,5R)-5-(6-amino-9H-purin-9-yl)-3,4-dihydroxyoxolan-2-yl]methyl}-2-nitro-4-methoxybenzenesulfonamide (**5**).* Following method E with **41e** (105 mg, 0.20 mmol), **5** was obtained as a beige solid (60 mg, 62%). R_f = 0.42 (1:9 MeOH/CH_2Cl_2). ^{1}H NMR (600 MHz, DMSO-d_6): δ 8.78 (t, J = 5.9 Hz, 1H), 8.29 (s, 1H), 8.13 (s, 1H), 7.85 (d, J = 8.8 Hz, 1H), 7.52 (d, J = 2.6 Hz, 1H), 7.44 (br s, 2H), 7.25 (dd, J = 8.9, 2.6 Hz, 1H), 5.81 (d, J = 6.5 Hz, 1H), 5.50 (br s, 1H), 5.34 (br s, 1H), 4.70 (t, J = 5.9 Hz, 1H), 4.09 (dd, J = 5.2, 2.7 Hz, 1H), 4.03 (td, J = 4.7, J = 2.7 Hz, 1H), 3.87 (s, 3H), 3.26−3.16 (m, 2H). ^{13}C NMR (150 MHz, DMSO-d_6): δ 162.6, 156.1, 152.2, 149.2, 148.8, 140.7, 131.5, 124.0, 119.6, 117.4, 109.9, 88.5, 83.6, 72.4, 71.2, 56.7, 44.9. HRMS (ESI+): m/z calculated for $C_{17}H_{20}N_7O_8S$ $[M+H]^+$: 482.1089, found 482.1094.

*N-{[(2R,5R)-5-(6-amino-9H-purin-9-yl)-3,4-dihydroxyoxolan-2-yl]methyl}-2-nitro-4-(trifluoro)benzenesulfonamide (**6**).* Following method E with **41f** (90 mg, 0.15 mmol), **6** was obtained as a beige solid (63 mg, 75%). R_f = 0.56 (1:9 MeOH/CH_2Cl_2). ^{1}H NMR (500 MHz, DMSO-d_6): δ 9.20 (t, J = 5.9 Hz, 1H), 8.49 (d, J = 1.7 Hz, 1H), 8.31 (s, 1H), 8.17−8.13 (m, 2H), 8.11 (dd, J = 8.3, 1.8 Hz, 1H), 7.53 (s, 2H), 5.82 (d, J = 6.4 Hz, 1H), 5.53 (br s, 1H), 5.35 (s, 1H), 4.73−4.56 (m, 1H), 4.10 (dd, J = 5.2, 3.0 Hz, 1H), 4.08−3.94 (m, 1H), 3.32 (t, J = 5.4 Hz, 2H). ^{13}C NMR (125 MHz, DMSO-d_6): δ 155.8, 151.8, 148.8, 147.8, 140.7, 136.5, 133.8, 133.6, 133.4, 133.1, 131.0, 129.5, 125.0,

https://doi.org/10.1021/acs.jmedchem.2c00120
J. Med. Chem. 2022, 65, 6231−6249

123.3, 121.5, 119.5, 122.1, 122.1, 119.5, 88.3, 83.5, 72.6, 71.1, 45.1. HRMS (ESI+): m/z calculated for $C_{17}H_{17}N_7O_7SF_3$ $[M+H]^+$: 520.0857, found 520.0858.

*N-{[(2R,5R)-5-(6-amino-9H-purin-9-yl)-3,4-dihydroxyoxolan-2-yl]methyl}-4-chloro-3-nitrobenzenesulfonamide (**7**).* Following method E with **41g** (105 mg, 0.20 mmol), **7** was obtained as a beige solid (80 mg, 89%). R_f = 0.48 (1:9 MeOH/CH_2Cl_2). ^{1}H NMR (600 MHz, DMSO-d_6): δ 8.80 (t, J = 6.0 Hz, 1H), 8.42 (d, J = 2.3 Hz, 1H), 8.28 (s, 1H), 8.14 (s, 1H), 8.02 (dd, J = 8.5 Hz, 2.3 Hz, 1H), 7.92 (d, J = 8.5 Hz, 1H), 7.37 (s, 2H), 5.82 (d, J = 6.4 Hz, 1H), 5.50 (d, J = 6.3 Hz, 1H), 5.31 (d, J = 4.7 Hz, 1H), 4.65 (q, J = 5.7 Hz, 1H), 4.11−4.06 (m, 1H), 3.98 (td, J = 4.9, 3.0 Hz, 1H), 3.26−3.15 (m, 2H). ^{13}C NMR (150 MHz, DMSO-d_6): δ 156.2, 152.3, 148.8, 147.3, 140.7, 140.3, 133.1, 131.2, 129.3, 123.9, 119.5, 88.1, 83.3, 72.5, 71.1, 44.9. HRMS (ESI+): m/z calculated for $C_{16}H_{17}N_7O_7SCl$ $[M+H]^+$: 486.0593, found 486.0597.

*N-{[(2R,5R)-5-(6-amino-9H-purin-9-yl)-3,4-dihydroxyoxolan-2-yl]methyl}-N-ethylbenzenesulfonamide (**8**).* Following method E using **42a** (108 mg, 0.24 mmol), **8** was obtained as a white solid (46 mg, 48%) with 99% purity determined by HPLC analysis at 260 nm. R_f = 0.54 (1:9 MeOH/CH_2Cl_2). ^{1}H NMR (600 MHz, DMSO-d_6): δ 8.35 (s, 1H), 8.14 (s, 1H), 7.83−7.78 (m, 2H), 7.68−7.62 (m, 1H), 7.61−7.55 (m, 2H), 7.27 (br s, 2H), 5.87 (d, J = 5.9 Hz, 1H), 5.49 (d, J = 6.1 Hz, 1H), 5.34 (d, J = 4.9 Hz, 1H), 5.47 (d, J = 6.2 Hz, 1H), 5.28 (d, J = 4.5 Hz, 1H), 4.81 (td, J = 6.0, 4.9 Hz, 1H), 4.21 (td, J = 5.0, 3.5 Hz, 1H), 4.06 (ddd, J = 8.2, 5.0, 3.5 Hz, 1H), 3.70 (dd, J = 14.8, 5.0 Hz, 1H), 3.28 (dd, J = 14.7, 7.8 Hz, 1H), 3.21 (dq, J = 14.2, 7.1 Hz, 1H), 3.11 (dt, J = 14.4, 7.2 Hz, 1H), 0.92 (t, J = 7.1 Hz, 3H). ^{13}C NMR (150 MHz, DMSO-d_6): δ 156.1, 152.5, 149.3, 140.3, 139.5, 132.7, 129.3, 126.8, 119.4, 87.9, 83.2, 72.1, 71.4, 49.7, 43.5, 13.6. HRMS (ESI+): m/z calculated for $C_{18}H_{23}N_6O_5S$ $[M+H]^+$: 435.1445, found 435.1449.

*N-{[(2R,5R)-5-(6-amino-9H-purin-9-yl)-3,4-dihydroxyoxolan-2-yl]methyl}-N-ethyl-2-nitro-4-(trifluoromethyl)benzene-1-sulfonamide (**9**).* Following method E with **42b** (100 mg, 0.17 mmol), **9** was obtained as a beige solid (64 mg, 69%). R_f = 0.58 (1:9 MeOH/CH_2Cl_2). ^{1}H NMR (600 MHz, DMSO-d_6): δ 8.53 (d, J = 1.7 Hz, 1H), 8.32 (s, 1H), 8.17 (d, J = 8.3 Hz, 1H), 8.13 (s, 1H), 8.03 (dd, J = 8.4, 1.8 Hz, 1H), 7.27 (br s, 2H), 5.86 (d, J = 5.4 Hz, 1H), 5.54 (d, J = 6.0 Hz, 1H), 5.37 (d, J = 5.2 Hz, 1H), 4.72 (q, J = 5.5 Hz, 1H), 4.19 (q, J = 4.9 Hz, 1H), 4.07 (dt, J = 8.3, 4.0 Hz, 1H), 3.79 (dd, J = 15.1, 3.9 Hz, 1H), 3.65 (dd, J = 15.1, 8.7 Hz, 1H), 3.41−3.28 (m, 2H), 1.00 (t, J = 7.1 Hz, 3H). ^{13}C NMR (150 MHz, DMSO-d_6): δ 156.1, 152.6, 149.2, 147.7, 140.1, 135.9, 134.0, 133.8, 133.5, 133.3, 131.1, 129.1, 124.9, 123.1, 121.3, 119.5, 121.9, 119.3, 88.0, 82.5, 72.4, 71.4, 49.5, 43.3, 13.5. HRMS (ESI+): m/z calculated for $C_{19}H_{21}F_3N_7O_7S$ $[M+H]^+$: 548.1170, found 548.1175.

*N-{[(2R,5R)-5-(6-amino-9H-purin-9-yl)-3,4-dihydroxyoxolan-2-yl]methyl}-3-nitrobenzenesulfonamide (**10**).* Following method E using **41h** (106 mg, 0.22 mmol), **10** (58 mg, 60%) was obtained as a white solid with 99% purity determined by HPLC analysis at 260 nm. R_f = 0.30 (1:9 MeOH/CH_2Cl_2). ^{1}H NMR (600 MHz, DMSO-d_6): δ 8.75 (br s, 1H), 8.50 (t, J = 2.0 Hz, 1H), 8.41 (ddd, J = 8.2, 2.3, 1.1 Hz, 1H), 8.27 (s, 1H), 8.18 (dt, J = 7.9, 1.4 Hz, 1H), 8.13 (s, 1H), 7.83 (t, J = 8.1 Hz, 1H), 7.35 (br s, 2H), 5.81 (d, J = 6.2 Hz, 1H), 5.48 (d, J = 6.2 Hz, 1H), 5.29 (d, J = 4.8 Hz, 1H), 4.65 (q, J = 6.0 Hz, 1H), 4.10−4.04 (m, 1H), 3.99−3.94 (m, 1H), 3.23−3.13 (m, 2H). ^{13}C NMR (150 MHz, DMSO-d_6): δ 156.7, 152.8, 149.3, 148.31, 142.6, 140.7, 132.9, 131.7, 127.5, 121.7, 119.9, 88.5, 83.7, 72.9, 71.6, 45.4. HRMS (ESI+): m/z calculated for $C_{16}H_{18}N_7O_7S$ $[M+H]^+$: 452.0983, found 452.0986.

*N-{[(2R,5R)-5-(6-amino-9H-purin-9-yl)-3,4-dihydroxyoxolan-2-yl]methyl}-4-fluoro-3-nitrobenzenesulfonamide (**11**).* Following method E with **41i** (109 mg, 0.21 mmol), **11** (65 mg, 74%) was obtained as a beige solid. R_f = 0.50 (1:9 MeOH/CH_2Cl_2). ^{1}H NMR (500 MHz, DMSO-d_6): δ 8.74 (t, J = 6.1 Hz, 1H), 8.45 (dd, J = 7.0, 2.4 Hz, 1H), 8.27 (s, 1H), 8.17−8.11 (m, 2H), 7.73 (dd, J = 10.9, 8.7 Hz, 1H), 7.35 (br s, 2H), 5.81 (d, J = 6.2 Hz, 1H), 5.49 (d, J = 6.2 Hz, 1H), 5.29 (d, J = 4.7 Hz, 1H), 4.65 (q, J = 6.0 Hz, 1H), 4.07 (td, J = 5.0, 3.2 Hz, 1H), 3.97 (td, J = 4.9, 3.2 Hz, 1H), 3.26−3.11 (m, 2H). ^{13}C NMR (125 MHz, DMSO-d_6): δ 157.5, 155.7 (C−F), 156.2, 152.3, 148.8, 140.2, 137.4, 137.4, 136.8, 136.7, 134.2, 134.1, 125.0, 120.1, 119.9, 119.4, 88.0, 83.2, 72.4, 71.1, 44.8. HRMS (ESI+): m/z calculated for $C_{16}H_{17}FN_7O_7S$ $[M+H]^+$: 470.0945, found 470.0941.

*N-{[(2R,5R)-5-(6-amino-9H-purin-9-yl)-3,4-dihydroxyoxolan-2-yl]methyl}-4-bromo-3-nitrobenzenesulfonamide (**12**).* Following method E with **41j** (94 mg, 0.17 mmol, 1.00 equiv), **12** (54 mg, 62%) was obtained as a beige solid. R_f = 0.50 (1:9 MeOH/CH_2Cl_2). ^{1}H NMR (500 MHz, DMSO-d_6): δ 8.83 (t, J = 5.9 Hz, 1H), 8.38 (d, J = 2.1 Hz, 1H), 8.30 (s, 1H), 8.13 (s, 1H), 8.09 (d, J = 8.4, 1H), 7.92 (dd, J = 8.4, 2.2 Hz, 1H), 7.41 (br s, 2H), 5.83 (d, J = 6.4 Hz, 1H), 5.53 (d, J = 6.2 Hz, 1H), 5.35 (d, J = 4.7 Hz, 1H), 4.66 (td, J = 6.3, 5.1 Hz, 1H), 4.07 (td, J = 4.9, 3.0 Hz, 1H), 3.98 (td, J = 4.9, 2.9 Hz, 1H), 3.24−3.12 (m, 2H). ^{13}C NMR (125 MHz, DMSO-d_6): δ 156.3, 152.4, 149.6, 148.9, 141.2, 140.3, 136.2, 131.0, 123.7, 119.5, 118.0, 88.0, 83.4, 72.4, 71.1, 44.9. HRMS (ESI+): m/z calculated for $C_{16}H_{17}BrN_7O_7S$ $[M+H]^+$: 530.0094, found 530.0095.

*N-{[(2R,5R)-5-(6-amino-9H-purin-9-yl)-3,4-dihydroxyoxolan-2-yl]methyl}-4-methyl-3-nitrobenzenesulfonamide (**13**).* Following method E with **41k** (75 mg, 0.15 mmol), **13** (50 mg, 72%) was obtained as a beige solid. R_f = 0.68 (1:9 MeOH/CH_2Cl_2). ^{1}H NMR (500 MHz, DMSO-d_6): δ 8.68 (t, J = 5.9 Hz, 1H), 8.31 (d, J = 2.0 Hz, 1H), 8.28 (s, 1H), 8.12 (s, 1H), 7.96 (dd, J = 8.0, 2.0 Hz, 1H), 7.65 (d, J = 8.1, 1H), 7.41 (br s, 2H), 5.81 (d, J = 6.3 Hz, 1H), 5.52 (d, J = 6.1 Hz, 1H), 5.34 (d, J = 4.6 Hz, 1H), 4.66 (td, J = 6.3, 5.1 Hz, 1H), 4.08 (td, J = 4.8, 3.0 Hz, 1H), 3.97 (td, J = 4.9, 3.0 Hz, 1H), 3.22−3.09 (m, 2H), 2.56 (s, 3H). ^{13}C NMR (125 MHz, DMSO-d_6): δ 156.3, 152.3, 148.9, 148.6, 140.4, 139.4, 137.7, 134.1, 130.6, 122.7, 119.5, 88.0, 83.3, 72.4, 71.1, 44.9, 19.7. HRMS (ESI+): m/z calculated for $C_{17}H_{20}N_7O_7S$ $[M+H]^+$: 466.1139, found 466.1145.

*N-{[(2R,5R)-5-(6-amino-9H-purin-9-yl)-3,4-dihydroxyoxolan-2-yl]methyl}-4-ethyl-3-nitrobenzenesulfonamide (**14**).* Following method E with **41l** (183 mg, 0.35 mmol), **14** (103 mg, 61%) was obtained as a white solid. R_f = 0.48 (1:9 MeOH/CH_2Cl_2). ^{1}H NMR (600 MHz, DMSO-d_6): δ 8.66 (br s, 1H), 8.28 (s, 1H), 8.26 (d, J = 2.0 Hz, 1H), 8.12 (s, 1H), 7.99 (dd, J = 8.2, 2.0 Hz, 1H), 7.69 (d, J = 8.2, 1H), 7.36 (br s, 2H), 5.82 (d, J = 6.4 Hz, 1H), 5.48 (d, J = 6.1 Hz, 1H), 5.29 (d, J = 4.7 Hz, 1H), 4.66 (q, J = 6.0, 1H), 4.09 (td, J = 5.0, 3.0 Hz, 1H), 3.98 (td, J = 4.9, 3.0 Hz, 1H), 3.21−3.12 (m, 2H), 2.86 (q, J = 7.5 Hz, 2H), 1.21 (t, J = 7.5 Hz, 3H). ^{13}C NMR (150 MHz, DMSO-d_6): δ 156.2, 152.3, 148.8, 148.7, 142.3, 140.2, 139.5, 132.6, 131.5, 122.5, 119.4, 88.0, 83.3, 72.4, 71.1, 44.9, 25.2, 14.4. HRMS (ESI+): m/z calculated for $C_{18}H_{22}N_7O_7S$ $[M+H]^+$: 480.1296, found 480.1297.

*N-{[(2R,5R)-5-(6-amino-9H-purin-9-yl)-3,4-dihydroxyoxolan-2-yl]methyl}-4-methoxy-3-nitrobenzenesulfonamide (**15**).* Following method E with **41m** (90 mg, 0.17 mmol), **15** (40 mg, 49%) was obtained as a white solid. R_f = 0.43 (1:9 MeOH/CH_2Cl_2). ^{1}H NMR (600 MHz, DMSO-d_6): δ 8.61 (t, J = 6.1 Hz, 1H), 8.29 (s, 1H), 8.13 (s, 1H), 7.95 (d, J = 2.1 Hz, 1H), 7.82 (d, J = 8.4, 1H), 7.73 (dd, J = 8.4, 2.2 Hz, 1H), 7.36 (br s, 2H), 5.83 (d, J = 6.3 Hz, 1H), 5.49 (d, J = 6.1 Hz, 1H), 5.30 (d, J = 4.6 Hz, 1H), 4.66 (q, J = 5.4, 1H), 4.10−4.06 (m, 1H), 3.99−3.95 (m, 1H), 3.23−3.11 (m, 2H). ^{13}C NMR (150 MHz, DMSO-d_6): δ 156.2, 152.3, 148.9, 140.8, 140.3, 135.5, 132.0, 131.6, 128.2, 126.5, 119.5, 88.0, 83.3, 72.4, 71.1, 44.8. HRMS (ESI+): m/z calculated for $C_{16}H_{17}Cl_2N_6O_5S$ $[M+H]^+$: 475.0358, found 475.0367.

*N-{[(2R,5R)-5-(6-amino-9H-purin-9-yl)-3,4-dihydroxyoxolan-2-yl]methyl}-N-ethyl-3-nitrobenzene-1-sulfonamide (**16**).* Following method E using **42c** (65 mg, 0.13 mmol), **16** (32 mg, 53%) was obtained as a white solid with 99% purity determined by HPLC analysis at 260 nm. R_f = 0.21 (1:9 MeOH/CH_2Cl_2). ^{1}H NMR (600 MHz, DMSO-d_6): δ 8.47−8.40 (m, 2H), 8.32 (s, 1H), 8.22 (dt, J = 7.9, 1.4 Hz, 1H), 8.13 (s, 1H), 7.82 (t, J = 8.0 Hz, 1H), 7.27 (br s, 2H) 5.85 (d, J = 5.6 Hz, 1H), 5.51 (d, J = 6.0 Hz, 1H), 5.36 (d, J = 4.9 Hz, 1H), 4.76 (q, J = 5.3 Hz, 1H), 4.20 (q, J = 4.1 Hz, 1H), 4.05 (dt, J = 8.3, 4.2 Hz, 1H), 3.74 (dd, J = 14.8, 4.5 Hz, 1H), 3.43 (dd, J = 14.8, 8.3 Hz, 1H), 3.24−3.15 (m, 2H), 0.99 (t, J = 7.1 Hz, 3H). ^{13}C NMR (150 MHz, DMSO-d_6): δ 156.6, 153.0, 149.7, 148.4, 141.7, 140.7, 133.3, 131.8, 127.7, 122.0, 119.8, 88.4, 83.1, 72.7, 71.8, 50.0, 44.0, 14.2. HRMS (ESI+): m/z calculated for $C_{18}H_{22}N_7O_7S$ $[M+H]^+$: 480.1296, found 480.1303.

*N-{[(2R,5R)-5-(6-amino-9H-purin-9-yl)-3,4-dihydroxyoxolan-2-yl]methyl}-N-ethyl-4-bromo-3-nitrobenzene-1-sulfonamide (**17**).* Following method E with **42d** (104 mg, 0.17 mmol), **17** (56 mg,

https://doi.org/10.1021/acs.jmedchem.2c00120
J. Med. Chem. 2022, 65, 6231−6249

57%) was obtained as a beige solid. R_f = 0.53 (1:9 MeOH/CH_2Cl_2). ^{1}H NMR (500 MHz, DMSO-d_6): δ 8.42 (d, J = 2.2 Hz, 1H), 8.35 (s, 1H), 8.14 (s, 1H), 8.04 (d, J = 8.4 Hz, 1H), 7.93 (dd, J = 8.4, 2.2 Hz, 1H), 7.32 (br s, 2H), 5.87 (d, J = 5.9 Hz, 1H), 5.56 (d, J = 6.1 Hz, 1H), 5.39 (d, J = 5.0 Hz, 1H), 4.77 (q, J = 5.8 Hz, 1H), 4.18 (td, J = 5.0, 3.5 Hz, 1H), 4.06 (dt, J = 8.2, 4.1 Hz, 1H), 3.70 (dd, J = 14.8, 4.4 Hz, 1H), 3.43 (dd, J = 14.9, 8.4 Hz, 1H), 3.33−3.09 (m, 2H), 0.97 (t, J = 7.1 Hz, 3H). ^{13}C NMR (125 MHz, DMSO-d_6): δ 156.6, 153.1, 150.3, 149.8, 140.7, 136.4, 136.4, 131.7, 124.2, 119.3, 118.6, 88.2, 83.3, 72.7, 71.8, 50.3, 44.2, 14.3. HRMS (ESI+): m/z calculated for $C_{18}H_{21}BrN_7O_7S$ $[M+H]^+$: 558.0401, found 558.0400.

*N-{[(2R,5R)-5-(6-amino-9H-purin-9-yl)-3,4-dihydroxyoxolan-2-yl]methyl}-N-ethyl-4-methyl-3-nitrobenzene-1-sulfonamide (**18**).* Following method E with **42e** (66 mg, 0.12 mmol), **18** (40 mg, 65%) was obtained as a beige solid. R_f = 0.60 (1:9 MeOH/CH_2Cl_2). ^{1}H NMR (500 MHz, DMSO-d_6): δ 8.34 (s, 1H), 8.29 (d, J = 1.9 Hz, 1H), 8.13 (s, 1H), 7.99 (dd, J = 8.1, 2.0 Hz, 1H), 7.63 (dd, J = 8.1, 0.8 Hz, 1H), 7.32 (br s, 2H), 5.85 (d, J = 5.8 Hz, 1H), 5.54 (d, J = 6.1 Hz, 1H), 5.39 (d, J = 5.0 Hz, 1H), 4.77 (q, J = 5.7 Hz, 1H), 4.19 (td, J = 5.0, 3.6 Hz, 1H), 4.05 (dt, J = 8.3, 4.2 Hz, 1H), 3.70 (dd, J = 14.8, 4.6 Hz, 1H), 3.43−3.35 (m, 1H), 3.30−3.11 (m, 2H), 2.55 (s, 3H), 0.97 (t, J = 7.1 Hz, 3H). ^{13}C NMR (125 MHz, DMSO-d_6): δ 156.1, 152.6, 149.3, 148.8, 140.3, 138.6, 137.7, 134.1, 130.9, 122.9, 119.3, 87.7, 82.8, 72.2, 71.3, 49.7, 43.5, 19.6, 13.8. HRMS (ESI+): m/z calculated for $C_{19}H_{24}N_7O_7S$ $[M+H]^+$: 494.1452, found 494.1459.

*N-{[(2R,5R)-5-(6-amino-9H-purin-9-yl)-3,4-dihydroxyoxolan-2-yl]methyl}-N-ethyl-3-nitrobenzene-1-sulfonamide (**19**).* Following method E with **42f** (96 mg, 0.18 mmol), **19** (51 mg, 57%) was obtained as a white solid. R_f = 0.45 (1:9 MeOH/CH_2Cl_2). ^{1}H NMR (500 MHz, DMSO-d_6): δ 8.42 (d, J = 2.2 Hz, 1H), 8.35 (s, 1H), 8.14 (s, 1H), 8.04 (d, J = 8.4 Hz, 1H), 7.93 (dd, J = 8.4, 2.2 Hz, 1H), 7.32 (br s, 2H), 5.87 (d, J = 5.9 Hz, 1H), 5.56 (d, J = 6.1 Hz, 1H), 5.39 (d, J = 5.0 Hz, 1H), 4.77 (q, J = 5.8 Hz, 1H), 4.18 (td, J = 5.0, 3.5 Hz, 1H), 4.06 (dt, J = 8.2, 4.1 Hz, 1H), 3.70 (dd, J = 14.8, 4.4 Hz, 1H), 3.43 (dd, J = 14.9, 8.4 Hz, 1H), 3.33−3.09 (m, 2H), 0.97 (t, J = 7.1 Hz, 3H). ^{13}C NMR (125 MHz, DMSO-d_6): δ 156.6, 153.1, 150.3, 149.8, 140.7, 136.4, 136.4, 131.7, 124.2, 119.3, 118.6, 88.2, 83.3, 72.7, 71.8, 50.3, 44.2, 14.3. HRMS (ESI+): m/z calculated for $C_{18}H_{21}BrN_7O_7S$ $[M+H]^+$: 558.0401, found 558.0400.

*N-{[(2R,5R)-5-(6-amino-9H-purin-9-yl)-3,4-dihydroxyoxolan-2-yl]methyl}-3-cyanobenzenesulfonamide (**20**).* Following method E using **41n** (102 mg, 0.22 mmol), **20** (57 mg, 61%) was obtained as a white solid with 99% purity determined by HPLC analysis at 260 nm. R_f = 0.29 (1:9 MeOH/CH_2Cl_2). ^{1}H NMR (600 MHz, DMSO-d_6): δ 8.65 (br s, 1H), 8.28 (s, 1H), 8.20 (t, J = 1.7 Hz, 1H), 8.14 (s, 1H), 8.11−8.05 (m, 2H), 7.76 (t, J = 7.9 Hz, 1H), 7.36 (br s, 2H), 5.82 (d, J = 6.2 Hz, 1H), 5.49 (d, J = 6.2 Hz, 1H), 5.30 (d, J = 4.5 Hz, 1H), 4.66 (q, J = 6.0 Hz, 1H), 4.07 (td, J = 4.9, 3.1 Hz, 1H), 3.97 (td, J = 5.0, 3.0 Hz, 1H), 3.20−3.12 (m, 2H). ^{13}C NMR (150 MHz, DMSO-d_6): δ 156.2, 152.3, 148.8, 141.7, 140.3, 136.0, 130.8, 130.7, 130.0, 119.5, 117.5, 112.4, 88.0, 83.4, 72.4, 71.1, 44.8. HRMS (ESI+): m/z calculated for $C_{17}H_{18}N_7O_5S$ $[M+H]^+$: 432.1085, found 432.1078.

*N-{[(2R,5R)-5-(6-amino-9H-purin-9-yl)-3,4-dihydroxyoxolan-2-yl]methyl}-3-cyano-4-fluorobenzenesulfonamide (**21**).* Following method E using **41o** (92 mg, 0.19 mmol), **21** (62 mg, 73%) was obtained as a white solid with 99% purity determined by HPLC analysis at 260 nm. R_f = 0.31 (1:9 MeOH/CH_2Cl_2). ^{1}H NMR (600 MHz, DMSO-d_6): δ 8.67 (br s, 1H), 8.32 (dd, J = 6.0, 2.4 Hz, 1H), 8.28 (s, 1H), 8.14 (s, 1H), 8.13 (ddd, J = 8.8, 4.9, 2.4 Hz, 1H) 7.67 (t, J = 9.0 Hz, 1H), 7.36 (br s, 2H), 5.82 (d, J = 6.3 Hz, 1H), 5.49 (d, J = 6.2 Hz, 1H), 5.29 (d, J = 4.7 Hz, 1H), 4.65 (q, J = 6.1 Hz, 1H), 4.05 (td, J = 4.9, 3.1 Hz, 1H), 3.97 (td, J = 4.9, 3.1 Hz, 1H), 3.23−3.16 (m, 2H). ^{13}C NMR (150 MHz, DMSO-d_6): δ 165.1, 163.3, 156.2, 152.3, 148.8, 140.3, 138.0, 134.2, 134.2, 132.6, 119.4, 117.9, 117.8, 112.8, 101.5, 101.4, 88.0, 83.3, 72.4, 71.1, 44.8. HRMS (ESI+): m/z calculated for $C_{17}H_{17}FN_7O_5S$ $[M+H]^+$: 450.0990, found 450.0989.

*N-{[(2R,5R)-5-(6-amino-9H-purin-9-yl)-3,4-dihydroxyoxolan-2-yl]methyl}-4-chloro-3-cyanobenzenesulfonamide (**22**).* Following method E using **41p** (99 mg, 0.20 mmol), **22** (59 mg, 65%) was obtained as a white solid with 99% purity determined by HPLC analysis at 260 nm. R_f = 0.26 (1:9 MeOH/CH_2Cl_2). ^{1}H NMR (600 MHz, DMSO-d_6): δ 8.71 (br s, 1H), 8.31 (d, J = 2.4 Hz, 1H), 8.28 (s, 1H), 8.14 (s, 1H), 8.03 (dd, J = 8.5, 2.1 Hz, 1H), 7.89 (d, J = 8.5 Hz, 1H), 7.37 (br s, 2H), 5.82 (d, J = 6.4 Hz, 1H), 5.50 (d, J = 6.2 Hz, 1H), 5.31 (d, J = 4.6 Hz, 1H), 4.65 (q, J = 6.0 Hz, 1H), 4.06 (td, J = 4.8, 3.1 Hz, 1H), 3.97 (td, J = 5.0, 3.0 Hz, 1H), 3.20 (d, J = 5.0 Hz, 2H). ^{13}C NMR (150 MHz, DMSO-d_6): δ 156.3, 152.4, 148.8, 140.4, 140.3, 139.4, 132.4, 132.3, 131.1, 119.4, 114.9, 113.1, 88.0, 83.3, 72.4, 71.1, 44.8. HRMS (ESI+): m/z calculated for $C_{17}H_{17}ClN_7O_5S$ $[M+H]^+$: 466.0695, found 466.0697.

*N-{[(2R,5R)-5-(6-amino-9H-purin-9-yl)-3,4-dihydroxyoxolan-2-yl]methyl}-3-cyano-4-methoxybenzenesulfonamide (**23**).* Following method E using **41q** (50 mg, 0.10 mmol), **23** (26 mg, 57%) was obtained as a white solid with 98% purity determined by HPLC analysis at 260 nm. R_f = 0.22 (1:9 MeOH/CH_2Cl_2). ^{1}H NMR (600 MHz, DMSO-d_6): δ 8.46 (br s, 1H), 8.28 (s, 1H), 8.14 (s, 1H) 8.09 (d, J = 2.3 Hz, 1H), 8.01 (dd, J = 9.0, 2.4 Hz, 1H), 7.40−7.34 (m, 3H), 5.82 (d, J = 6.4 Hz, 2H), 5.49 (d, J = 6.2 Hz, 1H), 5.30 (d, J = 4.6 Hz, 1H), 4.66 (q, J = 5.9 Hz, 1H), 4.07 (td, J = 4.7, 3.0 Hz, 1H), 4.00−3.95 (m, 4H), 3.14−3.06 (m, 2H). ^{13}C NMR (150 MHz, DMSO-d_6): δ 163.3, 156.2, 152.3, 148.9, 140.3, 133.4, 132.9, 132.3, 119.5, 115.1, 113.1, 100.9, 88.1, 83.4, 72.4, 71.1, 57.1, 44.8. HRMS (ESI+): m/z calculated for $C_{18}H_{20}N_7O_6S$ $[M+H]^+$: 462.1190, found 462.1189.

*N-{[(2R,5R)-5-(6-amino-9H-purin-9-yl)-3,4-dihydroxyoxolan-2-yl]methyl}-3-cyano-N-ethylbenzene-1-sulfonamide (**24**).* Following method E using **42g** (85 mg, 0.17 mmol), **24** (59 mg, 75%) was obtained as a white solid with 99% purity determined by HPLC analysis at 260 nm. R_f = 0.18 (1:9 MeOH/CH_2Cl_2). ^{1}H NMR (600 MHz, DMSO-d_6): δ 8.34 (s, 1H), 8.28 (t, J = 1.8 Hz, 1H), 8.14 (s, 1H), 8.13−8.07 (m, 2H), 7.74 (t, J = 7.9 Hz, 1H), 7.28 (br s, 2H), 5.87 (d, J = 5.9 Hz, 1H), 5.52 (d, J = 6.0 Hz, 1H), 5.36 (d, J = 4.9 Hz, 1H), 4.78 (q, J = 5.5 Hz, 1H), 4.20 (q, J = 4.2 Hz, 1H), 4.06 (m, 1H), 3.71 (dd, J = 14.8, 4.6 Hz, 1H), 3.39 (dd, J = 14.9, 8.3 Hz, 1H), 3.27 (dq, J = 14.2, 7.0 Hz, 1H), 3.16 (dq, J = 14.1, 7.0 Hz, 1H), 0.95 (t, J = 7.1 Hz, 3H). ^{13}C NMR (150 MHz, DMSO-d_6): δ 156.1, 152.5, 149.3, 140.9, 140.2, 136.3, 131.2, 130.7, 130.4, 119.3, 117.5, 112.6, 87.8, 83.0, 72.2, 71.4, 49.7, 43.6, 13.7. HRMS (ESI+): m/z calculated for $C_{19}H_{22}N_7O_5S$ $[M+H]^+$: 460.1398, found 460.1404.

*N-{[(2R,5R)-5-(6-amino-9H-purin-9-yl)-3,4-dihydroxyoxolan-2-yl]methyl}-3-cyano-N-ethyl-4-methoxybenzene-1-sulfonamide (**25**).* Following method E using **42h** (76 mg, 0.08 mmol), **25** (24 mg, 65%) was obtained as a white solid with 98% purity determined by HPLC analysis at 260 nm. R_f = 0.19 (1:9 MeOH/CH_2Cl_2). ^{1}H NMR (600 MHz, DMSO-d_6): δ 8.34 (s, 1H), 8.17 (d, J = 2.4 Hz, 1H), 8.15 (s, 1H), 8.03 (dd, J = 8.9, 2.4 Hz, 1H), 7.33 (d, J = 9.0 Hz, 1H), 7.28 (br s, 2H) 5.87 (d, J = 5.9 Hz, 1H), 5.52 (s, 1H), 5.36 (s, 1H), 4.78 (s, 1H) 4.19 (t, J = 4.0 Hz, 1H), 4.05 (dt, J = 8.1, 4.3 Hz, 1H), 3.99 (s, 3H), 3.67 (dd, J = 14.8, 4.7 Hz, 1H), 3.40−3.30 (m, 1H), 3.24 (dq, J = 14.2, 7.0 Hz, 1H), 3.11 (dq, J = 14.2, 7.1 Hz, 1H), 0.95 (t, J = 7.1 Hz, 3H). ^{13}C NMR (150 MHz, DMSO-d_6): δ 163.5, 156.1, 152.6, 149.3, 140.2, 133.8, 132.7, 132.1, 119.3, 115.0, 113.0, 101.2, 87.8, 83.0, 72.2, 71.3, 57.1, 49.7, 43.5, 13.7. HRMS (ESI+): m/z calculated for $C_{23}H_{28}N_7O_6S$ $[M+H]^+$: 490.1503, found 490.1504.

*N-{[(2R,5R)-5-(6-amino-9H-purin-9-yl)-3,4-dihydroxyoxolan-2-yl]methyl}-4-chlorobenzenesulfonamide (**26**).* Following method E using **41r** (157 mg, 0.33 mmol), **26** (100 mg, 69%) was obtained as a white solid with 99% purity determined by HPLC analysis at 260 nm. R_f = 0.21 (1:9 MeOH/CH_2Cl_2). ^{1}H NMR (600 MHz, DMSO-d_6): δ 8.59 (dd, J = 6.8, 5.3 Hz, 1H), 8.30 (s, 1H), 8.14 (s, 1H), 7.81−7.76 (m, 2H), 7.67−7.60 (m, 2H), 7.36 (br s, 2H), 5.82 (d, J = 6.5 Hz, 1H), 5.48 (d, J = 6.2 Hz, 1H), 5.29 (d, J = 4.5 Hz, 1H), 4.67 (q, J = 6.0 Hz, 1H), 4.06 (td, J = 4.7, 2.9 Hz, 1H), 3.98 (td, J = 4.8, 2.9 Hz, 1H), 3.14−3.06 (m, 2H). ^{13}C NMR (150 MHz, DMSO-d_6): δ 156.3, 152.3, 148.8, 140.4, 139.2, 137.3, 129.4, 128.4, 119.5, 88.2, 83.5, 72.4, 71.1, 44.9. HRMS (ESI+): m/z calculated for $C_{16}H_{18}ClN_6O_5S$ $[M+H]^+$: 441.0742, found 441.0728.

*N-{[(2R,5R)-5-(6-amino-9H-purin-9-yl)-3,4-dihydroxyoxolan-2-yl]methyl}-3-chlorobenzenesulfonamide (**27**).* Following method E using **41s** (80 mg, 0.17 mmol), **27** (52 mg, 71%) was obtained as a white solid with 99% purity determined by HPLC analysis at 260 nm. R_f

https://doi.org/10.1021/acs.jmedchem.2c00120
J. Med. Chem. 2022, 65, 6231−6249

= 0.18 (1:9 MeOH/CH_2Cl_2). ^{1}H NMR (600 MHz, DMSO-d_6): δ 8.56 (dd, J = 6.8, 5.1 Hz, 1H), 8.30 (s, 1H), 8.13 (s, 1H), 7.78 (t, J = 1.9 Hz, 1H), 7.75 (ddd, J = 7.9, 1.7, 1.0 Hz, 1H), 7.70 (ddd, J = 8.1, 2.3, 1.1 Hz, 1H), 7.60 (t, J = 8.0 Hz, 1H), 7.36 (br s, 2H), 5.83 (d, J = 6.3 Hz, 1H), 5.48 (d, J = 6.2 Hz, 1H), 5.30 (d, J = 4.6 Hz, 1H), 4.67 (td, J = 6.3, 5.2 Hz, 1H), 4.09 (td, J = 4.9, 3.0 Hz, 1H), 3.98 (td, J = 4.9, 3.0 Hz, 1H), 3.19−3.07 (m, 2H). ^{13}C NMR (150 MHz, DMSO-d_6): δ 156.3, 152.3, 148.9, 142.3, 140.3, 133.8, 132.4, 131.4, 126.0, 125.1, 119.5, 88.1, 83.4, 72.4, 71.1, 44.9. HRMS (ESI+): m/z calculated for $C_{16}H_{18}ClN_6O_5S$ $[M+H]^+$: 441.0742, found 441.0737.

*N-{[(2R,5R)-5-(6-amino-9H-purin-9-yl)-3,4-dihydroxyoxolan-2-yl]methyl}-3,4-dichlorobenzenesulfonamide (**28**).* Following method E with **41t** (80 mg, 0.16 mmol), **28** (30 mg, 41%) was obtained as a white solid. R_f = 0.49 (1:9 MeOH/CH_2Cl_2). ^{1}H NMR (600 MHz, DMSO-d_6): δ 8.61 (t, J = 6.1 Hz, 1H), 8.29 (s, 1H), 8.13 (s, 1H), 7.95 (d, J = 2.1 Hz, 1H), 7.82 (d, J = 8.4, 1H), 7.73 (dd, J = 8.4, 2.2 Hz, 1H), 7.36 (br s, 2H), 5.83 (d, J = 6.3 Hz, 1H), 5.49 (d, J = 6.1 Hz, 1H), 5.30 (d, J = 4.6 Hz, 1H), 4.66 (q, J = 5.4, 1H), 4.10−4.06 (m, 1H), 3.99−3.95 (m, 1H), 3.23−3.11 (m, 2H). ^{13}C NMR (150 MHz, DMSO-d_6): δ 156.2, 152.3, 148.9, 140.8, 140.3, 135.5, 132.0, 131.6, 128.2, 126.5, 119.5, 88.0, 83.3, 72.4, 71.1, 44.8. HRMS (ESI+): m/z calculated for $C_{16}H_{17}Cl_2N_6O_5S$ $[M+H]^+$: 475.0358, found 475.0367.

*N-{[(2R,5R)-5-(6-amino-9H-purin-9-yl)-3,4-dihydroxyoxolan-2-yl]methyl}-3-chloro-4-methylbenzenesulfonamide (**29**).* Following method E using **41u** (100 mg, 0.20 mmol), **29** (70 mg, 76%) was obtained as a white solid with 99% purity determined by HPLC analysis at 260 nm. R_f = 0.22 (1:9 MeOH/CH_2Cl_2). ^{1}H NMR (600 MHz, DMSO-d_6): δ 8.47 (dd, J = 6.9, 4.9 Hz, 1H), 8.29 (s, 1H), 8.13 (s, 1H), 7.75 (d, J = 1.8 Hz, 1H), 7.63 (dd, J = 8.0, 1.9 Hz, 1H), 7.53 (dd, J = 7.9, 0.9 Hz, 1H), 7.36 (br s, 2H), 5.82 (d, J = 6.4 Hz, 1H), 5.47 (d, J = 6.2 Hz, 1H), 5.29 (d, J = 4.6 Hz, 1H), 4.67 (td, J = 6.2, 5.1 Hz, 1H), 4.09 (td, J = 5.0, 3.0 Hz, 1H), 3.98 (td, J = 4.9, 2.9 Hz, 1H), 3.16−3.05 (m, 2H), 2.38 (s, 3H). ^{13}C NMR (150 MHz, DMSO-d_6): δ 156.3, 152.3, 148.9, 140.6, 140.4, 139.6, 133.8, 132.0, 126.5, 125.1, 119.5, 88.1, 83.4, 72.4, 71.1, 44.9, 19.6. HRMS (ESI+): m/z calculated for $C_{17}H_{20}ClN_6O_5S$ $[M+H]^+$: 455.0899, found 455.0894.

*N-{[(2R,5R)-5-(6-amino-9H-purin-9-yl)-3,4-dihydroxyoxolan-2-yl]methyl}-3-chloro-N-ethylbenzene-1-sulfonamide (**30**).* Following method E using **42i** (45 mg, 0.09 mmol), **30** (25 mg, 61%) was obtained as a white solid with 99% purity determined by HPLC analysis at 260 nm. R_f = 0.22 (1:9 MeOH/CH_2Cl_2). ^{1}H NMR (600 MHz, DMSO-d_6): δ 8.35 (s, 1H), 8.15 (s, 1H), 7.82 (t, J = 1.9 Hz, 1H), 7.77 (dt, J = 7.9, 1.4 Hz, 1H), 7.73 (ddd, J = 5.0, 3.5 Hz, 1H), 4.06 (ddd, J = 8.2, 4.7, 3.3 Hz, 1H), 3.72 (dd, J = 14.7, 4.8 H, J = 8.0, 2.2, 0.9 Hz, 1H), 7.59 (t, J = 8.0 Hz, 1H), 7.27 (br s, 2H), 5.88 (d, J = 5.9 Hz, 1H), 5.50 (d, J = 6.1 Hz, 1H), 5.35 (d, J = 4.9 Hz, 1H), 4.81 (q, J = 5.8 Hz, 1H), 4.21 (td, J = 5.1, 3.6 Hz, 1H), 3.36 (dd, J = 14.8, 8.1 Hz, 1H), 3.24 (dt, J = 14.3, 7.1 Hz, 1H), 3.14 (dq, J = 14.2, 6.6 Hz, 1H), 0.95 (t, J = 7.1 Hz, 3H). ^{13}C NMR (150 MHz, DMSO-d_6): δ 156.1, 152.5, 149.3, 141.5, 140.3, 134.0, 132.7, 131.3, 126.3, 125.6, 119.4, 87.9, 83.0, 72.1, 71.3, 49.7, 43.5, 13.6. HRMS (ESI+): m/z calculated for $C_{18}H_{22}ClN_6O_5S$ $[M+H]^+$: 469.1055, found 469.1041.

*N-{[(2R,5R)-5-(6-amino-9H-purin-9-yl)-3,4-dihydroxyoxolan-2-yl]methyl}-3,4-dichloro-N-ethylbenzene-1-sulfonamide (**31**).* Following method E with **42j** (113 mg, 0.21 mmol, 1.00 equiv), **31** (60 mg, 57%) was obtained as a white solid. R_f = 0.53 (1:9 MeOH/CH_2Cl_2). ^{1}H NMR (600 MHz, DMSO-d_6): δ 8.35 (s, 1H), 8.15 (s, 1H), 8.00 (d, J = 2.1 Hz, 1H), 7.79 (d, J = 8.4 Hz, 1H), 7.75 (dd, J = 8.4, 2.2 Hz, 1H), 7.27 (br s, 2H), 5.87 (d, J = 5.9 Hz, 1H), 5.51 (d, J = 6.1 Hz, 1H), 5.35 (d, J = 5.0 Hz, 1H), 4.78 (q, J = 5.7 Hz, 1H), 4.20 (td, J = 5.0, 3.6 Hz, 1H), 4.07−4.03 (m, 1H), 3.70 (dd, J = 14.8, 4.6 Hz, 1H), 3.45−3.39 (m, 1H), 3.30−3.23 (m, 1H), 3.18−3.10 (m, 1H), 0.97 (t, J = 7.1 Hz, 3H). ^{13}C NMR (150 MHz, DMSO-d_6): δ 156.6, 152.5, 149.3, 140.2, 139.9, 135.8, 132.2, 131.6, 128.5, 126.9, 119.3, 87.8, 82.8, 72.2, 71.3, 49.6, 43.4, 13.7. HRMS (ESI+): m/z calculated for $C_{18}H_{20}Cl_2N_6O_5S$ $[M+H]^+$: 504.4521, found 504.4529.

*N-{[(2R,5R)-5-(6-amino-9H-purin-9-yl)-3,4-dihydroxyoxolan-2-yl]methyl}-3-chloro-N-ethyl-4-methylbenzene-1-sulfonamide (**32**).* Following method E using **42k** (92 mg, 0.19 mmol), **32** (45 mg, 53%) was obtained as a white solid with 99% purity determined by HPLC analysis at 260 nm. R_f = 0.23 (1:9 MeOH/CH_2Cl_2). ^{1}H NMR (600 MHz, DMSO-d_6) 8.34 (s, 1H), 8.15 (s, 1H), 7.78 (d, J = 1.9 Hz, 1H), 7.66 (dd, J = 8.0, 1.9 Hz, 1H), 7.52 (d, J = 8.0 Hz, 1H), 7.27 (br s, 2H), 5.87 (d, J = 6.0 Hz, 1H), 5.49 (d, J = 6.1 Hz, 1H), 5.34 (d, J = 4.8 Hz, 1H), 4.80 (q, J = 5.8 Hz, 1H), 4.21 (td, J = 4.9, 3.4 Hz, 1H), 4.06 (ddd, J = 8.3, 4.8, 3.4 Hz, 1H), 3.70 (dd, J = 14.8, 4.9 Hz, 1H), 3.41−3.31 (m, 1H), 3.23 (dq, J = 14.2, 7.2 Hz, 1H), 3.11 (dq, J = 14.1, 7.0 Hz, 1H), 2.38 (s, 3H), 0.95 (t, J = 7.1 Hz, 3H). ^{13}C NMR (150 MHz, DMSO-d_6): δ 156.6, 153.0, 149.8, 141.4, 140.8, 139.3, 134.5, 132.5, 127.3, 126.0, 119.9, 88.4, 83.4, 72.6, 71.8, 50.1, 43.9, 20.1, 14.2. HRMS (ESI+): m/z calculated for $C_{19}H_{24}ClN_6O_5S$ $[M+H]^+$: 483.1212, found 483.1211.

*ethyl 5-(N-{[(2R,5R)-5-(6-amino-9H-purin-9-yl)-3,4-dihydroxyoxolan-2-yl]methyl}4-methoxy-3-nitrobenzenesulfonamido)-pentanoate (**33**).* Following method E with **43a** (140 mg, 0.22 mmol, 1.00 equiv), **33** (76 mg, 58%) was obtained as a white solid. R_f = 0.34 (5:95 MeOH/CH_2Cl_2). ^{1}H NMR (600 MHz, DMSO-d_6): δ 8.32 (s, 1H), 8.27 (d, J = 2.3 Hz, 1H), 8.13 (s, 1H), 8.01 (dd, J = 9.0, 2.4 Hz, 1H), 7.43 (d, J = 9.0, 1H), 7.27 (br s, 2H), 5.85 (d, J = 5.8 Hz, 1H), 5.50 (d, J = 6.1 Hz, 1H), 5.33 (d, J = 5.0 Hz, 1H), 4.78 (q, J = 5.9 Hz, 1H), 4.17 (td, J = 4.9, 3.5 Hz, 1H), 4.08−4.02 (m, 1H), 4.02−3.94 (m, 5H), 3.67 (dd, J = 14.9, 4.3 Hz, 1H), 3.38−3.34 (m, 1H), 3.18 (ddd, J = 14.5, 8.7, 6.4 Hz, 1H), 3.00 (ddd, J = 14.2, 8.7, 5.3 Hz, 1H), 2.11 (td, J = 7.2, 1.2 Hz, 2H), 1.49−1.22 (m, 4H), 1.14 (t, J = 7.0 Hz, 3H). ^{13}C NMR (150 MHz, DMSO-d_6): δ 173.0, 156.1, 154.7, 152.5, 149.3, 140.2, 138.8, 132.8, 130.9, 124.0, 119.3, 115.1, 87.9, 82.8, 72.1, 71.4, 59.6, 57.3, 50.4, 48.4, 32.8, 27.2, 21.3, 14.1. HRMS (ESI+): m/z calculated for $C_{24}H_{32}N_7O_{10}S$ $[M+H]^+$: 610.1943, found 610.1949.

*4-(N-{[(2R,5R)-5-(6-amino-9H-purin-9-yl)-3,4-dihydroxyoxolan-2-yl]methyl}4-methoxy-3-nitrobenzenesulfonamido)butyl acetate (**34**).* Following method E with **43b** (140 mg, 0.22 mmol, 1.00 equiv), **34** (79 mg, 60%) was obtained as a white solid. R_f = 0.34 (5:95 MeOH/CH_2Cl_2). ^{1}H NMR (600 MHz, $CDCl_3$): δ 8.33 (s, 1H), 8.27 (d, J = 2.4 Hz, 1H), 8.13 (s, 1H), 8.02 (dd, J = 9.0, 2.4 Hz, 1H), 7.44 (d, J = 9.0, 1H), 7.27 (br s, 2H), 5.86 (d, J = 5.9 Hz, 1H), 5.50 (d, J = 6.1 Hz, 1H), 5.34 (d, J = 5.0 Hz, 1H), 4.79 (q, J = 5.8 Hz, 1H), 4.18 (td, J = 5.0, 3.6 Hz, 1H), 4.08−4.03 (m, 1H), 4.00 (s, 3H), 3.83 (t, J = 6.4 Hz, 2H), 3.68 (dd, J = 14.9, 4.4 Hz, 1H), 3.20 (dd, J = 14.7, 8.7 Hz, 1H), 3.06−2.98 (m, 2H), 1.95 (s, 3H), 1.52−1.29 (m, 4H), 1.37 (s, 3H). ^{13}C NMR (150 MHz, $CDCl_3$): δ 170.3, 156.1, 154.7, 152.5, 149.3, 140.3, 138.8, 132.8, 130.9, 124.0, 119.4, 115.1, 87.9, 82.9, 72.1, 71.4, 63.2, 57.3, 50.5, 48.4, 25.1, 24.5, 20.6. HRMS (ESI+): m/z calculated for $C_{26}H_{34}N_7O_{10}S$ $[M+H]^+$: 636.2082, found 636.2092.

*N-{[(2R,5R)-5-(6-amino-9H-purin-9-yl)-3,4-dihydroxyoxolan-2-yl]methyl}-N-[4-(1,3-dioxo-2,3-dihydro-1H-isoindol-2-yl)butyl]-4-methoxy-3-nitrobenzene-1-sulfonamide (**35**).* Following method E with **43c** (140 mg, 0.19 mmol, 1.00 equiv), **35** (118 mg, 89%) was obtained as a white foam. R_f = 0.41 (5:95 MeOH/CH_2Cl_2). ^{1}H NMR (600 MHz, DMSO-d_6): δ 8.29 (s, 1H), 8.19 (d, J = 2.4 Hz, 1H), 8.15 (s, 1H), 7.89 (dd, J = 9.0, 2.4 Hz, 1H), 7.86−7.81 (m, 4H), 7.7 (d, J = 9.0, 1H), 7.37 (br s, 2H), 6.16 (d, J = 2.3 Hz, 1H), 5.42 (dd, J = 6.2, 2.3 Hz, 1H), 5.03 (dd, J = 6.3, 3.1 Hz, 1H), 4.30 (ddd, J = 8.4, 5.4, 3.1 Hz, 1H), 3.97 (s, 3H), 3.59 (dd, J = 14.8, 5.5 Hz, 1H), 3.42 (td, J = 6.8, 2.5 Hz, 2H), 3.28 (dd, J = 14.7, 8.0 Hz, 1H), 3.07−2.94 (m, 2H), 3.18−2.97 (m, 2H), 1.49 (s, 3H), 1.40−1.23 (m, 7H). ^{13}C NMR (150 MHz, DMSO-d_6): δ 167.8, 156.1, 154.7, 152.6, 148.5, 140.3, 138.7, 134.3, 131.5, 130.7, 124.0, 123.0, 119.2, 115.0, 113.3, 89.2, 85.0, 83.1, 82.0, 57.3, 49.7, 48.4, 36.8, 26.8, 25.2, 25.1, 25.0. HRMS (ESI+): m/z calculated for $C_{29}H_{31}N_8O_{10}S$ $[M+H]^+$: 683.1878, found 683.1881.

*N-{[(2R,5R)-5-(6-amino-9H-purin-9-yl)-3,4-dihydroxyoxolan-2-yl]methyl}benzamide (**36**).* Following method E using **44a** (230 mg, 0.56 mmol), **36** (160 mg, 77%) was obtained as a white solid. R_f = 0.38 (1:9 MeOH/CH_2Cl_2). ^{1}H NMR (600 MHz, DMSO-d_6): δ 8.71 (t, J = 5.9 Hz, 1H), 8.35 (s, 1H), 8.05 (s, 1H), 7.88−7.83 (m, 2H), 7.56−7.50 (m, 1H), 7.46 (dd, J = 8.3, 6.9 Hz, 2H), 7.29 (s, 2H), 5.87 (d, J = 6.2 Hz, 1H), 5.45 (d, J = 6.3 Hz, 1H), 5.27 (d, J = 4.7 Hz, 1H), 4.76 (td, J = 6.1, 5.0 Hz, 1H), 4.19 (td, J = 4.9, 3.2 Hz, 1H), 4.31 4.10 (td, J = 5.7, 3.2 Hz, 1H), 3.61 (t, J = 5.8 Hz, 2H). ^{13}C NMR (150 MHz, DMSO-d_6): δ 166.8, 156.1, 152.5, 149.3, 140.3, 134.5, 131.2, 128.3, 127.3, 119.5, 87.7,

https://doi.org/10.1021/acs.jmedchem.2c00120
J. Med. Chem. 2022, 65, 6231−6249

83.3, 72.6, 71.3, 41.7. HRMS (ESI+): m/z calculated for $C_{17}H_{19}N_6O_4$ $[M+H]^+$: 371.1462, found 371.1458.

*N-{[(2R,5R)-5-(6-amino-9H-purin-9-yl)-3,4-dihydroxyoxolan-2-yl]methyl}-4-chloro-3-nitrobenzamide (**37**).* Following method E using **44b** (80 mg, 0.16 mmol), **37** (66 mg, 90%) was obtained as a white solid. R_f = 0.38 (1:9 $MeOH/CH_2Cl_2$). ^1H NMR (600 MHz, DMSO-d_6): δ 9.03 (t, J = 5.8 Hz, 1H), 8.50 (d, J = 2.2 Hz, 1H) 8.35 (s, 1H), 8.14 (dd, J = 8.5, 2.1 Hz, 1H), 8.07 (s, 1H), 7.90 (d, J = 8.4 Hz, 1H), 7.28 (s, 2H), 5.88 (d, J = 5.8 Hz, 1H), 5.48 (d, J = 5.9 Hz, 1H), 5.29 (d, J = 4.8 Hz, 1H), 4.76 (q, J = 5.6 Hz, 1H), 4.22 (q, J = 4.7 Hz, 1H), 4.11−4.05 (m, 1H), 3.68 (dt, J = 13.8, 5.5 Hz, 1H), 3.58 (dt, J = 13.8, 6.2 Hz, 1H). ^{13}C NMR (150 MHz, DMSO-d_6): δ 163.7, 156.1, 152.6, 149.3, 147.3, 140.3, 134.4, 132.5, 132.0, 127.9, 124.5, 119.4, 87.8, 82.8, 72.6, 71.3, 42.0. HRMS (ESI+): m/z calculated for $C_{17}H_{17}N_7O_6Cl$ $[M+H]^+$: 450.0929, found 450.0934.

*N-{[(2R,5R)-5-(6-amino-9H-purin-9-yl)-3,4-dihydroxyoxolan-2-yl]methyl}-4-methyl-3-nitrobenzamide (**38**).* Following method E using **44c** (80 mg, 0.17 mmol), **38** (45 mg, 62%) was obtained as a white solid. R_f = 0.40 (1:9 $MeOH/CH_2Cl_2$). ^1H NMR (600 MHz, DMSO-d_6): δ 8.96 (t, J = 5.9 Hz, 1H), 8.45 (d, J = 1.9 Hz, 1H), 8.35 (s, 1H), 8.11−8.06 (m, 2H), 7.62 (d, J = 8.0 Hz, 1H), 7.28 (br s, 2H), 5.87 (d, J = 5.9 Hz, 1H), 5.46 (d, J = 6.1 Hz, 1H), 5.28 (d, J = 5.0 Hz, 1H), 4.75 (q, J = 5.8 Hz, 1H), 4.21 (td, J = 5.0, 3.6 Hz, 1H), 4.11−4.06 (m, 1H), 3.70−3.55 (m, 2H), 2.57 (s, 3H). ^{13}C NMR (150 MHz, DMSO-d_6): δ 164.4, 156.1, 152.6, 149.3, 148.7, 140.2, 136.0, 133.3, 133.0, 131.7, 123.2, 119.4, 87.7, 83.0, 72.5, 71.3, 41.9, 19.5. HRMS (ESI+): m/z calculated for $C_{18}H_{20}N_7O_6$ $[M+H]^+$: 430.1475, found 430.1480.

*N-{[(2R,5R)-5-(6-amino-9H-purin-9-yl)-3,4-dihydroxyoxolan-2-yl]methyl}-2-nitro-4-(trifluoromethyl)benzamide (**39**).* Following method E using **44d** (56 mg, 0.107 mmol), **39** (42 mg, 81%) was obtained as a white solid. R_f = 0.43 (1:9 $MeOH/CH_2Cl_2$). ^1H NMR (600 MHz, DMSO-d_6): δ 9.25 (t, J = 5.8 Hz, 1H), 8.44 (d, J = 1.7 Hz, 1H), 8.33 (s, 1H), 8.22 (dd, J = 8.1, 1.7 Hz, 1H), 7.88 (d, J = 8.0 Hz, 1H), 7.77 (s, 1H), 7.31 (br s, 2H), 5.87 (d, J = 6.2 Hz, 1H), 5.47 (d, J = 6.1 Hz, 1H), 5.34 (d, J = 4.7 Hz, 1H), 4.73 (q, J = 6.0 Hz, 1H), 4.19 (td, J = 4.9, 3.2 Hz, 1H), 4.11 (td, J = 5.1, 3.2 Hz, 1H), 3.70−3.58 (m, 2H). ^{13}C NMR (150 MHz, DMSO-d_6): δ 164.6, 156.2, 152.2, 149.0, 147.1, 140.5, 135.9, 130.9, 130.7, 130.5, 130.3, 130.6, 130.5, 125.4, 123.6, 121.8, 120.0, 121.6, 119.5, 88.1, 83.3, 72.5, 71.3, 41.7. HRMS (ESI+): m/z calculated for $C_{18}H_{17}N_7O_6F_3$ $[M+H]^+$: 484.1192, found 484.1198.

Molecular Docking. All calculations were performed using Autodock Vina (The Scripps Research Institute, La Jolla, CA) on an MSI computer with a 2.30 GHz Intel Core i5-8300H. The solved X-ray crystal structure of SARS-CoV nsp14 (PDB 5C8T) was used as a static receptor for docking. Both the co-crystalized ligand SAM and ions were removed from the SARS-CoV nsp14 protein using VMD 1.9.3 software. The ligand structures were drawn and minimized using MarvinSketch (ChemAxon). Targeted protein and ligand structures with polar hydrogens were converted to the required PDBQT format using MGL Tools (version 1.5.6). The docking was performed with a search box located at x = −11.155, y = −40.77, z = −3.688 coordinates, with a search box size of 25 × 25 × 25 Å^3. After calculations, PDB files were analyzed using Pymol (version 2.3).

Expression and Purification of Recombinant Proteins. Dengue virus serotype 2 methyltransferase (NS5 MTase) and human RNA N7-methyltransferase (hRNMT) coding sequences were cloned in fusion with a N-terminus hexa-histidine tag in Gateway plasmids. The proteins were expressed in *E. coli* and purified following previously described protocols.[34,36] Vaccinia virus capping enzyme (D1/D12 complex) and mRNA Cap 2′-*O*-methyltransferase (VP39) were purchased (New England Biolabs). SARS-CoV-2 nsp14, nsp10, and nsp16 coding sequences were cloned in fusion with a N-terminus hexa-histidine tag in pET28 plasmids. The proteins were expressed in *E. coli* C2566 and purified in a two-step IMAC using cobalt beads. Cells were lysed by sonication in a buffer containing 50 mM Tris pH 6.8, 300 mM NaCl, 10 mM imidazole, 5 mM $MgCl_2$, and 1 mM BME, supplemented with 0.25 mg/mL lysozyme, 10 μg/mL DNase, and 1 mM PMSF. The protein was purified through affinity chromatography with HisPur Cobalt resin 480 (Thermo Scientific), washing with an increased concentration of salt (1 M NaCl) and imidazole (20 mM), prior to elution in buffer supplemented with 250 mM imidazole. The protein was further purified by a size exclusion chomatography (GE Superdex S200) in a final buffer of 50 mM Tris pH 6.8, 300 mM NaCl, 5 mM $MgCl_2$, and 1 mM βME.

MTase Filter-Binding Assay (FBA). The transfer of tritiated methyl from [^{3}H] SAM onto RNA substrate was monitored by filter-binding assay, performed according to the method described previously.[37] For hRNMT and SARS CoV-2 nsp14, assays were carried out in reaction mixture [40 mM Tris-HCl (pH 8.0), 1 mM DTT, 1 mM $MgCl_2$, 2 μM SAM, and 0.1 μM ^{3}H-SAM (Perkin Elmer)] in the presence of 0.7 μM $GpppAC_4$ synthetic RNA and human RNA N7 MTase (hRNMT) (50 nM) and SARS-CoV-2 nsp14 (50 nM). For SARS CoV-2 nsp10/nsp16 (1.2 μM/0.2 μM) the reaction was performed in the presence of 0.7 μM $mGpppAC_4$ synthetic RNA. For NS5 MTase (500 nM) the reaction buffer does not contain $MgCl_2$ and the reaction was performed in the presence of 0.7 μM $mGpppAC_4$ synthetic RNA. For vaccinia virus capping enzyme (D1−D12) (41 U), the commercial buffer (New England Biolabs) at 1× concentration was used and the reaction was performed in the presence of 0.7 μM $GpppAC_4$ synthetic RNA. For vaccinia virus VP39 (24 U) the commercial buffer (New England Biolabs) at 1× concentration was used and the reaction was performed in the presence of 0.7 μM $mGpppAC_4$ synthetic RNA.

The enzymes were first mixed with the compound suspended in 100% DMSO (5% final DMSO) before the addition of RNA substrate and SAM and then incubated at 30 °C. For hRNMT, 3% DMSO final concentration was used. Control reactions were performed in the presence of 5% DMSO or 3% DMSO for hRNMT. Reactions mixtures were stopped after 30 min by their 10-fold dilution in ice-cold water. Samples were transferred to diethylaminoethyl (DEAE) filtermat (Perkin Elmer) using a Filtermat Harvester (Packard Instruments). The RNA-retaining mats were washed twice with 10 mM ammonium formate pH 8.0, twice with water and once with ethanol. They were soaked with scintillation fluid (Perkin Elmer), and ^{3}H-methyl transfer to the RNA substrates was determined using a Wallac MicroBeta TriLux liquid scintillation counter (Perkin Elmer). For IC_{50} measurements, values were normalized and fitted with Prism (GraphPad software) using the following equation: $Y = 100/[1 + ((X/IC_{50})$ ^Hillslope)]. IC_{50} is defined as the inhibitory compound concentration that causes 50% reduction in enzyme activity.

Thermal Shift Assays. TSA experiments were performed on a Bio-Rad C1000 thermal cycler CFX96 real-time system. Briefly, freshly purified nsp14 protein (5 μM 20 mM Hepes pH 7.5, 150 mM NaCl and do not exceed 5% of DMSO) was incubated with compounds at a concentration ranging from 500 μM to 8.4 nM (3-to-3 serial dilution) in the presence of Sypro Orange dye (SIGMA) used at 0.00056×. The TSA was performed in 96-well plates (4titude FrameStar 96 Well Skirked PCR plate) with a melt temperature increment of 1 °C each minute from 25 to 95 °C. The T_m was determined using the Boltzmann nonlinear regression formula (Graph-Pad PRISM 9) and ΔT_m was calculated by subtracting the compound T_m with that of negative control DMSO. The experiments were performed in duplicate and K_d was determined from the inflection point of the melting curve (ΔT_m in function of the concentration).

■ ASSOCIATED CONTENT

Supporting Information

The Supporting Information is available free of charge at https://pubs.acs.org/doi/10.1021/acs.jmedchem.2c00120.

Modeling results in SARS-CoV nsp14 (PDB ID: 5C8S, resolution 3.2 Å), pivot of the benzenesulfonamide ring with hydrophobic substituents, interaction between phthalimide moiety of **35** and Arg289, and overlay of SAM with compound **25**; melting temperatures (T_m °C) of SARS-CoV-2 nsp14; curves of fluorescence intensity versus temperature for SARS-CoV-2 nsp14 upon ligand binding; ^1H and ^{13}C NMR spectra of compounds **1**−**39** and intermediates (except for known compounds

https://doi.org/10.1021/acs.jmedchem.2c00120
J. Med. Chem. 2022, 65, 6231−6249

41b,c,e−g); and HPLC analysis of final compounds **1**−**32** (PDF)

Molecular formula strings (CSV)

Modeling of SARS-CoV nsp14_Compound **25** (ZIP)

AUTHOR INFORMATION

Corresponding Authors

Françoise Debart − *IBMM, University of Montpellier, 34293 Montpellier, cedex 5, France*; orcid.org/0000-0003-3422-3926; Email: francoise.debart@umontpellier.fr

Etienne Decroly − *AFMB, University of Aix-Marseille, 13288 Marseille, cedex 9, France*; Email: etienne.decroly@univ-amu.fr

Authors

Rostom Ahmed-Belkacem − *IBMM, University of Montpellier, 34293 Montpellier, cedex 5, France*

Marcel Hausdorff − *IBMM, University of Montpellier, 34293 Montpellier, cedex 5, France*

Adrien Delpal − *AFMB, University of Aix-Marseille, 13288 Marseille, cedex 9, France*

Priscila Sutto-Ortiz − *AFMB, University of Aix-Marseille, 13288 Marseille, cedex 9, France*; orcid.org/0000-0001-8672-690X

Agathe M. G. Colmant − *IHU Méditerranée Infection, Unité Virus Emergents, University of Aix-Marseille, 13005 Marseille, France*; orcid.org/0000-0002-2004-4073

Franck Touret − *IHU Méditerranée Infection, Unité Virus Emergents, University of Aix-Marseille, 13005 Marseille, France*

Natacha S. Ogando − *Department of Medical Microbiology, Leiden University Medical Center, 2333 ZA Leiden, The Netherlands*

Eric J. Snijder − *Department of Medical Microbiology, Leiden University Medical Center, 2333 ZA Leiden, The Netherlands*

Bruno Canard − *AFMB, University of Aix-Marseille, 13288 Marseille, cedex 9, France*

Bruno Coutard − *IHU Méditerranée Infection, Unité Virus Emergents, University of Aix-Marseille, 13005 Marseille, France*

Jean-Jacques Vasseur − *IBMM, University of Montpellier, 34293 Montpellier, cedex 5, France*; orcid.org/0000-0002-4379-6139

Complete contact information is available at: https://pubs.acs.org/10.1021/acs.jmedchem.2c00120

Notes

The authors declare no competing financial interest.

ACKNOWLEDGMENTS

The research described here was part of the MetInCoV project (F.D., J.-J.V., R.A.-B., M.H.), supported by grant ANR-21-CO14-0004-01 from the French National Research Agency, and this project has received funding from the European Union's Horizon 2020 Research and Innovation program under grants no. 101003627 (the SCORE project) and no. 101005077 (the CARE project) (E.D., B.C., A.D., and E.J.S.). R.A.-B. and M.H. thank the ANR for the financial support of the postdoc and Master 2 fellowships, ANR-21-CO14-0004-01 (MetInCoV) and ANR-20-CE11-0024-02 (VIRAGE), respectively.

ABBREVIATIONS USED

CoV, coronavirus; EDG, electron-donating group; EWG, electron-withdrawing group; MTase, methyltransferase; nsp, non-structural protein; SAH, *S*-5′-adenosyl-L-homocysteine; SAM, *S*-5′-adenosyl-L-methionine; SARS-CoV, severe acute respiratory syndrome coronavirus; TSA, thermal shift assay

REFERENCES

(1) Rota, P. A.; Oberste, M. S.; Monroe, S. S.; Nix, W. A.; Campagnoli, R.; Icenogle, J. P.; Penaranda, S.; Bankamp, B.; Maher, K.; Chen, M. H.; Tong, S.; Tamin, A.; Lowe, L.; Frace, M.; DeRisi, J. L.; Chen, Q.; Wang, D.; Erdman, D. D.; Peret, T. C.; Burns, C.; Ksiazek, T. G.; Rollin, P. E.; Sanchez, A.; Liffick, S.; Holloway, B.; Limor, J.; McCaustland, K.; Olsen-Rasmussen, M.; Fouchier, R.; Gunther, S.; Osterhaus, A. D.; Drosten, C.; Pallansch, M. A.; Anderson, L. J.; Bellini, W. J. Characterization of a novel coronavirus associated with severe acute respiratory syndrome. *Science* **2003**, *300*, 1394−1399.

(2) de Wit, E.; van Doremalen, N.; Falzarano, D.; Munster, V. J. SARS and MERS: recent insights into emerging coronaviruses. *Nat. Rev. Microbiol.* **2016**, *14*, 523−534.

(3) Seley-Radtke, K. L.; Yates, M. K. The evolution of nucleoside analogue antivirals: A review for chemists and non-chemists. Part 1: Early structural modifications to the nucleoside scaffold. *Antiviral Res.* **2018**, *154*, 66−86.

(4) Yates, M. K.; Seley-Radtke, K. L. The evolution of antiviral nucleoside analogues: A review for chemists and non-chemists. Part II: Complex modifications to the nucleoside scaffold. *Antiviral Res.* **2019**, *162*, 5−21.

(5) Decroly, E.; Canard, B. Biochemical principles and inhibitors to interfere with viral capping pathways. *Curr. Opin. Virol.* **2017**, *24*, 87−96.

(6) Benoni, R.; Krafcikova, P.; Baranowski, M. R.; Kowalska, J.; Boura, E.; Cahová, H. Substrate specificity of SARS-CoV-2 nsp10-nsp16 methyltransferase. *Viruses* **2021**, *13*, 1722.

(7) Bouvet, M.; Debarnot, C.; Imbert, I.; Selisko, B.; Snijder, E. J.; Canard, B.; Decroly, E. In vitro reconstitution of SARS-coronavirus mRNA cap methylation. *PLoS Pathol.* **2010**, *6*, No. e1000863.

(8) Romano, M.; Ruggiero, A.; Squeglia, F.; Maga, G.; Berisio, R. A structural view of SARS-CoV-2 RNA replication machinery: RNA synthesis, proofreading and final capping. *Cells* **2020**, *9*, 1267.

(9) Ogando, N. S.; El Kazzi, P.; Zevenhoven-Dobbe, J. C.; Bontes, B. W.; Decombe, A.; Posthuma, C. C.; Thiel, V.; Canard, B.; Ferron, F.; Decroly, E.; Snijder, E. J. Structure−function analysis of the nsp14 N7−guanine methyltransferase reveals an essential role in *Betacoronavirus* replication. *Proc. Natl. Acad. Sci. U. S. A.* **2021**, *118*, No. e2108709118.

(10) Aouadi, W.; Eydoux, C.; Coutard, B.; Martin, B.; Debart, F.; Vasseur, J. J.; Contreras, J. M.; Morice, C.; Quérat, G.; Jung, M.-L.; Canard, B.; Guillemot, J.-C.; Decroly, E. Toward the identification of viral cap-methyltransferase inhibitors by fluorescence screening assay. *Antiviral Res.* **2017**, *144*, 330−339.

(11) Wilamowski, M.; Sherrell, D. A.; Minasov, G.; Kim, Y.; Shuvalova, L.; Lavens, A.; Chard, R.; Maltseva, N.; Jedrzejczak, R.; Rosas-Lemus, M.; Saint, N.; Foster, I. T.; Michalska, K.; Satchell, K. J. F.; Joachimiak, A. 2′-O methylation of RNA cap in SARS-CoV-2 captured by serial crystallography. *Proc. Natl. Acad. Sci. U. S. A.* **2021**, *118*, No. e2100170118.

(12) Kasprzyk, R.; Jemielity, J. Enzymatic assays to explore viral mRNA capping machinery. *Chembiochem* **2021**, *22*, 3236−3253.

(13) Ferron, F.; Subissi, L.; Silveira De Morais, A. T.; Le, N. T. T.; Sevajol, M.; Gluais, L.; Decroly, E.; Vonrhein, C.; Bricogne, G.; Canard, B.; Imbert, I. Structural and molecular basis of mismatch correction and ribavirin excision from coronavirus RNA. *Proc. Natl. Acad. Sci. U. S. A.* **2018**, *115*, E162−E171.

(14) Basu, S.; Mak, T.; Ulferts, R.; Wu, M.; Deegan, T.; Fujisawa, R.; Tan, K. W.; Lim, C. T.; Basier, C.; Canal, B.; Curran, J. F.; Drury, L. S.; McClure, A. W.; Roberts, E. L.; Weissmann, F.; Zeisner, T. U.; Beale, R.; Cowling, V. H.; Howell, M.; Labib, K.; Diffley, J. F. X. Identifying SARS-CoV-2 antiviral compounds by screening for small molecule

inhibitors of nsp14 RNA cap methyltransferase. *Biochem. J.* **2021**, *478*, 2481−2497.
(15) Devkota, K.; Schapira, M.; Perveen, S.; Yazdi, A. K.; Li, F. L.; Chau, I.; Ghiabi, P.; Hajian, T.; Loppnau, P.; Bolotokova, A.; Satchell, K. J. F.; Wang, K.; Li, D. Y.; Liu, J.; Smil, D.; Luo, M. K.; Jin, J.; Fish, P. V.; Brown, P. J.; Vedadi, M. Probing the SAM binding site of SARS-CoV-2 nsp14 in vitro using SAM competitive inhibitors guides developing selective bisubstrate inhibitors. *SLAS Discovery* **2021**, *26*, 1200−1211.
(16) Kasprzyk, R.; Spiewla, T. J.; Smietanski, M.; Golojuch, S.; Vangeel, L.; De Jonghe, S.; Jochmans, D.; Neyts, J.; Kowalska, J.; Jemielity, J. Identification and evaluation of potential SARS-CoV-2 antiviral agents targeting mRNA cap guanine N7-Methyltransferase. *Antiviral Res.* **2021**, *193*, 105142.
(17) Pearson, L. A.; Green, C. J.; Lin, D.; Petit, A. P.; Gray, D. W.; Cowling, V. H.; Fordyce, E. A. F. Development of a high-throughput screening assay to identify inhibitors of the SARS-CoV-2 guanine-N7-methyltransferase using RapidFire mass spectrometry. *SLAS Discovery* **2021**, *26*, 749−756.
(18) Bobrovs, R.; Kanepe, I.; Narvaiss, N.; Patetko, L.; Kalnins, G.; Sisovs, M.; Bula, A. L.; Grinberga, S.; Boroduskis, M.; Ramata-Stunda, A.; Rostoks, N.; Jirgensons, A.; Tars, K.; Jaudzems, K. Discovery of SARS-CoV-2 nsp14 and nsp16 methyltransferase inhibitors by high-throughput virtual screening. *Pharmaceuticals* **2021**, *14*, 1243.
(19) Bobiļeva, O.; Bobrovs, R.; Kaņepe, I.; Patetko, L.; Kalniņš, G.; Šišovs, M.; Bula, A. L.; Grīnberga, S.; Borodušķis, M. r.; Ramata-Stunda, A.; Rostoks, N.; Jirgensons, A.; Tars, K.; Jaudzems, K. Potent SARS-CoV-2 mRNA cap methyltransferase inhibitors by bioisosteric replacement of methionine in SAM cosubstrate. *ACS Med. Chem. Lett.* **2021**, *12*, 1102−1107.
(20) Otava, T.; Šála, M.; Li, F.; Fanfrlík, J.; Devkota, K.; Perveen, S.; Chau, I.; Pakarian, P.; Hobza, P.; Vedadi, M.; Boura, E.; Nencka, R. The structure-based design of SARS-CoV-2 nsp14 methyltransferase ligands yields nanomolar inhibitors. *ACS Infect. Dis.* **2021**, *7*, 2214−2220.
(21) Ahmed-Belkacem, R.; Sutto-Ortiz, P.; Guiraud, M.; Canard, B.; Vasseur, J.-J.; Decroly, E.; Debart, F. Synthesis of adenine dinucleosides SAM analogs as specific inhibitors of SARS-CoV nsp14 RNA cap guanine-N7-methyltransferase. *Eur. J. Med. Chem.* **2020**, *201*, 112557.
(22) Ma, Y.; Wu, L.; Shaw, N.; Gao, Y.; Wang, J.; Sun, Y.; Lou, Z.; Yan, L.; Zhang, R.; Rao, Z. Structural basis and functional analysis of the SARS coronavirus nsp14-nsp10 complex. *Proc. Natl. Acad. Sci. U. S. A.* **2015**, *112*, 9436−9441.
(23) Yang, N. J.; Hinner, M. J. Getting across the cell membrane: an overview for small molecules, peptides, and proteins. *Methods Mol. Biol.* **2015**, *1266*, 29−53.
(24) Lu, R.; Zhao, X.; Li, J.; Niu, P.; Yang, B.; Wu, H.; Wang, W.; Song, H.; Huang, B.; Zhu, N.; Bi, Y.; Ma, X.; Zhan, F.; Wang, L.; Hu, T.; Zhou, H.; Hu, Z.; Zhou, W.; Zhao, L.; Chen, J.; Meng, Y.; Wang, J.; Lin, Y.; Yuan, J.; Xie, Z.; Ma, J.; Liu, W. J.; Wang, D.; Xu, W.; Holmes, E. C.; Gao, G. F.; Wu, G.; Chen, W.; Shi, W.; Tan, W. Genomic characterisation and epidemiology of 2019 novel coronavirus: implications for virus origins and receptor binding. *Lancet* **2020**, *395*, 565−574.
(25) Nepali, K.; Lee, H.-Y.; Liou, J.-P. Nitro-group-containing drugs. *J. Med. Chem.* **2019**, *62*, 2851−2893.
(26) Kan, T.; Fukuyama, T. Ns strategies: a highly versatile synthetic method for amines. *Chem. Commun.* **2004**, 353−359.
(27) Korzyński, M. D.; Borys, K. M.; Białek, J.; Ochal, Z. A novel method for the synthesis of aryl trihalomethyl sulfones and their derivatization: the search for new sulfone fungicides. *Tetrahedron Lett.* **2014**, *55*, 745−748.
(28) Wu, W. L.; Asberom, T.; Bara, T.; Bennett, C.; Burnett, D. A.; Clader, J.; Domalski, M.; Greenlee, W. J.; Josien, H.; McBriar, M.; Rajagopalan, M.; Vicarel, M.; Xu, R.; Hyde, L. A.; Del Vecchio, R. A.; Cohen-Williams, M. E.; Song, L.; Lee, J.; Terracina, G.; Zhang, Q.; Nomeir, A.; Parker, E. M.; Zhang, L. Structure activity relationship studies of tricyclic bispyran sulfone γ-secretase inhibitors. *Bioorg. Med. Chem. Lett.* **2013**, *23*, 844−849.
(29) Chan, M.; Lao, F. S.; Chu, P. J.; Shpigelman, J.; Yao, S.; Nan, J.; Sato-Kaneko, F.; Li, V.; Hayashi, T.; Corr, M.; Carson, D. A.; Cottam, H. B.; Shukla, N. M. Structure−activity relationship studies to identify affinity probes in bis-aryl sulfonamides that prolong immune stimuli. *J. Med. Chem.* **2019**, *62*, 9521−9540.
(30) Wei, W.; Liu, Q.; Li, Z.-Z.; Shi, W.-K.; Fu, X.; Liu, J.; Zhu, X.; Wang, X.-C.; Xu, N.; Li, T.-F.; Jiang, F.-R.; Xiao, Z.-P.; Zhu, H.-L. Synthesis and evaluation of adenosine containing 3-arylfuran-2(5H)-ones as tyrosyl-tRNA synthetase inhibitors. *Eur. J. Med. Chem.* **2017**, *133*, 62−68.
(31) Byun, Y.; Vogel, S. R.; Phipps, A. J.; Carnrot, C.; Eriksson, S.; Tiwari, R.; Tjarks, W. Synthesis and biological evaluation of inhibitors of thymidine monophosphate kinase from Bacillus anthracis. *Nucleosides Nucleotides Nucleic Acids* **2008**, *27*, 244−260.
(32) van Wandelen, L. T.; van Ameijde, J.; Mady, A. S.; Wammes, A. E.; Bode, A.; Poot, A. J.; Ruijtenbeek, R.; Liskamp, R. M. Directed modulation of protein kinase C isozyme selectivity with bisubstrate-based inhibitors. *ChemMedChem.* **2012**, *7*, 2113−2121.
(33) Soukarieh, F.; Nowicki, M. W.; Bastide, A.; Pöyry, T.; Jones, C.; Dudek, K.; Patwardhan, G.; Meullenet, F.; Oldham, N. J.; Walkinshaw, M. D.; Willis, A. E.; Fischer, P. M. Design of nucleotide-mimetic and non-nucleotide inhibitors of the translation initiation factor eIF4E: Synthesis, structural and functional characterisation. *Eur. J. Med. Chem.* **2016**, *124*, 200−217.
(34) Peyrane, F.; Selisko, B.; Decroly, E.; Vasseur, J. J.; Benarroch, D.; Canard, B.; Alvarez, K. High-yield production of short GpppA- and 7MeGpppA-capped RNAs and HPLC-monitoring of methyltransfer reactions at the guanine-N7 and adenosine-2′O positions. *Nucleic Acids Res.* **2007**, *35*, No. e26.
(35) Trott, O.; Olson, A. J. AutoDock Vina: improving the speed and accuracy of docking with a new scoring function, efficient optimization, and multithreading. *J. Comput. Chem.* **2009**, *31*, 455−461.
(36) Egloff, M. P.; Benarroch, D.; Selisko, B.; Romette, J. L.; Canard, B. An RNA cap (nucleoside-2′-O-)-methyltransferase in the flavivirus RNA polymerase NS5: crystal structure and functional characterization. *EMBO J.* **2002**, *21*, 2757−2768.
(37) Paesen, G. C.; Collet, A.; Sallamand, C.; Debart, F.; Vasseur, J. J.; Canard, B.; Decroly, E.; Grimes, J. M. X-ray structure and activities of an essential Mononegavirales L-protein domain. *Nature Comm.* **2015**, *6*, 8749.

https://doi.org/10.1021/acs.jmedchem.2c00120
J. Med. Chem. 2022, 65, 6231−6249